www.reanimatology.com
ISSN 2411-7110 (online)

GENERAL REANIMATOLOGY

SCIENTIFIC-AND-PRACTICAL JOURNAL

ОБЩАЯ РЕАНИМАТОЛОГИЯ

научно-практический журнал

Volume 21 Том 21

№ 5

THIS ISSUE:
Cerebrovascular Diseases

Basic information for the manuscript submission (v. April 21, 2025)

1. Initial submission

Authors should submit a single Word file containing the complete manuscript. Language of submission: Russian — for Russian-speaking authors. English — for non-Russian-speaking authors.

The file must include the following components:

- Title of the paper
- Full names of all authors
- Institutional affiliations of all authors
- Full manuscript text, including all sections
- Tables, figures, and photographs with captions and explanatory note
- Reference list

2. File Naming Format

Name the file using the first author's last name and the submission date in the format: LastName_YYYYMMDD.docx . For revised versions, only the date should be updated.

3. Manuscript Length

Original article: approximately 40,000 characters with spaces

Short communication: no more than 2,500 words

Review or meta-analysis: between 25,000 and 40,000 characters with spaces

4. Title Page Information

Title: must not exceed 12 words

Authors: full names (e.g., Peter A. Johnson)

Affiliations: full institutional names and postal addresses with zip code

Corresponding author: full name, email address, and phone number

5. Structure of summary, body text, References

Summary (Abstract): must be between 250 and 300 words and structured into the following sections:

- Introduction (background/scope of the problem)
- Aim
- Materials and Methods
- Results
- Conclusion

Highlights (optional): one to three main messages may be presented either in textual or infographic form. Text highlights should not exceed 40 words each.

Keywords: 6–8 keywords, separated by semicolons (;). Do not place a period at the end.

Post-keyword Informational Sections:

- Conflict of interest
- Study funding
- Acknowledgements (optional)
- Information about the Authors (ID, contributions)

Body text:

- Introduction (Background)
- Materials and Methods
- Results
- Discussion
- Conclusion

References: at least 70% of the references should be published within the last 5 years, and at least 30% within the last 3 years. Number of references: original articles — 25 to 45; short communications — 10 to 25; reviews — 80 to 120. Formatting: must comply with the Author Guidelines «3.14. References» section.

Illustrations (including tables): for original articles — up to 8; for short communications — up to 3; for reviews — up to 8.

6. Formatting

Font: Times New Roman, 12 pt. Section headings: bold. Line spacing: 5. Paragraph formatting: no extra space before or after paragraphs; one additional line between sections. First-line indent: 1.25 cm. Margins: 2.5 cm on all sides. Page numbers: bottom right corner of each page

ISSN 1813-9779 (print) ISSN 2411-7110 (online)

GENERAL REANIMATOLOGY

OBSHCHAYA REANIMATOLOGIYA

Scientific-and-Practical Peer-Reviewed Journal
Since 2005

• Covers issues of critical care medicine
• Manuscripts in Russian and English are published free-of-charge
• Included in SCOPUS (since 2015), RINTs, RSCI, DOAJ, and other databases, as well as in the Official list of editions recommended for publication of dissertations (PhD, DSci) by the Russian Higher Attestation Commission

Registration certificate of the Journal «Obshchaya reanimatologiya» (General Reanimatology): ПИ № ФС77-18690, November 2, 2004, Federal Service for Supervision of Compliance with Legislation in the Sphere of Mass Communications and Protection of Cultural Heritage
Publication Frequency: 6 numbers per year.
Founder:

ОБЩАЯ РЕАНИМАТОЛОГИЯ

OBŜAÂ REANIMATOLOGIÂ

научно-практический рецензируемый журнал
Выходит с 2005 г.

• охватывает вопросы медицины критических состояний
• публикует рукописи на русском и английском языках бесплатно
• включен в базы данных SCOPUS (с 2015 г.), РИНЦ, RSCI, DOAJ и др. базы данных; Перечень изданий, рекомендованных ВАК для публикации результатов диссертационных работ

Свидетельство о регистрации: ПИ № ФС77-18690 от 02 ноября 2004 г. Печатное издание журнал «Общая реаниматология» зарегистрирован Федеральной службой по надзору за соблюдением законодательства в сфере массовых коммуникаций и охране культурного наследия.
Периодичность: 6 раз в год
Учредитель: © Фонд «Медицина критических состояний», Москва, Россия

Publisher:
Federal Research and Clinical Center of Intensive Care Medicine and Rehabilitology, Moscow, Russia
Издатель:
Федеральный научно-клинический центр реаниматологии и реабилитологии (ФНКЦ РР), Москва, Россия

Supported by Russian Federation of Anesthesiologists and Reanimatologists
При поддержке Общероссийской общественной организации «Федерация анестезиологов и реаниматологов»

Artwork: Natalia V. Golubeva
Page-proof: Sergey V. Shishkov
Printing House:
Printed at LLC «Advanced Solutions». 19, Leninsky prospekt, build. 1, Moscow, 119071. www.aov.ru
Contacts:
25 Petrovka Str., Bldg. 2, 107031 Moscow, Russia.
Tel. +7-495-694-17-73.
E-mail: **journal_or@mail.ru;**
Web: **www.reanimatology.com**

Subscription:
Index 46338, refer to catalog of «Книга-Сервис»
Signed for printing: 24.11.2025

Оригинал-макет: Н. В. Голубева
Верстка: С. В. Шишков
Типография: отпечатано в ООО «Адвансед солюшнз». 119071, г. Москва, Ленинский пр-т, д. 19, стр. 1. www.aov.ru
Контакты с редакцией:
Россия, 107031, г. Москва, ул. Петровка, д. 25, стр. 2.
Тел.: +7-495-694-17-73.
E-mail: **journal_or@mail.ru;**
сайт: **www.reanimatology.com**

Подписка и распространение: индекс издания по каталогу «Книга-Сервис» — 46338.
Цена свободная
Подписано в печать: 24.11.2025

CONTENTS **СОДЕРЖАНИЕ**

ERRATUM [Russian Version of the Issue, No. 3, 2025]

Location	Printed	Correct Option
C. 3, Contents, Experimental Studies	Changes in Neutrophil Membranes Induced by Plasma from Newborns with Infection	Assessment of Structural Changes in Neutrophil Membranes Induced by Plasma from Newborns with Infection
C. 51, Summary, Conclusion	…pathogens that are not capable…	…pathogens that are capable…

https://doi.org/10.15360/1813-9779-2025-5-2580

Morphological Classification of Neuronal Damage

Arkady M. Golubev*

V. A. Negovsky Research Institute of General Reanimatology,
Federal Research and Clinical Center of Intensive Care Medicine and Rehabilitology,
25 Petrovka Str., Bldg. 2, 107031 Moscow, Russia

For citation: *Arkady M. Golubev.* Morphological Classification of Neuronal Damage. *Obshchaya Reanimatologiya = General Reanimatology.* 2025; 21 (5): 4–14. https://doi.org/10.15360/1813-9779-2025-5-2580 [In Russ. and Engl.]

***Correspondence to:** Arkady M. Golubev, arkadygolubev@mail.ru

Summary

Objectives. To develop a morphological classification of neuronal damage for use in practical activities by researchers, pathologists, and forensic experts.

Material and methods. The neurons of the cerebral cortex of 30 experimental animals (Wistar rats) were studied. Of these: with circulatory arrest *N*=10, with clozapine poisoning in combination with alcohol *N*=20 (clozapine dose 150 mg/kg, alcohol dose 5 ml/kg); morphological material of the human cerebral cortex was studied in subarachnoid hemorrhages (SAH) *N*=23, sudden cardiac death *N*=10, coronavirus infection *N*=18. Histological preparations were stained with hematoxylin and eosin, according to Nissl, according to Feulgen (for DNA), according to Brachet (for RNA and RNP), caspase-3 was detected by immunohistochemistry.

Results. A morphological classification of neuronal damage was proposed, including: decentralization of the nucleus within a neuron, morphological changes in the nucleolus, dark neurons, chromatin remodeling, lipofuscinosis, neuronal edema, Nissl substance lysis, neuronal calcification, neuronophagia, necrosis, and neuronal apoptosis. Functional disorders that occur in the studied variants of neuronal alteration were considered. As a result of developing neuronal damage, the function of the neuronal cytoskeleton, synthesis of ribosome subunits, synthesis of ribonucleoproteins, and DNA reparation are impaired, apoptosis is activated, lysosomes are damaged, the formation of reactive oxygen species is activated, and irreversible forms of neuronal damage (neuronophagia, necrosis, apoptosis) are recorded.

Conclusion. The proposed morphological classification complements existing classifications based on the study of molecular markers of neuronal damage and can be used in experimental studies and in the practical work of pathologists and forensic experts.

Keywords: neurons, neuronal damage, morphological classification

Conflict of interest. The author declares that he has no conflict of interest.

Funding. The work was carried out within the framework of the target assignment of the Ministry of Science and Higher Education (FGWS-2025-0016).

Information about the authors/Информация об авторе:
Arkady M. Golubev/Аркадий Михайлович Голубев: https://orcid.org/0000-0002-3165-0378

Introduction

Morphological studies are of great importance in understanding the processes occurring in the central nervous system, allowing for the verification of general pathological processes under the influence of damaging factors and the assessment of the nature of structural damage to neurons. In their everyday practical activities, pathologists and forensic experts solve the problems of identifying damage to neurons, their varieties, topographic localization with subsequent substantiation of their significance in the occurrence of functional disorders in various diseases of the central nervous system (CNS). Morphological classification of non-specific damage to neurons, developed at the Institute of Human Morphology [1] includes: acute swelling of nerve cells, primary irritation of neurons, hydropic changes in nerve cells, fatty degeneration, pigment dystrophies, calcification of neurons, shrinkage of nerve cells, severe changes in neurons, ischemic injury to neurons, karyocytolysis, satellitosis, neuronophagia. This classification includes not only morphological signs of neuronal damage, but also etiological factors (primary irritation, ischemic injury), as well as the intensity of damage (severe changes in neurons). Over the course of the existence of this classification, new data has been found characterizing new variants of neuronal damage, clarifying the mechanisms of alteration, and variants for assessing neuronal damage based on the identification of molecular markers have been proposed. In 1990 [2], a classification of irreversible cell damage was proposed: I — apoptosis, II — autophagy, III — necrosis. In 2005 (Nomenclature Committee on Cell the National Cancer Institute (NCCD) [3] recommended a classification that characterizes other types of cell alteration. A cell can be considered nonviable if one of three morphological criteria is detected: loss of cytoplasmic membrane integrity, complete cell fragmentation (including its nucleus) with formation of apoptotic bodies,

and absorption of the dead cell (or its fragments) by another cell. Researchers came to the understanding that morphological types of cell alteration (including neurons) indicate functional, biochemical, and immunological heterogeneity of the mechanisms of their damage. Visualization of morphological changes and determination of biochemical changes in the cell are recommended to determine the type of cell death. The NCCD proposed criteria for determining morphological types of cell death and gave recommendations on the use of terminology associated with cell death [4]. At the same time, this classification does not take into account a number of morphological changes that are reversible at a certain stage, but with prolonged and intense exposure to damaging factors lead to irreversible structural changes.

In addition to existing classifications, a classification of variants of alteration of CNS neurons was proposed taking into account morphological signs of damage, including the identification of molecular markers by histochemical and immunohistochemical research methods.

The aim of the study is to develop a morphological classification of neuronal damage for use in practical activities by researchers, pathologists, and forensic experts.

Material and Methods

The neurons of the cerebral cortex of 30 experimental animals (Wistar rats) were studied. Of these, 10 of which had circulatory arrest, and 20 had poisoning by clozapine in combination with alcohol (clozapine dose 150 mg/kg, alcohol — 5 ml/kg). In addition, the morphological material of the human cerebral cortex was examined in subarachnoid hemorrhages (SAH) (*N*=23), sudden cardiac death (*N*=10), COVID-19 (*N*=18). Histological preparations were stained with hematoxylin and eosin, according to Nissl, according to Feulgen, according to Brachet, luxol blue and cresyl violet, caspase-3 was detected by the immunohistochemical method.

Research Results

Decentralization of the neuron nucleus. One of the most common variants of neuron damage was the displacement of the nucleus to the periphery of the cell. This was most clearly recorded in large neurons, in which a significant volume belonged to the cytoplasm, due to which the nucleus could change its position in the cell (Fig. 1, *a*). The process of migration of the neuron nucleus is regulated by complex molecular mechanisms, considered in the discussion of the results of the study.

Morphological changes in the nucleolus of the neuron nucleus. Histological examination often revealed a shift (decentralization) of the nucleolus of neuronal nuclei, recorded in some neurons, while in other neurons the nucleolus retained a central position in the cell nucleus. In addition, neuron damage was accompanied by the disappearance of nucleoli and a decrease in the intensity of their staining. The diameter of nucleoli in cells synthesizing ribosome subunits varied from 0.5 to 7 μm. In cells where ribosome formation decreased or ceased, the size of nucleoli decreased to 0.1–0.3 μm. The shape, size, and number of nucleoli depended on the functional state of the nucleus: the larger the nucleolus, the higher its activity (Fig. 1, *b*, *c*).

Morphological changes in Nissl substance. Basophilic Nissl substance, revealed by staining with methylene blue (Nissl method), was located in the perinuclear zone. Electron microscopic examination showed that the basophilic substance was formed by flattened cisterns of the granular endoplasmic reticulum, where ribosomes were located, providing protein synthesis in the cell. Granules of Nissl substance contained ribonucleoproteins and protein-polysaccharide complexes. Basophilia, revealed by staining histological sections using the Nissl method, was due to RNA in the ribosomes.

Acute cerebrovascular events were accompanied by a significant decrease in the intensity of Nissl staining or a complete absence of staining. Spraying of Nissl substance in the cytoplasm of neurons was noted, as well as a shift to the peripheral zones of the neuron cytoplasm (Fig. 1, *d*).

Lipofuscinosis (acquired). Lipofuscin, which is formed in the cytoplasm of neurons and has autofluorescence, is one of the main markers of damage to neurons in the brain in cerebrovascular diseases. Lipofuscin exhibits variability in its properties: protein, lipid and/or carotenoid composition (Fig. 1, *e*).

Neuronal edema. Cellular (cytotoxic) edema was characterized by intracellular accumulation of fluid as a result of redistribution, rather than an increase in the fluid volume of brain tissue. Neuronal edema developed as a result of the entry of Na^+ and Cl^-, water from the interstitial spaces into the cell after damage to the central nervous system. At the light-optical level, swelling of cells and vacuolization of the cytoplasm of neurons were noted. Intracellular edema was observed in oncosis, which is one of the variants of neuronal damage. (Fig. 2, *a*).

Dark neurons. One of the histological variants of neuronal damage were the so-called dark neurons, which appeared as a result of damaging factors acting upon the central nervous system. Dark neurons are hyperchromic basophilic neurons with cytoplasm intensely stained with hematoxylin and eosin, according to Nissl and Brashe. Dark neurons are often subject to shrinkage and irreversible morphological changes (Fig. 2, *b*).

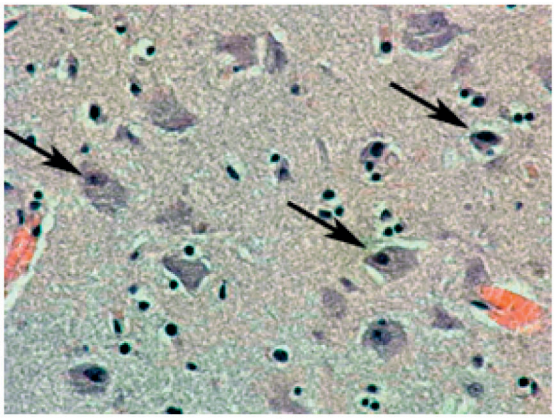

a

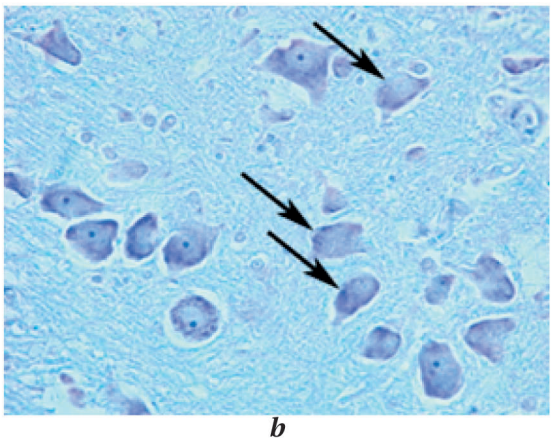

b

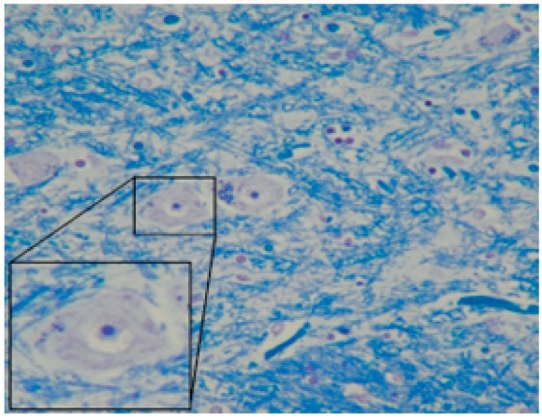

c

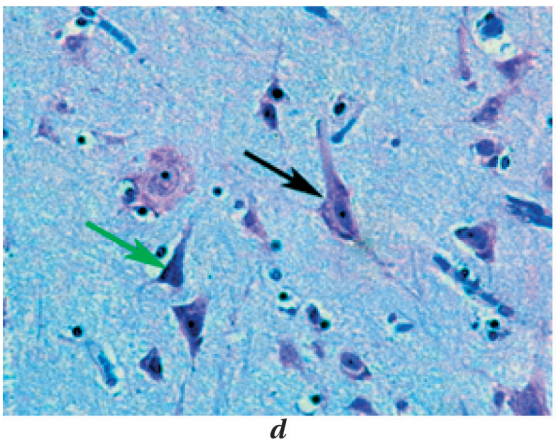

d

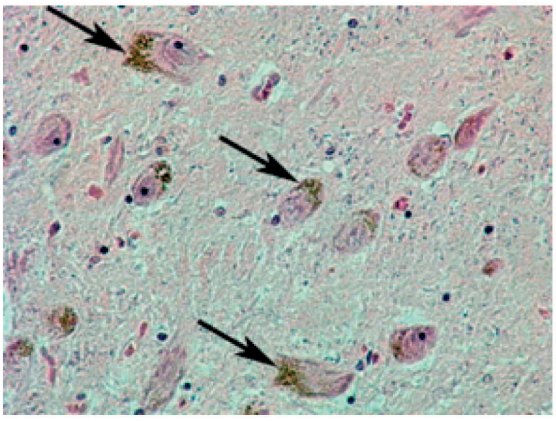

e

Calcification of neurons. One of the causes of damage to neurons is an increase of intracellular calcium. When staining histological sections with hematoxylin, calcification is characterized by the appearance of dark blue granules in the cytoplasm of neurons. Irreversible damage to neurons during their calcification develops through apoptosis or necrosis.

Remodeling (morphological changes) of chromatin. Chromatin in the nucleus of neurons during histological examination was represented by very small granules (euchromatin) or large aggregates (heterochromatin). The localization of chromatin in the nucleus varied. In some nuclei it was located throughout the entire area of the nucleus, while in others it was concentrated in the region of the inner nuclear membrane. When a neuron was damaged, chromatin changed intensity of staining, chromatin clumps became hypochromic, and during cell necrosis, chromatin was not stained with nuclear dyes. (Fig. 2, *c*). The chromatin of the nuclei contained despiralized forms of chromosomes responsible for the implement genetic information. Its chemical basis is deoxyribonucleoproteins — a complex of DNA with histone and non-histone proteins. Proteins make up a significant part of the chromosome substance, as well as performing a structural function, providing spatial organization of DNA in chromosomes.

Fig. 1. Damage to neurons of the human cerebral cortex in subarachnoid hemorrhages (*a, b, d, e*) and COVID-19 (*c*), magnification 400.

Note. *a* — Neurons of the 5th layer of the human cerebral cortex. Arrows show the displacement (decentralization) of neuronal nuclei. Hematoxylin and eosin staining. b — Arrows show that in some neurons the nucleoli are not stained. Nissl staining. *c* — Nucleoli are stained blue, indicating an acidic reaction. Staining with luxol blue and cresyl violet. *d* — Tigrolysis (black arrow), dark neurons (green arrow). Staining with Nissl. *e* — Lipofuscinosis of neurons. Staining with hematoxylin and eosin.

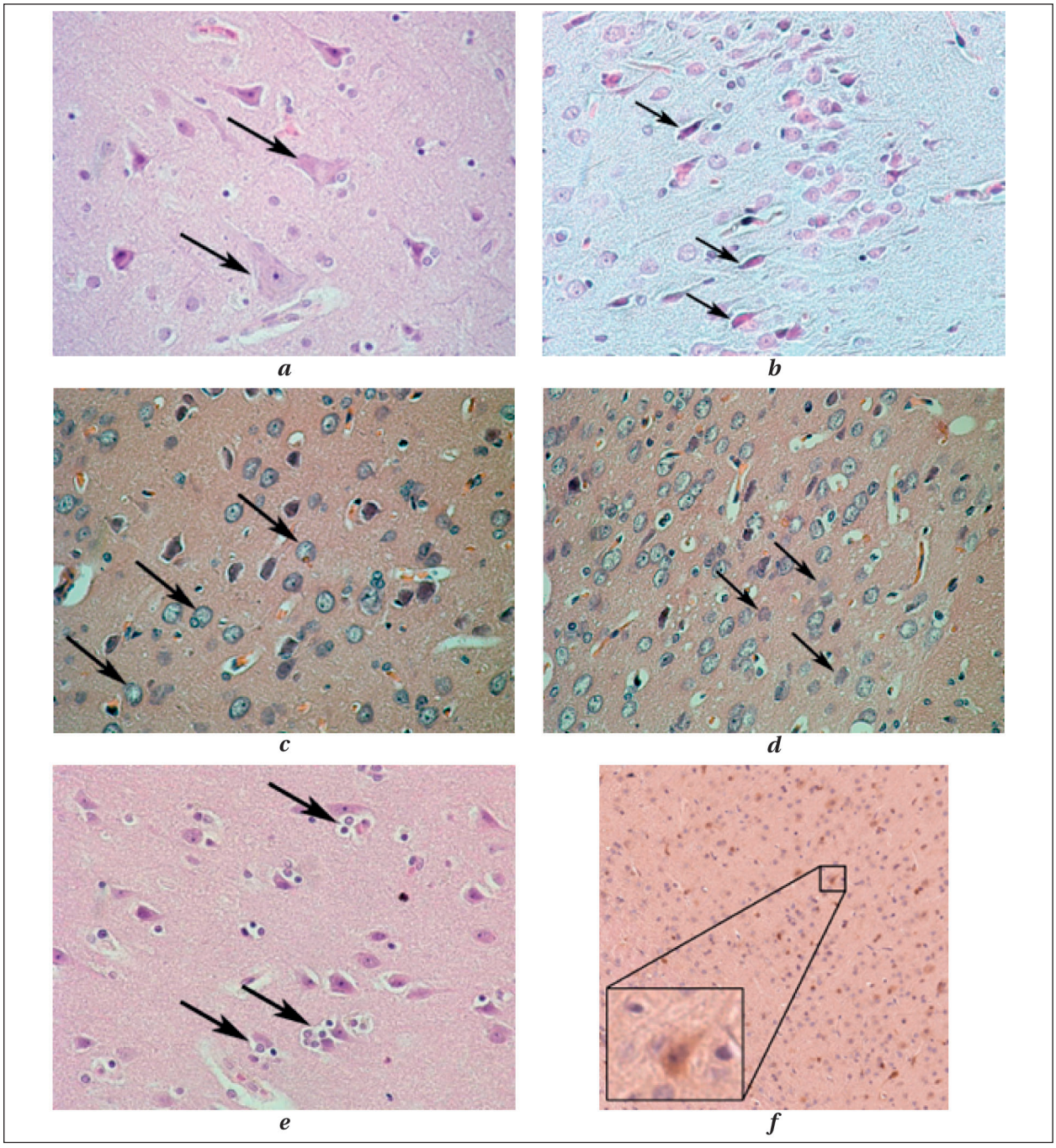

Fig. 2. Neuronal damage of the cerebral cortex of rats in cases of poisoning with clozapine in combination with alcohol (*a–e*) and in cases of circulatory arrest (*f*).
Note. *a–e*: hematoxylin and eosin staining. *a* — 5th layer of the cerebral cortex. Edema (swelling) of neurons. Magnification 400. *b* — 2–3rd layers of the cerebral cortex. Dark deformed neurons. Magnification 200. *c* — Chromatin of nuclei is not stained. Magnification 200. *d* — Necrosis of neurons, shadow cells. Chromatin is not stained. Magnification 200. *e* — Neuronophagia. Magn. 400. *f* — Circulatory arrest. Neurons with positive IHC reaction to Cas-3. Magn. 200

Necrosis. Necrosis is one of the irreversible types of neuronal damage. During necrosis, the integrity of the cells is preserved (unlike apoptosis, in which the cell is fragmented with the formation of apoptotic bodies). The neuron nucleus was not stained with nuclear dyes as a result of damage to nucleic acids. The cells turned into shadow cells, which were difficult to distinguish during microscopic examination. Karyolysis characterized the transition from necrobiosis to necrosis proper and was verified by hematoxylin and eosin staining (Fig. 2, *d*).

Phagocytosis of neurons (neuronophagy). Neuronophagy, as a variant of lethal cell damage, was caused by contact of a neuron with microglial

cells (satellitosis). Subsequently, microglia penetrate into the cytoplasm of the neuron, completing the process of phagocytosis. During histological examination, successive stages of this process were recorded (Fig. 2, *e*).

Apoptosis. During apoptosis, the neuron disintegrated into separate apoptotic bodies limited by the plasmalemma. Morphological changes in the early stages of apoptosis were not expressed and were associated with the activity of molecular factors — caspase-3, etc. Chromatin condensation, nuclear fragmentation, cell compaction and blebbing (the appearance of protrusions on the cell surface) were manifested in later stages of apoptosis (Fig. 2, *f*).

Discussion

Mechanisms of development of the considered morphological changes and their functional significance.

Decentralization of the core. Migration of nuclei in postmitotic neurons, remodeling of cell structure are caused by the interaction of the cytoskeleton and associated proteins present on the plasma membrane, which not only determine the shape of the cell, but also regulate intracellular transport [5].

Cell migration and nuclear movement within the cell are complex molecular events. In many cases, the microtubule motor proteins dynein and kinesin directly interact with the neuronal nucleus via the LINC (linker of the nucleoskeleton and cytoskeleton) complex, a protein complex associated with both the inner and outer membranes of the nucleus, and drive directional nuclear movement. Microtubule motors act on small points on the nuclear envelope through assembly with the LINC complex, directing the nucleus in a specific direction. Notably, dynein and kinesin are not simply segregated into exclusive microtubule «lanes» but can synergistically drive unidirectional nuclear movement along uniformly oriented microtubules. Such coordinated activity of opposing motors is particularly important for nuclear migration in narrow spaces. In addition, actomyosin contractility influences nuclear deformation and movement. Unlike the control forces of microtubule motors, actomyosin acts on a large area of the cell and nucleus, leading to nuclear deformation and its translocation. Actomyosin affects intracellular transport and cell shape [6].

Thus, the movement of the nucleus in the cell indicates changes in the cytoskeleton and nucleoskeleton, which underlie functional disorders of the neuron. The most important functions of cells, such as phagocytosis, pinocytosis, chemotaxis are entirely associated with damage to the cytoskeleton. Changes in the cytoskeleton of neurons disrupt the functioning of synapses, energy metabolism and RNA transport, and also contribute to protein aggregation and irreversible alteration of nerve cells [7].

Morphological changes in the nucleolus of the neuron nucleus. In addition to the «traditional» role of rRNA synthesis and ribosome assembly, the nucleolus controls physiological processes in the cell and homeostasis. The function of the nucleolus is essential for the vital activity of neurons and its features differ between cell types. The function of the nucleolus is also critical in the presence of damaging factors, since it controls mitochondrial activity and stress signaling pathways [8].

The nucleolus is the major site of ribosomal subunit biogenesis in eukaryotic cells. Specific chromosomal structures known as nucleolar organizing zones are formed in association with ribosomal DNA genes. The presence of proteins unrelated to ribosomal subunit production suggests additional functions for the nucleolus, such as regulation of mitosis, cell cycle progression, stress response, and biogenesis of various ribonucleoprotein complexes [9].

In interphase cells, ribosomal DNA (rDNA) is localized inside and near the nucleoli, and its location indicates the transcriptional activity of ribosomal genes — inactive rDNA outside, and active inside. Moreover, the nucleolus itself acts as a spatial organizer of chromatin. Microscopic studies make it possible to study the spatially different localization of various DNA populations in relation to the nucleolar structure [10].

Inhibition of neuronal RNA polymerase-1, which transcribes rRNA (transfer of genetic information from DNA to RNA) [11], leads to structural disruption of the nucleolus and apoptosis.

Measurements of nucleolar diameter and nucleolar PARP-1 (nuclear protein (ADP-ribose) polymerase-1, which regulates gene expression) content in the hippocampus of people with cognitive impairment showed a decrease in the diameter of neuronal nucleoli and a decrease in the number of nucleoli containing PARP-1. These studies indicate that disruption of nucleolar shape and function is an early and important feature in the progression of cognitive impairment [12].

Nissl substance: morphological changes. One of the variants of neuronal damage is tigrolysis — dust-like decay of Nissl substance, detected in cortical neurons 20 minutes after a 4-minute cessation of blood flow. Disturbances in protein synthesis are of exceptional importance in the process of development of neuronal alteration in cerebrovascular diseases. At the same time, ribosome biogenesis affects the stimulation of neuronal recovery after a stroke [13].

Under stress, the basis of protein synthesis disruption is a change in rRNA processing. Stress

promotes the breakdown of tRNA (transport RNA that delivers amino acids to ribosomes that synthesize proteins, which leads to the cessation of ribosome formation). These events, developing at the molecular level, contribute to the suppression of protein translation (implementation of the amino acid sequence in the synthesized protein molecule) [14].

Neuronal edema. A decrease in plasma osmolarity causes rapid water uptake by astrocytes but not neurons. Astrocytes osmotically swell because they express functional water channels (aquaporins), whereas neurons lack functional aquaporins. However, neuronal edema develops when blood flow to the brain is disrupted (cytotoxic edema), such as in strokes, sudden cardiac arrest, or traumatic brain injury. Ischemic neuronal edema is not osmotic but results from depolarization due to dysfunction of the ATP-dependent sodium/potassium ATPase (Na^+/K^+ pump). In addition, ion/water cotransporters and the amino acid water pump are involved in ischemia [15].

The resistance of pyramidal neurons to osmotic swelling is explained by the absence of functional AQP4 water channels. Neurons are not osmoresistant, and their swelling is controlled by an AQP4-independent mechanism [16].

Cerebral edema impairs cerebral perfusion and may lead to transtentorial herniation. The blood-brain barrier plays an important role in maintaining a stable microenvironment of the central nervous system. In ischemic stroke, disruption of the blood-brain barrier structures leads to increased paracellular permeability, which promotes extravasation of blood components and causes vasogenic cerebral edema. The glymphatic system and meningeal lymphatic vessels provide a channel for the penetration of cerebrospinal fluid into the brain [17].

Following acute CNS injury, cells of the neurovascular unit undergo pre- and posttranscriptional changes in the activity of ion channels and transporters. These changes result in inadequate ion transport and the generation of abnormal osmotic forces, which ultimately manifest as cerebral edema [18].

Dark neurons. The hyperchromic dark neuron is a cell with active protein synthesis, in which irreversible alteration processes develop under prolonged and intense exposure to unfavorable factors [19].

Dark neurons resulting from alteration must be differentiated from artificial (artifactual) dark neurons damaged during fixation, wiring and staining, in which there were no damage processes during life. It has been shown that the number of artificial neurons increases with non-compliance with the methods of fixation of preparations: namely, replacing 4% buffered paraformaldehyde solution with immersion. An important feature of artifactual neurons is isomorphism [20].

Most of the altered neurons are at the stage of reversible changes. The structure of some dark neurons in the cerebral cortex of rats was restored within 2 days as a result of hypoglycemic seizures. Non-restoring dark neurons were removed from the cortex in two different ways. If neurons were present in an undamaged environment, they were removed by apoptosis, and neurons present in a damaged environment were removed by necrosis [21].

One hypothesis explains the formation of dark neurons by the sol-gel transition of the cytoplasm of compacted neurons. Changes in the molecular composition of the glycocalyx lead to a decrease in the volume of the neuron as a result of the effect on the cytoskeleton, the nucleus, the membrane of which is associated with the cytoskeleton, and actin. As a result, contraction of the cytoskeleton and increase in intracellular pressure leads to loss of water and shrinkage of neurons. Another hypothesis explains the phenomenon of spreading dark neurons through dendritic connections. Research provides evidence indicating the presence of physical contact at the synaptic zone. The presynaptic and postsynaptic membranes of dendrites are linked by β neurexin and neuroligin. The intercellular regions of these adhesive proteins provide a connection between the presynaptic zone and the postsynaptic densification. This type of connection provides for rapid intercellular interaction as a result of actin polymerization of two closely located neurons. It is suggested that the role of β neurexin-neuroligin is to polymerize actin and transmit information from one neuron to neighboring neurons, which forms new populations of dark neurons [22].

Calcification of neurons. In a cohort of 1130 patients with acute ischemic stroke, hippocampal calcification was detected on CT scans. Hippocampal calcification was detected in 381 (34%) patients. The prevalence increased with age from 8% at age ⩽40 years to 45% at age ⩾80 years [23].

Photodynamic effects on neurons and glial cells, causing oxidative stress and ischemic damage, are accompanied by a violation of calcium homeostasis. Oxidative stress and ischemia-induced processes in nervous tissue lead to an apoptotic or necrotic scenario of cell death [24].

Reperfusion carries a risk of acute calcium-dependent damage to the blood-brain barrier, however, its mechanism is unknown. Measurement of the activity of NADPH-oxidase type 5 (NOX5), a calcium-activated enzyme that generates ROS, showed that reoxygenation or calcium overload increases ROS levels in the brain in a NOX5-dependent manner *in vivo*, post-ischemic ROS generation, infarct volume, and functional outcomes were wors-

ened in mice by NOX5-KI activation. Pharmacological inhibition of NOX5 prevented acute reoxygenation-induced injury [25].

Remodeling (morphological changes) of chromatin. Chromatin is formed by despiralized forms of chromosomes in a non-dividing nucleus, implementing genetic information. The chemical basis of chromatin is deoxyribonucleoprotein — a complex of DNA with histone and non-histone proteins. Chromosome proteins account for about 65% of the mass of these structures. The content of non-histone proteins in chromosomes is significantly less than histones, but they are extremely diverse (more than 100 fractions). Morphologically, heterochromatin and euchromatin (open chromatin) are distinguished, differing in functional properties. Based on the morphological features of chromatin (its shape and location), various types of neurons can be catogorized [26].

Regulation of chromatin by epigenetic mechanisms plays a central role in gene expression. Aberrant chromatin regulation observed in many diseases is due to defects in epigenetic gene regulation, which leads to abnormal gene expression programs. These defects are caused by mutations in genes encoding enzymes that modify DNA, histones, and shape chromatin architecture [27].

Chromatin is an active participant in the DNA repair process. Changing the patterns of histone modifications formed by numerous histone-modifying enzymes and chromatin remodeling are key to high-quality DNA repair [28].

Regulation of open chromatin formation is an important mechanism for controlling gene expression patterns. Genome-wide studies of various cell tissues, including cells of the nervous system, have revealed tissue- and cell-type-specific landscapes of chromatin accessibility [29].

Hypoxia, inadequate nutrient supply cause chromatin compaction associated with ATP depletion. The mobility of the linker histone H1 is significantly reduced. Studies illustrate the ability of chromatin architecture to physically respond to environmental conditions, directly link cellular energy status to chromatin compaction, and provide insight into the effects of ischemia on cellular nuclear architecture [30].

Chromatin structure varies across cell types, with neuronal chromatin showing greater regional variability than other cells [31].

Enzymes and metabolites can modulate chromatin by regulating the activity of chromatin proteins, including histone-modifying enzymes. Dysregulation of this metabolic activity has been implicated in cerebrovascular diseases, among others [32].

In the mammalian cell nucleus, a clear spatial separation of active euchromatic and inactive heterochromatic genomic regions is observed. In normal nuclei, as shown by microscopy, euchromatin is localized inside the nucleus, and heterochromatin is located at the periphery of the nucleus. Interactions with the nuclear lamina are necessary for constructing an architecture from separated chromatin phases [33].

Euchromatin spatially organized into transcriptionally inactive domains interspersed with foci of transcriptional activity. RNA induces the formation of transcriptional pockets that displace transcriptionally inactive chromatin [34].

Lipofuscinosis (acquired). Lipofuscin formation is promoted by oxidative stress, aging and other factors. Accumulation of oxidized protein aggregates and highly cross-linked materials such as lipofuscin affects cell viability. Postmitotic neurons cannot remove lipofuscin via phagocytosis and autophagy, which accumulates as endocytoplasmic granules in the cell cytoplasm, impairing neuronal function. In addition to being a potent source of oxidants, lipofuscin induces apoptosis. The cytotoxicity of lipofuscin is closely related to the presence of iron in the material. As with the formation of other large protein aggregates, the process responsible for their engulfment and degradation is macroautophagy. Autophagosomes and lysosomes are the storage sites for this type of biomolecular aggregate, contributing to the mitigation of their cytotoxicity [35].

The presence of lipofuscin in neurons coexists with its localization in microglia. Glial cells deposit lipofuscin clusters in pericapillary areas, which has a negative impact on the homeostasis of neurons and glia [36].

An increase in the lipofuscin content in neurons is associated with the aging process. At the same time, pigment formation has been demonstrated not only in old but also in young animals, as well as in individuals subjected to stress, dietary and environmental interventions. Electron microscopic studies on animals have shown significant variability in the structure of individual lipofuscin granules, but the presence of «transparent vacuoles» surrounded by a single membrane is one of the characteristic features of neuronal lipofuscin in older people [37].

Lipofuscin, being a photosensitizer, potentiates intracellular dyshomeostasis, playing a decisive role in inhibiting the function of the proteasome (a multiprotein complex that carries out proteolysis of defective proteins), activating mitophagy, autophagy, disrupting lysosomal stability and producing reactive oxygen species [38].

Isolated lipofuscin aggregates containing elevated concentrations of proline, calcium, and iron cause cellular damage via a pyroptosis-like mechanism. Lipofuscin activates mitochondrial ROS production and induces lysosomal dysfunction via alterations in the lysosomal membrane, resulting in

decreased lysosome numbers and impaired cathepsin D activity. CTSD gene deficiency is considered to be the main cause of neuronal lipofuscinosis [39].

Necrosis. It was believed that necrosis in stroke, traumatic brain injury, has no genetic regulation. Modeling of neuronal injury by calcium overload revealed that JIL-1/mitogen — and stress-activated proteinkinase-1, 2 are regulators of neuronal necrosis through phosphorylation of serine 28 of histone H3 (H3S28ph). In addition, activation of Trithorax (Trx) was identified. To test the role of the JIL-1/PRC1/Trx cascade in mammals, glutamate-induced necrosis was studied in rat cortical neuron cultures and in models of cerebral ischemia. It was found that the cascade is activated under these conditions, and inhibition of the cascade suppresses necrosis both *in vitro* and *in vivo* [40].

It has been established that responses to damage, including DNA repair, DNA methylation and autonomous mechanisms of neuronal necrosis, are different in humans and experimental animals [41].

RNA plays an important role in the mechanisms of neuronal damage. RNA-binding proteins are crucial for the regulation of RNA processing and transport. RNA processing defects are increasingly recognized as critical determinants of neurological diseases. These mechanisms underlie changes in neuronal function, increased susceptibility of neurons to the influence of damaging factors, changes in RNA expression, where RNA-binding proteins play a central role in maintaining neuronal function and morphology [42].

One of the variants of necrotic damage to neurons is ferroptosis, which develops when the balance of free iron and lipid peroxidation is disrupted. This process leads to the disruption of the structure and functions of plasma membranes. Morphological manifestations of ferroptosis in nervous tissue are a decrease in the number of mitochondria, compaction, and (or) disorganization of the cristae mitochondria, rupture of their outer membrane, and an increase in the density of internal membranes. The etiological factor of ferroptosis is a deficiency of GPx4 (Glutathione peroxidase 4, glutathione peroxidase 4), which is necessary for the reduction of toxic lipid peroxides. In ischemic stroke, when blood flow to the brain is limited, there is increased iron absorption, oxidative stress, and disruption of the integrity of the blood-brain barrier. An imbalance of proteins involved in the transport and storage of iron increases lipid oxidation and contributes to neuronal damage, indicating the possibility of brain cell death, especially neurons, as a result of ferroptosis [43].

Phagocytosis of neurons (neuronophagy). Following stroke, neurons undergo damage due to ongoing ischemia and excitotoxicity. They release «find me» (ATP), «eat me» (phosphatidylserine) signals that bind to the opsonins complement components C1q and C3b, inducing microglia to phagocytose damaged neurons. Blocking these neuronal factors or microglial phagocytic receptors prevents delayed neuronal loss and behavioral impairment in rodent models of ischemic stroke [44].

Microglia engulf and remove opsonized and non-opsonized targets such as pathogens, apoptotic cells, and cellular debris. Phagocytosis is also critical in neural development, homeostasis, and repair mechanisms [45]. In addition to the microglia, astrocytes have been shown to respond to neuronal injury [46].

Apoptosis. There are two types of apoptosis: extrinsic (caspase-dependent) and intrinsic (non-caspase-related). The intrinsic pathway is triggered by intracellular factors that detect DNA damage, the presence of viral pathogens, or respond to the absence of external signals from other cells. In contrast, the extrinsic pathway of apoptosis is triggered by an external signal, most often from natural killer (NK) cells or CD8-positive cytotoxic T lymphocytes (CTLs). The extrinsic pathway of apoptosis induction begins with the binding of specific ligands (TNFα, FASL, etc.) to plasma membrane receptors whose cytoplasmic regions contain death domains. The resulting complex of molecules is called the Death Inducing Signaling Complex (DISC). Subsequent activation of caspase-8 leads to activation of effector caspases 3 and 7 and subsequent irreversible cell damage [47].

The internal triggering of apoptosis is associated with mitochondria, changes in their membrane potential and the release of pro-apoptotic proteins of the Bcl-2 family. It depends on the activation and release of cytochrome C, flavoprotein AIF (apoptosis-inducing factor), and procaspase-2 into the cytoplasm. The causes of the release of intracellular apoptotic signals by a damaged cell are varied: hypoxia, radiation, viral infection, increased intracellular calcium concentration, etc. Mitochondria also play an important role in other forms of cell damage: pyroptosis, ferroptosis and necroptosis [48].

Conclusion

The proposed morphological classification of neuronal damage is based on the structural changes in nerve cells detected by histological, histochemical and immunohistochemical methods.

Taking into account the unity of structure and function, we examined functional disorders that arise during neuron alteration. In particular, the displacement of the nucleus is caused by damage to the cytoskeleton of neurons. Morphological changes in the nucleoli are associated with a violation of the synthesis of ribosome subunits. A decrease or absence of staining of the Nissl substance indicates a violation of the synthesis of ribonucleoproteins.

Dark neurons indicate the accumulation of protein products in the cytoplasm of cells and a violation of their utilization. Chromatin remodeling leads to violations of DNA repair, synthesis processes, etc. Lipofuscin is a marker of neuronal damage, activates apoptosis, damages lysosomes. Calcinosis promotes the formation of active oxygen species. Neuronophagia, necrosis, and apoptosis are irreversible forms of neuronal damage.

The proposed morphological classification of neuronal damage complements existing classifications that primarily take into account molecular mechanisms of damage.

References

1. *Ермохин П. Н.* Гистопатология центральной нервной системы. Под редакцией академика АМН СССР проф. *А. П. Авцина*. М.: «Медицина»; 1969: 245. УДК 616.831/832-001.8 (084.4). *Yermokhin P. N.* Histopathology of the central nervous system. Ed. by prof. A. P. Avtsyn, member of the USSR Academy of Medical Sciences. M.: Meditsina; 1969: 245. UDC 616.831/832-001.8 (084.4). (in Russ.).
2. *Clarke G. D.* Developmental cell death: morphological diverciti and multiple mechanisms. *Anatomy Embryology (Berl)*. 1990; 181: 195–201. DOI: 10.1007/BF00174615. PMID: 2186664.
3. *Kroemer G., El-Deiry W. S., Golstein P.* Nomenclature Committee on Cell Death Classification of cell death: recommendations of the Nomenclature Committee on Cell Death. *Cell Death Differentiation*. 2005; 2: 1463–1467. DOI: 10.1038/sj.cdd.4401724. PMID: 16247491.
4. *Galluzzi L., Vitale I., Abrams J. M., Alnemri E. S., Baehrecke E. H., Blagosklonny M. V., Dawson T. M., et al.* Molecular definitions of cell death subroutines: recommendations of the Nomenclature Committee on Cell Death. *Cell Death & Differentiation*. 2012; 19: 07–120. DOI: 10.1038/cdd.2011.96. PMID: 21760595.
5. *Di Giaimo R., PennaE., Pizzella A., Cirillo R., Perrone-Capano C., Crispino M.* Cross talk at the cytoskeleton–plasma membrane interface: impact on neuronal morphology and functions. *Int J Mol Sci*. 2020; 21 (23): 9133. DOI: 10.3390/ijms21239133. PMID: 33266269.
6. *Kengaku M.* Cytoskeletal control of nuclear migration in neurons and non-neuronal cells. *Proc Jpn Acad Ser B Phys Biol Sci*. 2018; 94 (9): 337–349. DOI: 10.2183/pjab.94.022. PMID: 30416174.
7. *Wilson D. M., Cookson M. R., Van Den Bosch L., Zetterberg H., Holtzman D. M., Dewachter I.* Hallmarks of neurodegenerative diseases. *Cell*. 2023; 186: 693–714. DOI: 10.1016/j.cell.2022.12.032. PMID: 36803602.
8. *Parlato R., Kreiner G.* Nucleolar activity in neurodegenerative diseases: a missing piece of the puzzle? *J Mol Med (Berl)*. 2013; 91 (5): 541–547. DOI: 10.1007/s00109-012-0981-1. PMID: 23179684.
9. *Dubois M.-L., Boisvert F.-M.* The nucleolus: structure and function. In the book: The Functional Nucleus. David P. Bazett-Jones, Graham Dellaire. (eds.). Springer Nature Link; 2016: 29–49. DOI: 10.1007/978-3-319-38882-3_2.
10. *Schufer C., Weipoltshammer K.* Nucleolus and chromatin. *Histochem Cell Biol*. 2018; 150 (3): 209–225. DOI: 10.1007/s00418-018-1696-3. PMID: 30046888.
11. *Slomnicki L. P., Hallgren J., Vashishta A., Smith S. C., Ellis S. R., Hetman M.* Proapoptotic requirement of ribosomal protein L11 in ribosomal stress-challenged cortical neurons. *Mol Neurobiol*. 2018; 55 (1): 538–553. DOI: 10.1007/s12035-016-0336-y. 14. PMID: 27975169.
12. *Regier M., Liang J., Choi A., Verma K., Libien J., Hernández A. I.* Evidence for decreased nucleolar PARP-1 as an early marker of cognitive impairment. *Neural Plast*. 2019; 2019: 4383258. DOI: 10.1155/2019/4383258. PMID: 31827497.
13. 13. *Wang X., Zhang X. Y., Liao N. Q., He Z.H., Chen Q. F.* Identification of ribosome biogenesis genes and subgroups in ischaemic stroke. *Front Immunol*. 2024; 15: 1449158. DOI: 10.3389/fimmu.2024.1449158. PMID: 39290696.
14. *Chen Q. M.* The Odds of protein translation control under stress. *Antioxid Redox Signal*. 2024; 40 (16–18): 943–947. DOI: 10.1089/ars.2023.0478. PMID: 38573012.
15. *Hellas J. A., Andrew R. D.* Neuronal swelling: a non-osmotic consequence of spreading depolarization. *Neurocrit Care*. 2021; 35 (Suppl 2): 112–134. DOI: 10.1007/s12028-021-01326-w. PMID: 34498208.
16. *Murphy T. R., Davila D., Cuvelier N., Young L.R, Lauderdale K., Binder D. K., Fiacco T. A.* Hippocampal and cortical pyramidal neurons swell in parallel with astrocytes during acute hypoosmolar stres. *Front Cell Neurosci*. 2017; 11: 275. DOI: 10.3389/fncel.2017.00275. PMID: 28979186.
17. *Chen S., Shao L., Ma L.* Cerebral edema formation after stroke: emphasis on blood-brain barrier and the lymphatic drainage system of the brain. *Front Cell Neurosci*. 2021; 15: 716825. DOI: 10.3389/fncel.2021.716825. PMID: 34483842.
18. *Stokum J. A., Gerzanich V., Simard J. M.* Molecular pathophysiology of cerebral edema. *J Cereb Blood Flow Metab*. 2016; 36 (3): 513–538. DOI: 10.1177/0271678X15617172. PMID: 26661240.
19. *Зиматкин С. М. Бонь Е. И.* Темные нейроны мозга. *Морфология*. 2017; 152 (6): 81–86. *Zimatkin S. M., Bon E. I.* Dark neurons of the brain. *Morphollogy = Morfologiya*. 2017; 152 (6): 81–86. (in Russ.). DOI: 10.17816/morph.398200.
20. *Авдеев Д. Б., Степанов С. С., Горбунова А. В., Шоронова А. Ю., Макарьева Л. М., Акулинин В. А., Коржук М. С., Заболотных М. В.* Темные нейроны сенсомоторной коры белых крыс после острой неполной ишемии в аспекте артефактов фиксации и нейроглиальных взаимоотношений. *Журнал анатомии и гистопатологии*. 2021; 10 (2): 9–20. *Avdeev D. B., Stepanov S. S., Gorbunova A. V., Shoronova A.Yu., Makar'eva L.M., Akulinin V. A., Korzhuk M. S., Zabolotnykh M. V.* Dark Neurons of the Sensorimotor Cortex of White Rats after Acute Incomplete Ischemia in Terms of Artifacts Fixation and Neuroglial Relationships. *Journal of Anatomy and Histopathology = Zhurnal Anatomii i Gistopatologii*. 2021; 10 (2): 9–22. (In Russ.). DOI: 10.18499/2225-7357-2021-10-2-9-22.
21. *Gallias F., CsordasA., Schwartz A., Mazlo M.* «Dark» (compacted) neurons may not die in a necrotic manner. *Exp Brain Res*. 2005; 160 (4): 473–86. DOI: 10.1007/s00221-004-2037-4. PMID: 15480602.
22. *Ahmadpour S., Behrad A., Fernández-Vega I.* Dark neurons: a protective mechanism or a mode of death. *Journal of Medical Histology*. 2019; 3 (2): 125–131. DOI: 10.21608/jmh.2020.40221.1081.
23. *Kockelkoren R., De Vis J. B., Stavenga M., Mali W. P. Th. M., Hendrikse J., Rozemuller A. M., Koek H. L., et al,* the DUST study group. Hippocampal calcification on brain CT: prevalence and risk factors in a cerebrovascular cohort. *Eur Radiol*. 2018; 28 (9): 3811–3818. DOI: 10.1007/s00330-018-5372-8. PMID: 29619516.

24. *Дзреян В. А., Хайтин А. М., Демьяненко С. В.* Нарушение кальциевого гомеостаза и ответные изменения в кальциевой сигнализации нейронов и глиальных клеток при фотодинамическом воздействии. *Биологические мембраны: Журнал мембранной и клеточной биологии.* 2022; 39 (4): 283–291. *Dzreyan V. A., Khaitin A. M., Demyanenko S. V.* Disruption of calcium homeostasis and following changes in calcium signaling in neurons and glial cells in response to photodynamic treatment. *Biological Membranes: Journal of Membrane and Cell Biology = Biologicheskiye Membrany: Zhurnal Membrannoy i Kletochnoy Biologii.* 2022; 39 (4): 283–291. (in Russ.). DOI: 10.31857/S0233475522040041.
25. *Casas A. I., Kleikers P.Wm., Geuss E., Langhauser F., Adler T., Busch D. H., Gailus-Durner V., et al.* Calcium-dependent blood-brain barrier breakdown by NOX5 limits postreperfusion benefit in stroke. *J Clin Invest.* 2019; 129 (4): 1772–1778. DOI: 10.1172/JCI124283. PMID: 30882367.
26. *Winick-Ng W., Kukalev A., Harabula I., Zea-Redondo L., Szabó D., Meijer M., SerebreniL., et al.* Cell-type specialization is encoded by specific chromatin topologies. *Nature.* 2021; 599 (7886): 684–691. DOI: 10.1038/s41586-021-04081-2. PMID: 34789882.
27. *Mirabella A. C., Foster B. M., Bartke T.* Chromatin deregulation in disease. *Chromosoma.* 2016; 125: 75–93. DOI: 10.1007/s00412-015-0530-0. PMID: 26188466.
28. *Aleksandrov R., Hristova R., Stoynov S., Gospodinov A.* The chromatin response to double-strand DNA breaks and their repair. *Cells.* 2020; 9 (8): 1853. DOI: 10.3390/cells9081853. PMID: 32784607.
29. *Su Y., Shin J., Zhong C., Wang S., Roychowdhury P., Lim J., Kim D., et al.* Neuronal activity modifies the chromatin accessibility landscape in the adult brain. *Nat Neurosci.* 2017; 20 (3): 476–483. DOI: 10.1038/nn.4494. PMID: 28166220.
30. *Kirmes I., Szczurek A., Prakash K., Charapitsa I., Heiser C., Musheev M., Schock F., et al.* A transient ischemic environment induces reversible compaction of chromatin. *Genome Biol.* 2015; 16: 246. DOI: 10.1186/ s13059-015-0802-2. PMID: 26541514.
31. *Fullard J. F., Hauberg M. E., Bendl J., Egervari G., Cirnaru M.-D., Reach S. M., Motl J., et al.* An atlas of chromatin accessibility in the adult human brain. *Genome Res.* 2018; 28 (8): 1243–1252. DOI: 10.1101/gr.232488.117. PMID: 29945882.
32. *Li X., Egervari G., Wang Y., Berger S. L., Nat Z. L.* Regulation of chromatin and gene expression by metabolic enzymes and metabolites. *Nat Rev Mol Cell Biol.* 2018; 19 (9): 563–578. DOI: 10.1038/s41580-018-0029-7. PMID: 29930302.
33. *Falk M., Feodorova Y., Naumova N., Imakaev M., Lajoie B. R., Leonhardt H., Joffe B., et al.* Heterochromatin drives compartmentalization of inverted and conventional nuclei. *Nature.* 2019; 570 (7761): 395–399. DOI: 10.1038/s41586-019-1275-3. PMID: 31168090.
34. *Hilbert L., Sato Y., Kuznetsova K., Bianucci T., Kimura H., Jülicher F., Honigmann A., et al.* Transcription organizes euchromatin via microphase separation. *Nat Commun.* 2021; 12: 1360. DOI: 10.1038/s41467-021-21589-3. PMID: 33649325.
35. *Di Guardo* G. Lipofuscin, lipofuscin-like pigments and autofluorescence. *Eur J Histochem.* 2015; 59 (1): 2485. DOI: 10.4081/ejh.2015.2485. PMID: 25820564.
36. *Riga D., Riga S., Halalau F., Schneider F.* Brain lipopigment accumulation in normal and pathological aging. *Ann N Y Acad Sci.* 2006; 1067: 158–163. DOI: 10.1196/annals.1354.019. PMID: 16803981.
37. *Glees P., Hasan M.* Lipofuscin in neuronal aging and diseases. *Norm Pathol Anat (Stuttg).* 1976; 32: 1–68. PMID: 639413.
38. *Snyder A. N., Crane J. S.* Histology, lipofuscin. 2023. In: StatPearls [Internet]. Treasure Island (FL): StatPearls Publishing; 2025. PMID: 30726043. Free Books & Documents.
39. *Baldensperger T., Jung T., Heinze T., Schwerdtle T., Höhn A., Grune T.* The age pigment lipofuscin causes oxidative stress, lysosomal dysfunction, and pyroptotic cell death. *Free Radic Biol Med.* 2024; 225: 871–880. DOI: 10.1016/j.freeradbiomed.2024.10.311. PMID: 39486751.
40. *Liu K., Ding L., Li Y., Yang H., Zhao C., Lei Y., Han S., et al.* Neuronal necrosis is regulated by a conserved chromatin-modifying cascade. *Proc Natl Acad Sci U S A.* 2014; 111 (38): 13960–13965. DOI: 10.1073/pnas.1413644111. PMID: 25201987.
41. *Martin L. J., Chang Q.* DNA damage response and repair, DNA methylation, and cell death in human neurons and experimental animal neurons are different. *J Neuropathol Exp Neurol.* 2018; 77 (7): 636–655. DOI: 10.1093/jnen/nly040. PMID: 29788379.
42. *Nussbacher J. K., Tabet R., Yeo G. W., Lagier-Tourenne C.* Disruption of RNA metabolism in neurological diseases and emerging therapeutic interventions. *Neuron.* 2019; 102 (2): 294–320. DOI: 10.1016/j.neuron.2019.03.014. PMID: 30998900.
43. *Delgado-Martín S., Martínez-Ruiz A.* The role of ferroptosis as a regulator of oxidative stress in the pathogenesis of ischemic stroke. *FEBS Lett.* 2024; 598 (17): 2160–2173. DOI: 10.1002/18733468.14894. PMID: 38676284.
44. *Brown G. C.* Neuronal loss after stroke due to microglial phagocytosis of stressed neurons. *Int J Mol Sci.* 2021; 22 (24): 13442. DOI: 10.3390/ijms222413442. PMID: 34948237.
45. *Galloway D. A., Phillips A. E. M., Owen D. R. J., Moore C. S.* Phagocytosis in the brain: homeostasis and disease. *Front Immunol.* 2019; 10: 790. DOI: 10.3389/fimmu.2019.00790. PMID: 31040847.
46. *Wakida N. M., Cruz G. M. S., Ro C. C., Moncada E. G., KhatibzadehN., Flanagan L. A., Berns M. W.* Phagocytic response of astrocytes to damaged neighboring cells. *PLoS One.* 2018; 13 (4): e0196153. DOI: 10.1371/journal.pone.019615.
47. *Yanumula A., Cusick J. K.* Biochemistry, extrinsic pathway of apoptosis. In: StatPearls [Internet]. Treasure Island (FL): StatPearls Publishing; 2025. PMID: 32809646. Free Books & Documents.
48. *Glover H. L., Schreiner A., Dewson G., Tait S. W. G.* Mitochondria and cell death. *Nat Cell Biol.* 2024; 26 (9): 1434–1446. DOI: 10.1038/s41556-024-01429-4. PMID: 38902422.

Received 26.05.2025
Accepted 30.06.2025
Online first 29.09.2025

https://doi.org/10.15360/1813-9779-2025-5-2579

Predictive Markers of Functional Outcome in Subtypes of Ischemic Stroke

Anastasia M. Tynterova*, Ekaterina M. Moiseeva,
Matvey S. Khoymov, Natalya N. Shusharina

Imannuel Kant Baltic Federal University,
14 Aleksandr Nevsky Str., 236041 Kaliningrad, Russia

For citation: *Anastasia M. Tynterova, Ekaterina M. Moiseeva, Matvey S. Khoymov, Natalya N. Shusharina.* Predictive Markers of Functional Outcome in Subtypes of Ischemic Stroke. *Obshchaya Reanimatologiya = General Reanimatology.* 2025; 21 (5): 15–25. https://doi.org/10.15360/1813-9779-2025-5-2579 [In Russ. and Engl.]

***Correspondence to:** Anastasia M. Tynterova, antynterova@mail.ru

Summary

The aim of the study was to identify potential predictors of functional outcome (FO) in patients with subtypes of ischemic stroke (IS) who did not receive reperfusion therapy.

Materials and methods. A prospective study included 229 patients with ischemic stroke divided . into three groups based on the IS subtype: Group 1 — 84 patients with cardioembolic IS; Group 2 — 65 patients with atherothrombotic IS; Group 3 — 80 patients with lacunar IS. Changes in the modified Rankin Scale (mRS) scores were considered as FO criteria calculated as the difference between the scores on admission and on the 21st day after IS onset — △mRS. In order to optimize the performance of the machine learning (ML) model, a binary FO approach was chosen for assessment on the 21st day after IS onset: mRS ⩾ 3 scores corresponded to an unfavorable non-lethal outcome, and mRS = 0–2 scores corresponded to a favorable FO. We analyzed the interrelation with FO (correlation coefficient, r) and the predictive ability (ML (decision tree), information gain, i. g.) of 29 parameters, including demographic features; comorbidities; instrumental examination findings; NIHSS, BI, CDR scores; serum concentrations of cytokines on the 2nd day of hospital stay.

Results. The following significant ($P<0.0001$) predictors of unfavorable non-lethal FO were identified: female sex (i. g. = 0.346), recurrent IS (i. g = 0.248), diabetes mellitus (i. g. = 0.442), and CXCL2 concentration (i.g. = 0.306) in Group 1; WMHs severity (i. g. = 0.206), diabetes mellitus (i. g. = 0.340), content of CCL2 (i. g. = 0.116), CCL3 (i. g. = 0.202) and CCL23 (i. g. = 0.101) in Group 2; age (i. g. = 0.106), 2nd–3rd degree obesity (i. g. = 0.150), WMHs severity (i. g. = 0.300), CXCL5 content (i. g. = 0.143) and MIF (i. g. = 0.145) in Group 3. Concentrations of CCL25 (i. g. = 0.108) and IL-6 (i. g. = 0.401) were found as predictors of favorable FO ($P<0.0001$) in Group 1; 1st degree obesity (i. g. = 0.118) and TNF-α concentration (i. g. = 0.211) in Group 2; arterial hypertension (AH) (i. g. = 0.113) and 1st degree obesity in Group 3.

Conclusion. Study results made evident the variances in combination of factors affecting FO, depending on IS pathogenetic subtype. Despite undoubtful value of the data obtained, further research is needed to expand the potentiality in predicting acute IS outcome and confirm the relevance of identified markers.

Keywords: ischemic stroke, acute phase, functional outcome, mRS, subtypes of ischemic stroke, prognostic markers

Conflict of interest. The authors declare no conflict of interest.

Information about the authors/Информация об авторах:
Anastasia M. Tynterova/Анастасия Михайловна Тынтерова: https://orcid.org/0000-0003-1743-4713
Ekaterina M. Moiseeva/Екатерина Михайловна Моисеева: https://orcid.org/0000-0003-4052-1604
Matvey S. Khoimov/Матвей Сергеевич Хоймов: https://orcid.org/0000-0001-8056-2019
Natalia N. Shusharina/Наталья Николаевна Шушарина: https://orcid.org/0000-0002-8848-6134

Introduction

Development of early prediction methods and identification of predictors of unfavorable functional outcome (FO) in patients with acute ischemic stroke (IS) is a crucial task in era of personalized medicine [1, 2]. There's a sound body of published data on national and international research in the field of development, evaluation, and implementation of prognostic models for ischemic stroke. However, the majority of these studies focus on longitudinal evaluation of patients' disability in the recovery period and later stages of ischemic stroke [3, 4]. Very few studies have demonstrated the potential for assessing the persistence or progression of neurological and cognitive deficits occurring in the acute phase of IS [5, 6]. The insufficient validity of risk prediction models for predicting unfavorable FO in some of them originates from the limited set of traditionally considered predictor variables, such as demographic characteristics, clinical and functional indicators, and laboratory and instrumental data. Search for potential biomarkers of functional recovery in patient's immunological status sounds promising and increases the value of stratified risk prediction models for unfavorable FO. This domain is currently in the focus of intensive research, and particularly, the role of «inducible» cytokines, such as CXC and CC chemokines in the pathogenesis of

IS, and regulation of immune response during the acute phase of ischemia in addition to well-established interleukin (IL), interferon gamma (IFN-γ), and tumor necrosis factor (TNF-α) mechanisms of action.

There's a building up amount of data evidencing involvement of various chemokines into pathogenetic mechanisms underlying the development of cerebrovascular disorders, cell apoptosis, and neuro- and angiogenesis during the acute period of stroke. In this context, the most promising chemokines are the ligands of the CXCR1 and CCR1/2 receptors, strongly associated with the acute period of stroke and post-stroke FO [7, 8]. Of particular interest is the verification of factors affecting the dynamics of patients' functional status, depending on pathogenetic mechanisms underlying IS and patient's comorbidities [9]. Therefore, focusing research on comprehensive patient assessment in the acute period of stroke, followed by modeling of FO prognosis based on advanced mathematical algorithms, is a promising trajectory in the context of personalized medicine.

The aim of the study is to identify potential predictors of functional outcome in patients with ischemic stroke subtypes who did not receive reperfusion therapy.

Material and Methods

The prospective study was approved by the Independent Ethics Committee of the Clinical Research Center at Immanuel Kant Baltic Federal University (Minutes of Meeting No. 2 dated April 27, 2021, and No. 34 dated September 29, 2022). The study included 229 patients with a diagnosis of ischemic stroke undergoing treatment from January 2023 to February 2025 at the Neurology Department of the Emergency Medical Care Hospital and the Department of Medical Rehabilitation for Patients with Central Nervous System Disorders at the Central City Clinical Hospital of Kaliningrad. The sample size of the study was not precalculated. The diagnosis of IS was made based on abrupt onset (minutes, hours) of focal neurologic deficits attributable to one of the vascular territories, and lasting at least 24 hours.

Clinical signs and symptoms attributable to diagnosis of «ischemic stroke in the carotid artery territory» were set as inclusion criteria. The exclusion criteria included: reperfusion therapy; transient ischemic attack; vertebrobasilar stroke, patient's death, and development of severe complications within 21 days. Patients were selected according to the inclusion/exclusion criteria from the initial sample (*N*=508, Fig. 1).

Patients' examinations were performed within the stroke care standards to verify IS subtype according to the TOAST criteria (Trial of Org 10172 in Acute Stroke Treatment). Standardized procedures on admission included clinical neurological evaluation, brain CT/MRI, transcranial Doppler ultrasonography of extracranial and intracranial vessels, electrocardiography, and laboratory tests.

Stroke severity and activities of daily living were quantified on admission using the NIH Stroke Scale (NIHSS) and the Barthel Index (BI). The degree of cognitive decline was assessed using the Clinical Dementia Rating (CDR) scale on the 14th day of hospital stay.

The laboratory tests included assessment of serum concentrations of biologically active molecules (cytokines) in samples collected on the 2nd day of hospital stay, including chemokines (Gro-a/CXCL1, Gro-b/CXCL-2, GCP-2/CXCL6, ENA-78/CXCL5, MIP-1a/CCL3, MIP-1d/CCL15, MPIF-1/CCL23, MCP-1/CCL2, TECK/CCL25), interleukins (IL-1b, IL-6, IL-16), interferon gamma (IFN-γ), macrophage migration inhibitory factor (MIF), and tumor necrosis factor (TNFa). Concentrations were measured by flow cytometry on a two-beam laser automatic analyzer (Bio-Plex® 200 Systems, Bio-Rad, USA) using a commercial test system (Bio-Plex Human Panel, 40-Plex Assay, Bio-Rad, USA). The results were expressed in pg/ml.

The neuroimaging parameters were assessed based on magnetic resonance imaging (MRI) data

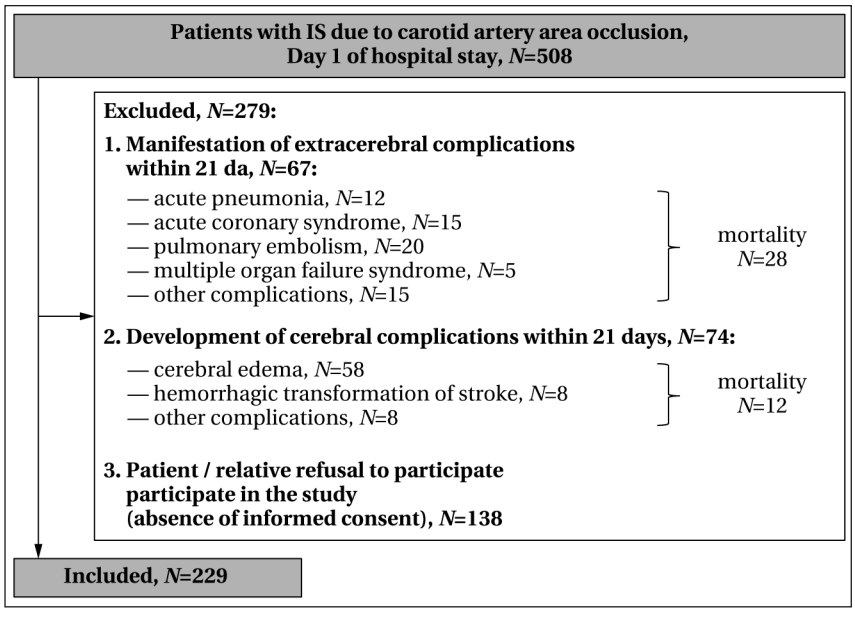

Fig. 1. Scheme of patient recruitment procedure.

(Optima MR450w 1.5T magnetic resonance scanner) using a DWI, T2* (hemo), and T2/Flair scanning protocol. White matter hyperintensity (WMH) grade was assessed using the Fazekas visual scale. The IS topography was related to the ischemic lesions in vascular territories of the anterior cerebral (ACA), middle cerebral (MCA), and anterior choroidal (AChA) arteries based on neuroimaging data.

Changes in the patient's disability index measured by the modified Rankin scale (mRS) as the difference between the mRS scores on admission and on day 21 from IS onset — △mRS were used as criteria of IS functional outcome (FO). In order to optimize the performance of the machine learning (ML) model, a binary FO approach was chosen for assessment on the 21st day after IS onset: mRS ⩾3 scores corresponded to an unfavorable non-lethal outcome, and mRS = 0–2 scores corresponded to a favorable FO.

Standard SPSS Statistics V23.0 software for Windows, the Python programming language, and the Pandas and SciPy libraries were used for statistical data processing. The distribution of quantitative variables was assessed using the Shapiro–Wilk test. Quantitative variables with a normal distribution were described using arithmetic means and standard deviations ($M\pm\sigma$). Data with a normal distribution was compared using the ANOVA test for dependent and independent samples. In case of abnormal distribution, quantitative variables were described using the median (*Me*), lower and upper quartiles [*Q1–Q3*]. The nonparametric Wilcoxon test was used when the dependent variable was not normally distributed. Quantitative variables in groups with non-normal distributions were compared using the Mann–Whitney *U* test. The Bonferroni correction was used for multiple comparisons to avoid false positives. Analysis of frequency differences in two independent groups was performed using the Fisher's exact test with two-sided confidence intervals and the χ^2 test with Yates's correction. The critical level of statistical significance was set at $P<0.05$. The Z-score was not used for rating cognitive measures by CDR scale in the absence of reference values from the control group.

For mathematical analysis, 29 parameters were selected as the initial data, and grouped into the following main categories: demographic data (age and gender); comorbidities (presence or absence of arterial hypertension, recurrent stroke, and diabetes mellitus; grade of obesity based on body mass index (BMI)); instrumental examinations data (laterality of stroke and localization of lesion, lesion size, presence of multiple lesions and WMH grade); NIHSS, BI, and CDR scores; immunological indicators, such as serum concentrations of cytokines.

To optimize dataset statistical processing, all data were classified based on their nature: continuous (cytokine concentrations, age, IS lesion size, CDR, NIHSS, and BI scores), categorical (lesion localization, WMH grade, obesity grade), and binary variables (comorbid conditions, multifocal lesions, IS lesion laterality, and gender).

The correlation coefficient (*R*) was calculated to assess the relationship of the functional outcome variables on the mRS scale with the studied indicators. The r value ranged from –1 to 1, where –1 represents a complete inverse relationship, 0 represents no relationship, and 1 represents a complete direct relationship. Biserial method was used to assess △mRS correlation with binary variables, and Spearman test — to assess the correlation with categorical and continuous variables. The conventional value of 0.05 was chosen as the threshold. When a *P*-value was less than 0.05, the significance of the correlation coefficient was considered statistically confirmed. Correlation coefficients with a *P*-value above 0.05 were excluded from consideration. Correlation analysis was performed separately for each group. In order to detect confounders — confusing variables, correlation coefficients between variables were calculated with subsequent exclusion from statistical analysis. Following the correlation analysis, variables with a correlation coefficient $R>0.300$ were selected to train mathematical analysis models based on ML algorithms. For machine learning, an algorithm for predicting the target variable value — a decision tree with a maximum depth and additional selection of features using the SelectFromModel in Python Scikit-learn library was chosen. Feature importance was determined by higher values in information gain (i. g.) following the selection of the feature.

Results

The patients were distributed into three groups based on IS subtype: Group 1 — 84 patients with cardioembolic IS; Group 2 — 65 patients with atherothrombotic IS; Group 3 — 80 patients with lacunar IS. All patients were managed according to specialized medical care standards for cerebral stroke. No thrombolytic therapy was used in view of contraindications or missed therapeutic window due to late hospital admission. Based on comprehensive examination findings, the following clinical and neuroimaging signs of ischemic stroke were verified (Table 1).

Arterial hypertension was more common in group 1 patients, compared to groups 2 and 3, ($P=0.0041$, $P=0.0007$), while risk of recurrent stroke was higher in patients from group 3 ($P=0.0017$, $P=0.0025$) compared to patients from groups 1 and 2. Patients from groups 2 and 3 had higher BMI values vs patients from group 1 ($P<0.0001$, $P=0.009$). Neuroimaging findings showed higher prevalence of multifocal brain lesions in group 3, compared to group 2 ($P<0.0001$), and MRI signs of grade 3 WMH according to the Fazekas scale were common in patients from groups 2 and 3, compared to group 1

Table 1. Demographic characteristics and characteristics of cerebral ischemic stroke in patients, groups 1, 2, and 3.

Parameters	Values in the groups			*P*
	1, *N*=84	2, *N*=65	3, *N*=80	
Demographic variables, *N* (%)				
Males, *N* (%)	46 (54.8)	32 (49.2)	46 (57.5)	P_1=0.497; P_2=0.727; P_3=0.318
Females, *N* (%)	38 (45.2)	33 (50.8)	34 (42.5)	P_1=0.497; P_2=0.727; P_3=0.318
Mean age, y., *M*±σ	66.65±3.2	66.48±2.9	67.03±3.9	P_1=0.738; P_2=0.495; P_3=0.305
Comorbid conditions				
Diabetes mellitus, type 2, *N* (%)	29 (34.5)	16 (24.6)	26 (32.5)	P_1=0.192; P_2=0.786; P_3=0.297
Arterial hypertension, *N* (%)	75 (89.3)	46 (70.8)	54 (67.5)	P_1=0.0041*; P_2=0.0007*; P_3=0.669
Recurrent IS, *N* (%)	15 (17.8)	11 (16.9)	32 (40.0)	P_1=0.887; P_2=0.0017*; P_3=0.0025*
BMI, kg/m², *M*±σ	25.15±3.8	28.14±2.5	27.04±3.3	P_1<0.0001*; P_2=0.009*; P_3=0.0169
Excess weight (BMI 25–30 kg/m²)	30 (25.2)	29 (44.6)	24 (30.0)	P_1=0.0130; P_2=0.491; P_3=0.0694
Grade 1 obesity (BMI = 30–35 kg/m²)	4 (4.8)	7 (10.8)	10 (12.5)	P_1=0.165; P_2=0.070; P_3=0.715
Grades 2–3 obesity (BMI > 35 kg/m²)	11 (13.1)	10 (15.4)	18 (22.5)	P_1=0.694; P_2=0.165; P_3=0.281
Neuroimaging parameters				
Multiple lesions, *N* (%)	8 (9.5)	0 (0)	18 (22.5)	P_1=0.106; P_2=0.023; P_3<0.0001*
Lesion size, *Me [Q1; Q3]*, mm	25 [23; 48]	23 [20; 36]	5 [3–10]	P_1=0.567; P_2=0.0111*; P_3<0.0001*
WMH (Fazekas 2), *N* (%)	46 (54.8)	28 (43.1)	48 (60.0)	P_1=0.156; P_2=0.846; P_3=0.110
WMH (Fazekas 3), *N* (%)	2 (2.4)	12 (18.5)	14 (17.5)	P_1=0.0009*; P_2=0.0039*; P_3=0.572
IS lesion in the right hemisphere	38 (45.2)	32 (49.2)	54 (67.5)	P_1=0.627; P_2=0.004*; P_3=0.026
IS lesion in the left hemisphere	46 (54.8)	33 (50.8)	26 (32.5)	P_1=0.627; P_2=0.004; P_3=0.026
MCA stroke	56 (66.7)	48 (73.8)	78 (97.5)	P_1=0.349; P_2<0.0001*; P_3<0.0001*
ACA stroke	21 (25.0)	10 (15.4)	2 (2.5)	P_1=0.152; P_2<0.0001*; P_3=0.0051
AChA stroke	7 (8.3)	7 (10.8)	0 (0)	P_1=0.603; P_2=0.0085*; P_3=0.0026*
Clinical scales (scores), *M*±σ				
NIHSS (on admission)	9.6±1.6	7.5±0.9	5.8 2.4	P_1<0.0001*; P_2<0.0001*; P_3<0.0001*
BI (on admission)	76.18±5.8	82.76±8.3	86.51±5.4	P_1=0.048; P_2<0.0001*; P_3=0.0131
CDR (day 14)	0.64±0.1	0.65±0.1	0.86±0.4	P_1=0.991; P_2<0.0001*; P_3<0.0001*
Functional outcome parameters				
mRS (1st day), (scores), *M*±σ	3.6±1.9	3.4±1.8	2.8±0.8	P_1=0.515; P_2=0.0018*; P_3=0.0083*
mRS (21st day), (scores), *M*±σ	2.40±1.3	2.17±1.9	1.35±0.9	P_1=0.382; P_2<0.0001*; P_3=0.0006*
Favorable outcome (mRS = 0–2 scores), *N* (%)	40 (47.6)	32 (49.2)	63 (78.8)	P_1=0.846; P_2<0.0001*; P_3=0.0002*
Unfavorable outcome (mRS ⩾ 3 scores), *N* (%)	44 (52.3)	33 (50.8)	17 (21.2)	P_1=0.846; P_2<0.0001*; P_3=0.0002*

Notes. P_1 — the indicator of statistical significance of the difference between the parameters of the 1st and 2nd groups; P_2 — the indicator of statistical significance of the difference between the parameters of the first and third groups; P_3 — the indicator of statistical significance of the difference between the parameters 2nd and 3d groups; * — the differences in indicators are statistically significant (P<0.0125 with the Bonferroni correction). ICA — internal carotid artery; IS — ischemic stroke; BMI — body mass index; WMH — white matter hyper-intensity; ACA — anterior cerebral artery; MCA — middle cerebral artery; AChA — anterior choroidal artery; CDR — Clinical Dementia Rating scale; mRS — the modified Rankin scale; NIHSS — National Institutes of Health Stroke Scale.

(*P*=0.0009, *P*=0.0039). Evaluation by clinical assessment scales showed higher baseline NIHSS scores in patients from group 1 (*P*<0.0001), and higher CDR scores in patients from group 3 on the 14th day of hospital stay (*P*<0.0001). Assessment of the mRS score dynamics showed a significant (*P*<0.0001) decrease in the mRS score by the 21st day of hospital stay in all study groups. Evaluation of cytokines revealed higher concentrations of MIP-1d/CCL15 in patients from group 2 compared to group 1 (*P*=0.0002), and higher MCP-1/ CCL2 concentrations in patients from group 3 compared to group 1 (*P*=0.0004, Fig. 1). Concentrations of other evaluated cytokines did not show statistically significant differences (*P*<0.0125, Fig. 2).

Assessment of relationships between the studied parameters and △mRS in the groups revealed correlations of varying strength. In all groups, significant correlations (*P*<0.0001) were found between △mRS and presence of diabetes mellitus (*R*=0.884, *R*=0.749, *R*=0.475). In groups 1 and 3 there was a significant correlation between △mRS and presence of recurrent IS (*R*=0.701, *P*=0.0021; *R*=0.413, *P*=0.0001) and IS laterality (*R*=0.359, *P*=0.0071; *R*=0.454, *P*=0.001). In groups 2 and 3, a positive correlation of △mRS was found with WMH grade (*R*=0.625, *P*<0.0001; *R*=0.601, *P*=0.004) and grades 2–3 obesity (*R*=0.343, *P*=0.011; *R*=0, 624, *P*<0.0001), and a negative correlation with grade 1 obesity (*R*=–0.427, *P*=0.0021; *R*=–0.518, *P*<0.0001). A correlation between △mRS and the baseline NIHSS scores was established in patients from groups 1 and 2 (*R*=0.338, *P*=0.01; *R*=0.547, *P*=0.012). The most significant △mRS correlation with gender was found in patients from group 1 (*R*=0.508, *P*<0.0001), while in group 3 — with presence of arterial hypertension (*R*=–0.329, *P*<0.0001) and with age (*R*=0.488, *P*=0.0001). Assessment of correlations between immunological indicators and FO parameters in patients from group 1 revealed significant positive associations of △mRS with concentrations of CXCL6 (*R*=0.413, *P*=0.001), CXCL1 (*R*=0.782, *P*=0.0017), CXCL-2 (*R*=0.635, *P*=0.0024), CCL23 (*R*=0.358, *P*<0.0001) and CCL3 (*R*=0.343, *P*=0.001). A negative correlation

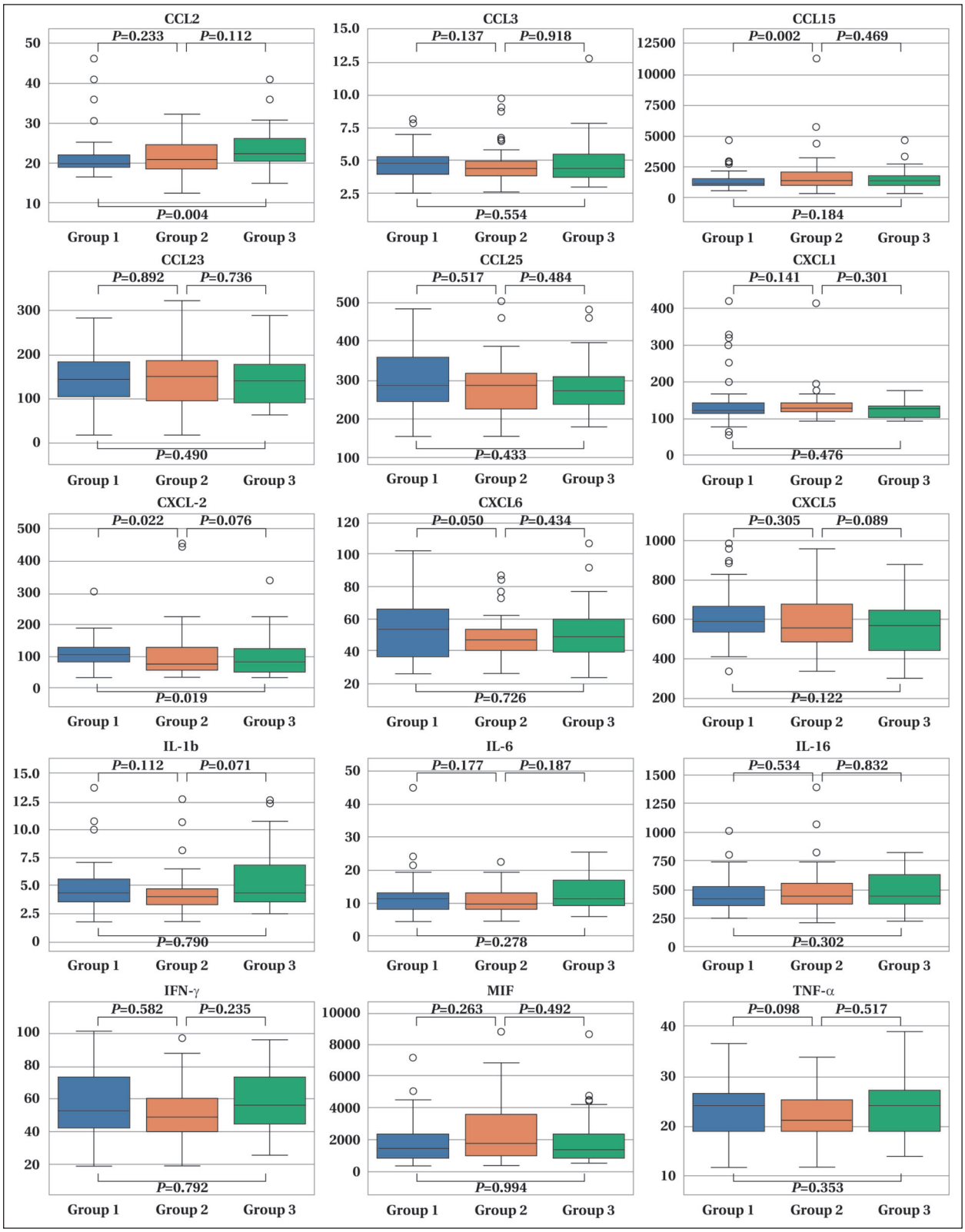

Fig. 2. Cytokine concentrations (pg/ml) in groups of patients with different subtypes of ischemic stroke ($P<0.0125$ with Bonferroni correction).

was found between △mRS and IL-6 (R=–0.474, P=0.0004), CCL25 (R=–0.508, P=0.002), and TNF-α (R=–0.401, P=0.001). In group 2, significant positive correlations of △mRS were found with concentrations of CCL2 (R=0.632, P=0.001), CCL3 (R=0.423, P=0.011), CCL23 (R=0.351, $P<0.0001$), IL-1b (R=0.365, P=0.0213), CXCL5 (R=0.341, $P<0.0001$), CXCL6 (R=0.334, $P<0.0001$) and IL-16 (R=0.328, P=0.0031).

A negative correlation was established between △mRS and IL-6 (R=–0.468, P=0.0004), and TNF-α (R=–0.358, P=0.011). In group 3, a significant correlation was found between △mRS and the concentrations of CXCL5 (R=0.741, P<0.0001), MIF (R=0.606, P<0.0001), and CXCL10 (R=0.499, P=0.0074, Fig. 3).

Performance of model in verification of binary FO reached 0,91 after training ML algorithms via feeding similar set of features for each group. Important features with higher information gain regarding an unfavorable non-fatal outcome (mRS⩾3 scores) in group 1 were: female gender (i.g.=0.346; P<0.0001), recurrent IS (i.g.=0.248; P<0.0001), diabetes mellitus (i.g.=0.442; P<0.0001) and concentrations of CXCL2 (i.g.=0.306, P<0.0001). In group 1, concentrations of CCL25 (i.g.=0.108, P<0.0001) and IL-6 (i.g.=0.401, P<0.0001) were identified as predictors of favorable FO. In group 2, WMH grade (i.g.=0.206; P<0.0001), diabetes mellitus (i.g.=0.340; P<0.0001), concentrations of CCL2 (i.g.=0.116; P<0.0001), CCL3 (i.g.= 0.202; P<0.0001), and CCL23 (i.g.=0.101; P<0.0001) were identified as relevant indicators associated with unfavorable FO. Grade 1 obesity (i.g.=0.118, P<0.0001) and TNF-α concentration (i.g.= 0.211, P<0.0001) were associated with favorable FO. In patients from group 3, age (i.g.=0.106; P<0.0001), grade 2 obesity (i.g. = 0.150; P<0.0001), WMH (i.g.=0.300; P<0.0001), CXCL5 (i.g.=0.143; P<0.0001) and MIF (i.g.=0.145; P<0.0001) concentrations were indicators of unfavorable FO, while AH (i.g.=0.113; P<0.0001) and grade 1 obesity were indicators of favorable FO. Given the high percentage of patients with arterial hypertension and diabetes mellitus in the overall cohort, a discriminant analysis was performed to identify relevant parameters for these categories of patients in the groups. In groups 1 and 2, CXCL1 concentration was identified as a predictor of unfavorable FO in patients with AH (i.g.=0.206, P<0.0001; i.g.=0.105, P<0.0001), in patients with diabetes

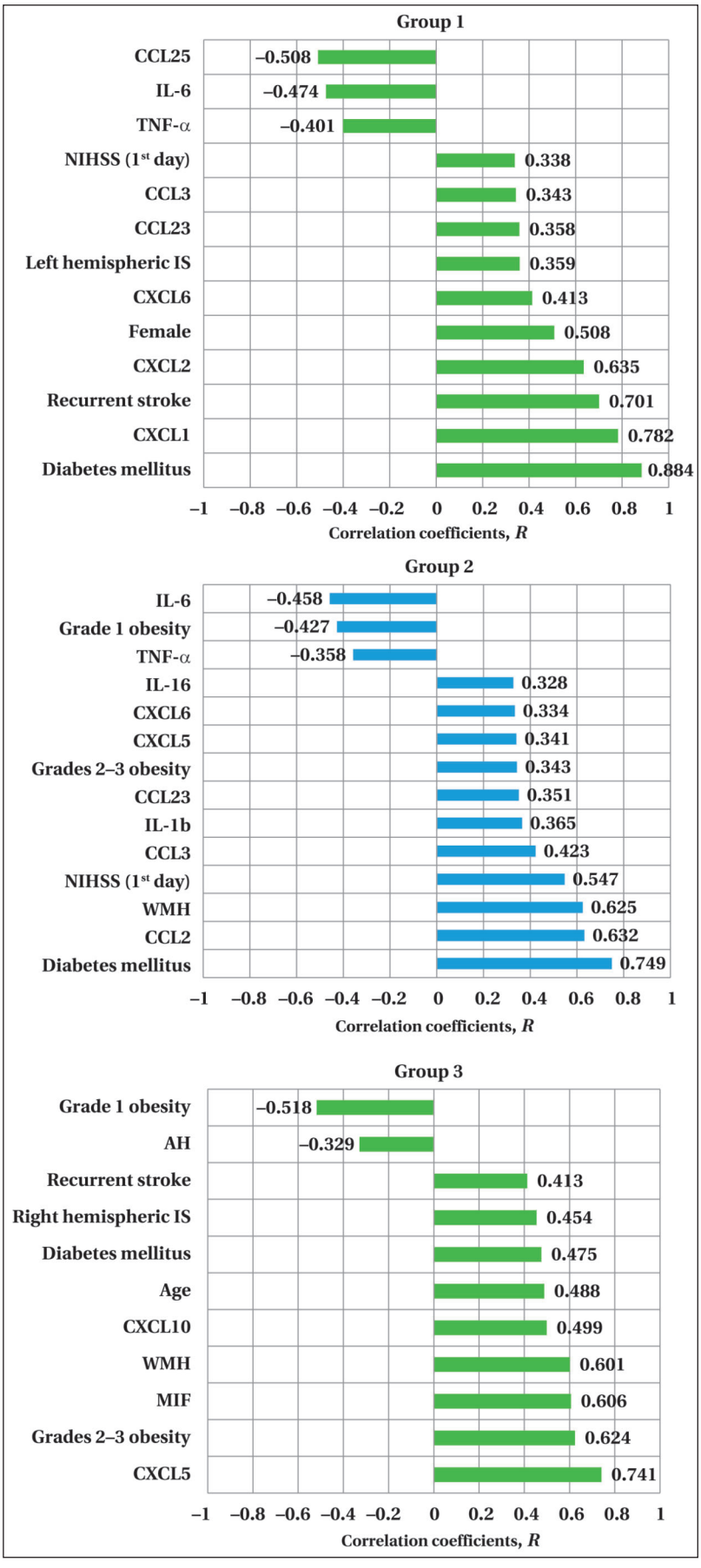

Fig. 3. Correlation of clinical parameters and cytokine concentrations (pg/ml) with △mRS scores in patients with different subtypes of IS.

mellitus from groups 1 and 3 it was the concentration of CXCL5 (i.g.=0.206, $P<0.0001$; i.g.=0.105, $P<0.0001$).

Discussion

An unfavorable non-lethal functional outcome in acute IS was documented in 50% of patients due to underlying atherosclerosis of large or medium-sized cerebral arteries and cerebral embolism originating from the heart. A tendency to an unfavorable outcome was established in 21.2% of patients with the lacunar IS, despite high average survival rate and a relatively good prognosis for functional recovery in this cohort. The results obtained are consistent with published evidence from other studies, which have demonstrated that early disabling functional impairments develop in 50–60% of patients with cardioembolic and atherothrombotic stroke, and in 20–30% of patients with lacunar IS [10–12]. Type 2 diabetes was identified as a predictor of unfavorable outcome, regardless of IS subtype, which is consistent with the findings of studies that contemplate the impact of carbohydrate metabolism disorders on mortality, patient recovery, frequency and timing of recurrent IS after the first-time stroke [13, 14].

Although the relationship between excessive weight and all IS subtypes has been demonstrated in cohort studies and meta-analyses [15–17], in this study, grades 2–3 obesity were significant predictors of unfavorable outcome only in patients with the lacunar IS. A favorable outcome in patients with atherothrombotic and lacunar IS who have a BMI of 30–35 kg/m² (grade 1 obesity) in this study is of interest. It can be interpreted on the context of the so-called «obesity paradox», linking extra weight and grade 1 obesity with better outcomes and reduced mortality in patients with IS [18]. However, definition of metabolic obesity as a marker of unfavorable outcome based only on BMI is insufficient, which necessitates verification of obesity significance (with thorough evaluation of central obesity, lipid profile, disorders of carbohydrate metabolism, and insulin resistance) as an important predictive factor for IS outcome in metabolic syndrome [19, 20].

Demographic characteristics were significant for prediction of IS outcome in the acute period in patients with cardioembolic (female gender) and lacunar (age) subtypes. These results are consistent with some recent studies that have demonstrated differences in non-fatal functional outcomes related to gender and age, as well as worse outcomes of cardioembolic IS in the acute period in women compared to men [21]. According to few references, these differences can be associated with higher content of molecular-genetic markers of atrial fibrillation, in particular, brain natriuretic peptide (NT-proBNP) and fibroblast growth factor-23 (FGF-23) in women compared to men [22, 23]. Age, identified as an important predictor of unfavorable outcome in lacunar IS, along with WMH and grade of cognitive decline, is most likely associated with age-dependent cerebral microangiopathy, established as the leading risk factor for lacunar stroke [24].

Severe damage to the microcirculatory vascular bed and progressive microangiopathy can lead to IS recurrence, which was a relevant indicator and marker of unfavorable outcome in patients with lacunar stroke in this study. Potential association of AH with favorable outcome in patients with lacunar IS remains controversial. Quite possible, that the obtained results prove more favorable functional outcomes of lacunar stroke in patients with hypertensive microangiopathy as compared to cases of atherosclerotic and embolic origin.

However, as there was no assessment of heterogeneity and verification of causes leading to development of this subtype of IS, the results require further confirmation in studies aimed at FO evaluation in patients with different pathogenetic subtypes of lacunar stroke. An increase in CXCL2 concentration was verified as the main immunological marker of unfavorable FO in patients with cardioembolic IS. Even though the role of CXC-chemokines in pathogenesis of cardiovascular diseases was competently investigated, nevertheless, the mechanisms of action of this family of cytokines in cerebral ischemia and hypoxia in the acute period of IS are not yet sufficiently studied.

Recent experimental studies have demonstrated the key role of the CXCR2 receptor in pathogenesis of atrial fibrillation, which is the main risk factor for development of cardioembolic stroke. In addition to its main effect of chemoattracting monocytes to the vascular endothelium and cardiac tissue, CXCL-2 expression also contributes to secretion of platelet-derived growth factor A (PDGF-A) and increase in pro-inflammatory cytokines, thereby promoting development of atrial fibrosis and heart remodeling, which are the key factors in pathogenesis of arrhythmias characterized by irregular electrical activity [25] Clinical studies have also revealed higher concentrations of circulating CXCL-2 in patients with atrial fibrillation compared to control group patients with sinus rhythm [26]. CXCL-1 is another member from the CXC family that had been shown to be predictive, as its increased concentration was associated with unfavorable prognosis in patients with AH developing atherothrombotic and cardioembolic IS. The obtained results are consistent with the data from studies revealing higher CXCL1 levels in patients with AH compared to healthy subjects, and demonstrating that CXCL1 promotes AH by potentiating the expression of angiotensin type 1 and 2 receptors, toll-like receptor 4 (TLR4), and production of transforming growth factor β (TGF-β) [27, 28].

Ligands CCL3 and CCL2 of chemokine receptors CCR1 and CCR2, respectively, have been identified as biomarkers of unfavorable FO in patients with atherothrombotic IS. The pro-atherogenic role of these chemokines has been well-studied and demonstrated in a number of experimental and clinical studies. Increased concentrations of both CCL2 and CCL3 induce migration of leukocytes into the arterial wall, formation of foam cells, destabilization, and rupture of the atherosclerotic plaque. Studies on animal models with induced hypercholesterolemia have shown a direct correlation between CCL2/CCL3 and LDL concentrations, as well as decrease in these cytokines following intake of statins, which further supports the association between increased CCL2 and CCL3 levels and the progression of early atherosclerotic processes [29]. The CCL23 pro-atherogenic effect is enacted when it is expressed into milieu with increased LDL via stimulation of monocytes and macrophages chemotaxis into the vascular wall, increased expression of adhesion molecules and release of matrix metalloproteinase 2 (MMP-2) from monocytes [30, 31]. A favorable outcome in patients with atherothrombotic and cardioembolic IS was associated with increased concentrations of CCL25 chemokine, TNF-α and IL-6. Despite sound body of accumulated knowledge of pro-inflammatory properties of these cytokines, a number of researchers have demonstrated their opposite effect in acute IS due to mitigation of hypoxic-ischemic damage, arteriodilatation, and antiapoptotic effects. CCL25 protection of neurons, endothelium, and microglia cells was explained by activation of NLR (NOD-like receptors) family, involved in regulation of inflammatory cascades by inhibiting the transcriptional nuclear factor-kappa B (NF-κB) processing and mitogen-activated protein kinases (MAPK), and also by activation of apoptosis regulator Bcl-2. [32]. IL-6 and TNF-α protection after excitotoxic damage, provided via modulation of neurogenesis, angiogenesis, and revascularization processes by activating the JAK/STAT (Janus kinase/signal transducers and activators of transcription) and PI3K (phosphoinositide 3-kinase) signaling pathways, was elucidated in a number of studies [33, 34].

Concentrations of CXCL5 and MIF were identified as immunological markers of unfavorable prognosis in patients with lacunar IS. Currently, scientific experience regarding the role of CXCL5 in the pathogenesis of lacunar stroke is limited to experimental studies, demonstrating expression of astrocytic and endothelial CXCL5 in progression of chronic cerebral ischemia and WMH via modulation of microglia activity and induction of interleukin-17 expression [35, 36]. In addition, CXCL5 concentration was established as a marker of unfavorable FO in patients with diabetes mellitus. These results are consistent with CXCL5 mechanism of action, which promotes insulin resistance via potentiation of TNFα effects and activation of JAK/STAT (Janus kinases/signal transducer and activator of transcription) [37, 38]. Unlike CXCL5, the MIF role in development of cerebral ischemia has been extensively studied, but remains controversial. Recent studies showed that increased MIF activity in hypoxic environment, driven by expression of hypoxia-inducible factor 1α (HIF-1-α), positively correlated with disease severity, ischemic lesion size, and neurological outcomes [39, 40]. The results of some studies show a direct correlation between the Fazekas scale score and concentration of MIF, suggesting that increase in MIF concentration may be a predictor of cerebral microangiopathy progression [41]. Given significant prevalence of patients with high BMI in the lacunar IS group, MIF expression can be associated with obesity. This is supported by studies demonstrating MIF involvement in the inhibition of hormone-sensitive lipase, which contributes to increase in triglyceride levels and exacerbation of obesity [42, 43]. MIF expression also contributes to endothelial dysfunction by regulating leukocyte trafficking into the endothelial wall, expression of adhesion molecules and TNF-α via stimulation of endothelial granular protein P-selectin [44].

Limitations. The main limitations of the study were exclusion of patients with fatal outcomes from the core data sheet, no monitoring of relevant cellular immunological parameters, and missed registration of the prospective study protocol.

Conclusion

The results of the study demonstrated differences in sets of factors affecting the functional outcome of patients with IS, depending on the pathogenetic subtype. Female gender, recurrent IS, an increase in CXCL-2F were the predictors of unfavorable outcome in patients with cardioembolic IS. For patients with the atherothrombotic subtype, WMH grade and contents of CCL2, CCL3 and CCL23 were the significant factors of unfavorable prognosis. Age, recurrent IS, BMI>35 kg/m², and WMH grade, along with increased levels of CXCL5 and MIF, were identified as indicators of unfavorable FO in patients with lacunar IS. Type 2 diabetes mellitus was verified as an independent predictor of eventual disabling disorders, regardless of the stroke pathogenetic mechanisms.

The parameters associated with a favorable FO in patients with the cardioembolic IS were CCL25 and IL-6 expression, with the atherothrombotic subtype — grade 1 obesity along with TNF-a expression, with lacunar IS — underlying AH and grade 1 obesity. Despite the potential value of these results for improving prediction of acute stroke outcomes, further research is needed to confirm the significance of these markers by monitoring key clinical indicators, expanding the sample size, and using diverse statistical analysis methods.

References

1. *Савелло А. В., Вознюк И. А., Бабичев К. Н., Кандыба Д. В., Шендеров С. В., Власенко С. В., Сараев Г. Б.* Шкала прогнозирования раннего функционального исхода после внутрисосудистой тромбоэмболэктомии при каротидном ишемическом инсульте. *Журнал неврологии и психиатрии им. С. С. Корсакова.* 2021; 121 (6): 34–39. *Savello A. V., Voznyuk I. A., Babichev K. N., Kandyba D. V., Shenderov S. V., Vlasenko S. V., Saraev G. B.* A prognosis scale for functional outcome at discharge after endovascular thrombectomy in the carotid artery territory. *S.S. Korsakov Journal of Neurology and Psychiatry.* 2021; 121 (6): 34–39. (in Russ.). DOI: 10.17116/jnevro202112106134.
2. *Силкин В. В., Ершов В. И., Бурдаков В. В., Бирюкова Т. В., Бредихин А. Ю., Лозинская Т. Ю.* Математическое моделирование тяжелого ишемического инсульта с полиорганной недостаточностью: ретроспективное наблюдательное исследование. *Вестник интенсивной терапии им. А. И. Салтанова.* 2023; 1: 91–100. *Silkin V. V., Ershov V. I., Burdakov V. V., Biryukova T. V., Bredikhin A. Yu., Lozinskaya T. Yu.* Mathematical modeling of severe ischemic stroke with multiple organ failure: a retrospective observational study. *Annals of Critical Care.* 2023; 1: 91–100. (in Russ.). DOI: 10.21320/1818-474X-2023-1-91-100.
3. *Manchi M. R., Venkatachalam A. M., Atem F. D., Stone S., Mathews A. A., Abraham A. M., Chavez A. A., et al.* Effect of inpatient rehabilitation facility care on ninety day modified Rankin score in ischemic stroke patients. *J Stroke Cerebrovasc Dis.* 2023 Jun; 32 (6): 107109. DOI: 10.1016/j.jstrokecerebrovasdis.2023.107109. PMID: 37031503.
4. *Guzek Z., Dziubek W., Stefańska M., Kowalska J.* Evaluation of the functional outcome and mobility of patients after stroke depending on their cognitive state. *Sci Rep.* 2024 Jan 17; 14 (1): 1515. DOI: 10.1038/s41598-024-52236-8. PMID: 38233519.
5. *Gardener H., Romano L. A., Smith E. E., Campo-Bustillo I., Khan Y., Tai S., Riley N., et al.* Functional status at 30 and 90 days after mild ischaemic stroke. *Stroke Vasc Neurol.* 2022 Apr 26; 7 (5): 375–380. DOI: 10.1136/svn-2021-001333. PMID: 35474180.
6. *Новикова Л. Б., Акопян А. П., Латыпова Р. Ф.* Анализ исхода острого периода ишемического инсульта. *Анналы клинической и экспериментальной неврологии.* 2022; 16 (4): 5–11. *Novikova L. B., Akopyan A. P., Latypova R. F.* Evaluation of the outcome in ischemic stroke acute period. *Annals of Clinical and Experimental Neurology.* 2022; 16 (4): 5–11. (In Russ.) DOI: 10.54101/ACEN.2022.4.1.
7. *Pawluk H., Woźniak A, Grześk G., Kołodziejska R., Kozakiewicz M., Kopkowska E., Grzechowiak E., Kozera G.* The Role of Selected Pro-Inflammatory Cytokines in Pathogenesis of Ischemic Stroke. *Clin Interv Aging.* 2020 Mar 23; 15: 469–484. DOI: 10.2147/CIA.S233909. PMID: 32273689.
8. *Klimiec-Moskal E., Koceniak P., Weglarczyk K., Slowik A., Siedlar M., Dziedzic T.* Circulating chemokines and short- and long-term outcomes after ischemic stroke. *Mol Neurobiol.* 2025 Jan; 62 (1): 421–428. DOI: 10.1007/s12035-024-04279-1. PMID: 38861234.
9. *Голубев А. М.* Модели ишемического инсульта (обзор). *Общая реаниматология.* 2020; 16 (1): 59–72. *Golubev A. M.* Models of Ischemic Stroke (Review). *General Reanimatology.* 2020; 16 (1): 59–72. (In Russ.) DOI: 10.15360/1813-9779-2020-1-59-72.
10. *Poomalai G., Prabhakar S., Sirala Jagadesh N.* Functional Ability and Health Problems of Stroke Survivors: An Explorative Study. *Cureus.* 2023 Jan 4; 15 (1): e33375. DOI: 10.7759/cureus.33375. PMID: 36751244.
11. *Hu Y., Jiang X., Li Y., Yang C., Ma M., Fang J., He L.* Endovascular treatment with or without intravenous thrombolysis for acute ischemic stroke due to tandem occlusion: a systematic review and meta-analysis. *J Am Heart Assoc.* 2024 Sep 3; 13 (17): e034829. DOI: 10.1161/JAHA.124.034829. PMID: 39206729.
12. *Максимова М. Ю., Гулевская Т. С.* Лакунарный инсульт. *Журнал неврологии и психиатрии им. С. С. Корсакова.* 2019; 119 (8 вып. 2): 13–27. *Maksimova M. Yu., Gulevskaya T. S.* Lacunar stroke. *S. S. Korsakov Journal of Neurology and Psychiatry.* 2019; 119 (8 vyp. 2): 13–27. (In Russ.). DOI: 10.17116/jnevro201911908213.
13. *Lau L. H., Lew J., Borschmann K., Thijs V., Ekinci E. I.* Prevalence of diabetes and its effects on stroke outcomes: A meta-analysis and literature review. *J Diabetes Investig.* 2019 May; 10 (3): 780–792. DOI: 10.1111/jdi.12932. PMID: 30220102.
14. *Воронина В. П., Загребельный А. В., Лукина Ю. В., Кутишенко Н. П., Дмитриева Н. А., Лерман О. В., Лукьянов М. М. с соавт.* Особенности течения мозгового инсульта у больных сахарным диабетом по данным регистра РЕГИОН-М. *Кардиоваскулярная терапия и профилактика.* 2019; 18 (5): 60–65. https://doi.org/10.15829/1728-8800-2019-5-60-65. *Voronina V. P., Zagrebelnyi A. V., Lukina Yu. V., Kutishenko N. P., Dmitrieva N. A., Lerman O. V., Lukyanov M. M., et al.* Features of cerebral stroke course in patients with diabetes mellitus according to the REGION-M register. *Cardiovascular Therapy and Prevention.* 2019; 18 (5): 60–65 (In Russ.). DOI: 10.15829/1728-8800-2019-5-60-65.
15. *Miwa K., Nakai M., Yoshimura S., Sasahara Y., Wada S., Koge J., Ishigami A., et al.* Clinical impact of body mass index on outcomes of ischemic and hemorrhagic strokes. *Int J Stroke.* 2024 Oct; 19 (8): 907–915. DOI: 10.1177/17474930241249370. PMID: 38651751.
16. *Захарычева Т. А., Широкова А. С., Поляков А. Г., Яицкая Е. О., Чекурина С. Л.* Лакунарные инсульты. Клинические наблюдения. *Регионарное кровообращение и микроциркуляция.* 2022; 21 (4): 94–101. https://doi.org/10.24884/1682-6655-2022-21-4-94-101. *Zakharycheva T. A., Shirokova A. S., Polyakov A. G., Yaitskaya E. O., Chekurina S. L.* Lacunary stroke. Clinical cases. *Regional blood circulation and microcirculation.* 2022; 21 (4): 94–101. (In Russ.). DOI: 10.24884/1682-6655-2022-21-4-94-101.
17. *Миклишанская С. В., Мазур Н. А., Соломасова Л. В., Чигинева В. В.* «Парадокс ожирения» и степень его доказанности. Терапевтический архив. 2020; 92 (4): 84–90. *Miklisanskaya S. V., Mazur N. A., Solomasova L. V., Chigineva V. V.* The «obesity paradox» and its degree of proof. Therapeutic Archive. 2020; 92 (4): 84–90. (In Russ.)] DOI: 10.26442/00403660.2020.04.000421.
18. *Антонова К. В., Танашян М. М., Раскуражев А. А., Спрышков Н. Е., Панина А. А., Лагода О. В.,*

Аметов А. С. с соавт. Ожирение и нервная система. *Ожирение и метаболизм.* 2024; 21 (1): 68–78. *Antonova K. V., Tanashyan M. M., Raskurazhev A. A., Spryshkov N. E., Panina A. A., Lagoda O. V., Ametov A. S., et al.* Obesity and the nervous system. *Obesity and metabolism.* 2024; 21 (1): 68–78. DOI: 10.14341/omet13019.
19. *Horn J. W., Feng T., Mørkedal B., Strand L. B., Horn J., Mukamal K., Janszky I.* Obesity and Risk for First Ischemic Stroke Depends on Metabolic Syndrome: The HUNT Study. *Stroke.* 2021 Nov; 52 (11): 3555–3561. DOI: 10.1161/STROKEAHA.120.033016. PMID: 34281375.
20. *Ruan H., Ran X., Li SS, Zhang Q.* Dyslipidemia versus obesity as predictors of ischemic stroke prognosis: a multi-center study in China. *Lipids Health Dis.* 2024 Mar 9; 23 (1): 72. DOI: 10.1186/s12944-024-02061-9. PMID: 38461258.
21. *Dahl S., Hjalmarsson C., Andersson B.* Sex differences in risk factors, treatment, and prognosis in acute stroke. *Womens Health (Lond).* 2020 Jan–Dec; 16. DOI: 10.1177/1745506520952039. PMID: 32997605.
22. *Ko D., Rahman F., Schnabel R. B., Yin X., Benjamin E. J., Christophersen I. E.* Atrial fibrillation in women: epidemiology, pathophysiology, presentation, and prognosis. *Nat Rev Cardiol.* 2016 Jun; 13 (6): 321–32. DOI: 10.1038/nrcardio.2016.45. PMID: 27053455.
23. *Santamarna M., López-Dequidt I., López-Loureiro I., Rodríguez-Pérez M., Hervella P., Sobrino T., Campos F. et al.* Influence of sex on stroke prognosis: a demographic, clinical, and molecular analysis. Front Neurol. 2019 Apr 17; 10: 388. DOI: 10.3389/fneur.2019.00388. PMID: 31057479.
24. *Мхитарян Э. А., Фатеева В. В.* Возраст-зависимая церебральная микроангиопатия, ассоциированная с сосудистыми факторами риска: как распознать на гериатрическом приеме. *Российский журнал гериатрической медицины.* 2024; (1): 49–55. *Mkhitaryan E. A., Fateeva V. V.* Age-dependent cerebral microangiopathy associated with vascular risk factors: how to recognize the signs? *Russian Journal of Geriatric Medicine.* 2024; (1): 49–55. (In Russ.) DOI: 10.37586/2686-8636-1-2024-49-55.
25. *Lu X., Wang Z., Ye D., Feng Y., Liu M., Xu Y., Wang M., et al.* The Role of CXC Chemokines in Cardiovascular Diseases. *Front Pharmacol.* 2022 May 20; 12: 765768. DOI: 10.3389/fphar.2021.765768. PMID: 35668739.
26. *Zhang Y. L., Cao H. J., Han X., Teng F., Chen C., Yang J., Yan X., et al.* Chemokine Receptor CXCR-2 Initiates Atrial Fibrillation by Triggering Monocyte Mobilization in Mice. *Hypertension.* 2020 Aug; 76 (2): 381–392. DOI: 10.1161/HYPERTENSIONAHA.120.14698. PMID: 32639881.
27. *Zhang R. M., McNerney K. P., Riek A. E., Bernal-Mizrachi C.* Immunity and Hypertension. *Acta Physiol.* (Oxf) 2021; 231: e13487. DOI: 10.1111/apha.13487. PMID: 32359222.
28. *Korbecki J., Maruszewska A., Bosiacki M., Chlubek D., Baranowska-Bosiacka I.* The potential importance of CXCL1 in the physiological state and in noncancer diseases of the cardiovascular system, respiratory system and skin. *Int J Mol Sci.* 2022 Dec 22; 24 (1): 205. DOI: 10.3390/ijms24010205. PMID: 36613652.
29. *Yan Y., Thakur M., van der Vorst E. P. C., Weber C., Döring Y.* Targeting the chemokine network in atherosclerosis. *Atherosclerosis.* 2021 Aug; 330: 95–106. DOI: 10.1016/j.atherosclerosis.2021.06.912. PMID: 34247863.
30. *Kim C. S., Kang J. H., Cho H. R., Blankenship T. N., Erickson K. L., Kawada T., Yu R.* Potential involvement of CCL23 in atherosclerotic lesion formation/progression by the enhancement of chemotaxis, adhesion molecule expression, and MMP-2 release from monocytes. *Inflamm Res.* 2011 Sep; 60 (9): 889–95. DOI: 10.1007/s00011-011-0350-5. PMID: 21656154.
31. *Tsioufis P., Theofilis P., Tsioufis K., Tousoulis D.* The impact of cytokines in coronary atherosclerotic plaque: current therapeutic approaches. *Int J Mol Sci.* 2022 Dec 14; 23 (24): 15937. DOI: 10.3390/ijms232415937. PMID: 36555579.
32. *Wu X., Sun M., Yang Z., Lu C., Wang Q., Wang H., Deng C., Liu Y., Yang Y.* The Roles of CCR9/CCL25 in Inflammation and Inflammation-Associated Diseases. *Front Cell Dev Biol.* 2021 Aug 19; 9: 686548. DOI: 10.3389/fcell.2021.686548. PMID: 34490243
33. *Kummer K. K., Zeidler M., Kalpachidou T., Kress M.* Role of IL-6 in the regulation of neuronal development, survival and function. *Cytokine.* 2021 Aug; 144: 155582. DOI: 10.1016/j.cyto.2021.155582. PMID: 34058569.
34. *Xue Y., Zeng X., Tu W. J., Zhao J.* Tumor Necrosis Factor-α: The Next Marker of Stroke. *Dis Markers.* 2022 Feb 27; 2022: 2395269. DOI: 10.1155/2022/2395269. PMID: 35265224.
35. *Cao Q., Chen J., Zhang Z., Shu S., Qian Y., Yang L., Xu L., et al.* Astrocytic CXCL5 hinders microglial phagocytosis of myelin debris and aggravates white matter injury in chronic cerebral ischemia. *J Neuroinflammation.* 2023 May 3; 20 (1): 105. DOI: 10.1186/s12974-023-02780-3. PMID: 37138312
36. *Xiao G., Kumar R., Komuro Y., Burguet J., Kakarla V., Azizkhanian I., Sheth S. A., et al.* IL-17/CXCL5 signaling within the oligovascular niche mediates human and mouse white matter injury. *Cell Rep.* 2022 Dec 20; 41 (12): 111848. DOI: 10.1016/j.celrep.2022.111848. PMID: 36543124
37. *Chen C., Chang T. T., Chen J. W.* Mechanistic role of CXCL5 in cardiovascular disease, diabetes mellitus, and kidney disease. *Life Sci.* 2023 Oct 1; 330: 122018. DOI: 10.1016/j.lfs.2023.122018. PMID: 37567498.
38. *Chen C., Lin L. Y., Wu Y. W., Chen J. W., Chang T. T.* CXCL5 inhibition improves kidney function by protecting renal tubular epithelial cells in diabetic kidney disease. *Clin Immunol.* 2024 Nov; 268: 110369. DOI: 10.1016/j.clim.2024.110369. PMID: 39326648.
39. *Zhang Y., Yu Z., Ye N., Zhen X.* Macrophage migration inhibitory factor (MIF) in CNS diseases: Functional regulation and potential therapeutic indication. *Fundam Res.* 2023 May 30; 4 (6): 1375–1388. DOI: 10.1016/j.fmre.2023.05.008. PMID: 39734533
40. *Li Y. S., Chen W., Liu S., Zhang Y. Y., Li X. H.* Serum macrophage migration inhibitory factor levels are associated with infarct volumes and long-term outcomes in patients with acute ischemic stroke. *Int J Neurosci.* 2017 Jun; 127 (6): 539–546. DOI: 10.1080/00207454.2016.1211648. PMID: 27402018.
41. *Zhao J., Wang X., Yu M., Zhang S., Li Q., Liu H., Zhang J., et al.* The relevance of serum macrophage migration inhibitory factor level and executive function in patients with white matter hyperintensity in

cerebral small vessel disease. *Brain Sci.* 2023 Apr 5; 13 (4): 616.
DOI: 10.3390/brainsci13040616. PMID: 37190581

42. *Chen L., Li L., Cui D., Huang Y., Tong H., Zabihi H., Wang S., et al.* Extracellular macrophage migration inhibitory factor (MIF) downregulates adipose hormone-sensitive lipase (HSL) and contributes to obesity. *Mol Metab.* 2024 Jan; 79: 101834.
DOI: 10.1016/j.molmet.2023.101834. PMID: 37935315
43. *Cui N., Li H., Dun Y., Ripley-Gonzalez J. W., You B., Li D., Liu Y., et al.* Exercise inhibits JNK pathway activation and lipotoxicity via macrophage migration inhibitory factor in nonalcoholic fatty liver disease. *Front Endocrinol (Lausanne).* 2022 Sep 6; 13: 961231.
DOI: 10.3389/fendo.2022.961231. PMID: 36147562
44. *Cheng Q., McKeown S. J., Santos L., Santiago F. S., Khachigian L. M., Morand E. F, Hickey M. J.* Macrophage migration inhibitory factor increases leukocyte-endothelial interactions in human endothelial cells via promotion of expression of adhesion molecules. *J Immunol.* 2010 Jul 15; 185 (2): 1238–47.
DOI: 10.4049/jimmunol.0904104. PMID: 20554956.

Received 05.05.2025
Accepted 09.09.2025
Online first 10.10.2025

https://doi.org/10.15360/1813-9779-2025-5-26-34

The Potential for Improving the Diagnostics of Nosocomial Meningitis and Ventriculitis

Medina I. Aybazova[1]*, Leonid A. Shmidt[2], Natalya V. Dryagina[1], Elena S. Borisova[2], Kristina A. Krivchikova[2], Nikita V. Goncharuk[2], Lubov M. Tsentsiper[1–4], Anatoly N. Kondratyev[1]

[1] A. L. Polenov Russian Research Neurosurgical Institute, branch of V. A. Almazov National Medical Research Center, Ministry of Health of Russia 12 Mayakovsky Str., 191014 St. Petersburg, Russia
[2] V. A. Almazov National Medical Research Center, Ministry of Health of Russia, 2 Akkuratova Str., 197341 Saint Petersburg, Russia
[3] St. Petersburg State Pediatric Medical University, Ministry of Health of Russia, 2 Litovskaya Str, 194100 Saint-Petersburg, Russia
[4] Medical Institute, Patrice Lumumba Peoples Friendship University of Russia, 6 Miklukho-Maclaya Str., 117198 Moscow, Russia

For citation: *Medina I. Aybazova, Leonid A. Shmidt, Natalya V. Dryagina, Elena S. Borisova, Kristina A. Krivchikova, Nikita V. Goncharuk, Lubov M. Tsentsiper, Anatoly N. Kondratyev.* The Potential for Improving the Diagnostics of Nosocomial Meningitis and Ventriculitis. *Obshchaya Reanimatologiya = General Reanimatology.* 2025; 21 (5): 26–34. https://doi.org/10.15360/1813-9779-2025-5-26-34 [In Russ. and Engl.]

***Correspondence to:** Medina I. Aybazova, aibazova.med@yandex.ru

Summary

The aim of the study was to identify the most specific and sensitive criteria for diagnosing nosocomial meningitis and ventriculitis.

Materials and methods. A retrospective case-control cohort study conducted at the department of anesthesiology and intensive care of the A. L. Polenov Russian Research Neurosurgical Institute (RRNI), a branch of the V. A. Almazov National Medical Research Center (NMRC) of the Ministry of Health of Russia included 120 patients who underwent intracranial neurosurgery: the main group (*N*=60) — patients with nosocomial meningitis (NM), and the comparison group (*N*=60) — patients without NM. Inclusion criteria: age over 18 years. Exclusion criteria: severe immunosuppressive condition (HIV infection), signs of central nervous system (CNS) infection (meningitis, ventriculitis, brain abscess) on admission, extracranial surgical interventions, pre-operative cerebrospinal fluid leakage, CNS trauma, and extracranial causes of CNS infection. The US Centers for Disease Control and Prevention (CDC) and the Burdenko National Medical Research Center for Neurosurgery criteria for NM diagnosis were used in the study.

Results. External validation of the NM diagnostic criteria in the analyzed patient cohort resulted in 81.67% sensitivity and 83.33% specificity of the CDC criteria. Sensitivity and specificity of the Burdenko National Medical Research Center for Neurosurgery criteria were 81.67% and 88.33%, respectively, for probable NM, and 51.67% and 100%, for confirmed NM. The CDC criteria demonstrated the highest sensitivity for protein concentration in cerebrospinal fluid (CSF) > 0.33 g/L (83.6%), with simultaneous extremely low specificity of 21%, and the highest specificity for the CSF positive culture (100%). As for the Burdenko National Research Medical Center for Neurosurgery criteria, in probable NM the highest sensitivity was established for CSF cell count > 65 cells/μL (64.4%), and the highest specificity — for CSF glucose < 2.6 mmol/l (93.9%) and CSF/serum glucose ratio (CSF/SGLU) < 0.45 (96.8%). In confirmed NM, CSF cell count > 65 cells/μL was also the most sensitive parameter (95.2%), although with 51% specificity. The highest specificity was found for the CSF lactate > 4.2 mmol/L (92.3%). The optimal threshold values were calculated for four parameters: body temperature > 37.7°C, CSF cell count > 245 cells/μL, CSF glucose < 2.0 mmol/L, and CSF lactate > 3.7 mmol/L. Using a combination of threshold values for all four parameters, we achieved a sensitivity of 90.00% and a specificity of 91.67%. CSF cell count (AUC=0.90; 95% CI 0.84–0.95), increased CSF lactate (AUC=0.85; 95% CI 0.75–0.93), total CSF protein (AUC=0.83; 95% CI 0.75–0.90) and body temperature (AUC=0.82; 95% CI 0.74–0.89) had the greatest diagnostic value. Positive CSF culture and the occipital muscle rigidity correlated with the diagnosis of NM (*rbp*=0.522 and *rbp*=0.415, respectively, *P*=0.0001), but did not show good predictive diagnostic capacity.

Conclusion. Fever, increase in CSF cell count and CSF lactate were identified as the most clinically significant signs of NM. A positive CSF culture traditionally used as the gold standard for diagnosis of NM showed low sensitivity of 69.2%. When taken together, the identified in the study threshold values of body temperature, CSF cell count, CSF glucose and lactate have a higher sensitivity and specificity than those used earlier.

Keywords: nosocomial meningitis; CNS infection; criteria for diagnosing nosocomial meningitis

Conflict of interest. The authors declare no conflict of interest.

Information about the authors/Информация об авторах:
Medina I. Aybazova/Медина Исламовна Айбазова: https://orcid.org/0000-0002-6280-3832
Leonid A. Shmidt/Леонид Александрович Шмидт: https://orcid.org/0009-0004-1205-7650
Natalya V. Dryagina/Наталья Владимировна Дрягина: https://orcid.org/0000-0001-8595-6666

Elena S. Borisova/Елена Сергеевна Борисова: https://orcid.org/0009-0006-3986-633X
Kristina A. Krivchikova/Кристина Александровна Кривчикова: https://orcid.org/0009-0006-9796-8799
Nikita V. Goncharuk/Никита Валерьевич Гончарук: https://orcid.org/0000-0002-2905-1587
Lubov M. Tsentsiper/Любовь Марковна Ценципер: https://orcid.org/0000-0001-7527-7707
Anatoly N. Kondratyev/Анатолий Николаевич Кондратьев: https://orcid.org/0000-0002-7648-2208

Introduction

Nosocomial meningitis (NM) remains a life-threatening complication that increases the duration of hospital stay, causes disability, and leads to adverse outcomes. The incidence of NM among neurosurgical patients is 1.49%, and it increases to 8.4% in selective surgical interventions. The mortality rate for NM reaches 28.9% (up to 78.12% in ventriculitis, according to Corona-Nakamura A. L.), and the incidence of drainage-associated meningoventriculitis is 19.8%, or 18.3 cases per 1.000 days of drainage [1–8]. Timely diagnosis and initiation of antibiotic therapy improve the NM prognosis [9, 10].

NM probability is considered based on deviations in cerebrospinal fluid (CSF) analysis. In global clinical practice, management of ventriculitis and meningitis is based on the criteria of the Centers for Disease Control and Prevention (CDC) [11] and guidelines developed by the Infectious Diseases Society of America (IDSA) as proposed in 2017 [12].

According to the CDC criteria, the diagnosis of nosocomial meningitis is made if at least one of the following criteria is met:

1. CSF pathogen is isolated, either from CSF culture, or using other available microbiological tests.

2. The patient has at least two of the following clinical manifestations:

— fever >38.0°C;

— headache;

— meningeal signs;

— signs of cranial nerve involvement;

And at least one of the following laboratory criteria:

— changes in CSF: increased leukocyte count with predominant neutrophils; increased protein concentration; decreased glucose concentration;

— serological confirmation of infection: diagnostic titer of specific IgM or a 4-fold increase in the titer of IgG antibody in paired sera.

N. N. Burdenko National Medical Research Center for Neurosurgery (NMRCN) NM diagnostic criteria (probable and confirmed) include assessment of patient's clinical status (cerebral, meningeal symptoms, fever), routine and biochemical CSF analyses, CSF cultures, hyponatremia. The N. N. Burdenko NMRCN criteria for probable NM include: a single episode of CSF cell count >65 cells/μL, increased CSF lactate >4.2 mmol/l, decreased CSF glucose <2.6 mmol/l, CSF/serum glucose ratio (CSF/SGLU) <0.45, or, in the absence of all above mentioned criteria, only a positive CSF culture. Additional criteria include fever ⩾38°C and plasma sodium < 135 mmol/l. NM is considered confirmed when CSF positive culture comes along with all pathological CSF tests [4].

However, as noted by N.V. Kurdyumova, clinical symptoms may not appear immediately that impedes early diagnosis [4].

Although CSF culture is considered the «gold standard», the results can be both false-positive and false-negative [13, 14]. Moreover, in 50% of cases bacteria are not detected in patients treated with antibiotics [15–17].

According to various sources, CSF leukocytosis in bacterial meningitis varies widely, from 11 cells/mm³ (according to the CDC) to 1.000 cells/mm³ [12].

The aim of the study was to determine the most specific and sensitive criteria for diagnosing nosocomial meningitis and ventriculitis.

Material and Methods

A retrospective case-control cohort study conducted at the department of anesthesiology and intensive care of A. L. Polenov Russian Research Neurosurgical Institute (RRNI), a branch of V. A. Almazov National Medical Research Center (NMRC) of the Russian Ministry of Health included 120 patients who underwent intracranial neurosurgery: the main group (*N*=60) — patients with nosocomial meningitis (NM), and the comparison group (*N*=60) — patients without NM.

Craniotomy or implantation of intracranial devices (shunts) was performed from January 2020 to January 2025.

Inclusion criteria: age over 18 years. Exclusion criteria: severe immunosuppressive condition (HIV infection), signs of central nervous system (CNS) infection (meningitis, ventriculitis, brain abscess) on admission, extracranial surgical interventions, pre-operative cerebrospinal fluid leakage, CNS trauma, and extracranial causes of CNS infection.

The following clinical features and laboratory findings were evaluated: patients' body temperature and meningeal symptoms; laboratory blood parameters, including RBC count, WBC count, concentrations of albumin and total protein; CSF parameters included cell count in 1 μl (lymphocytes, neutrophils, macrophages, plasma cells, monocytes, degenerated cells, granulocytes); RBC count, CSF glucose, protein, and lactate, CSF to serum glucose ratio (CSF/SGLU), CSF culture and microbiological examination. Presented CSF data were obtained from samples that were collected in the comparison group on the next day after surgery, and in the main group — on the day when meningitis was confirmed.

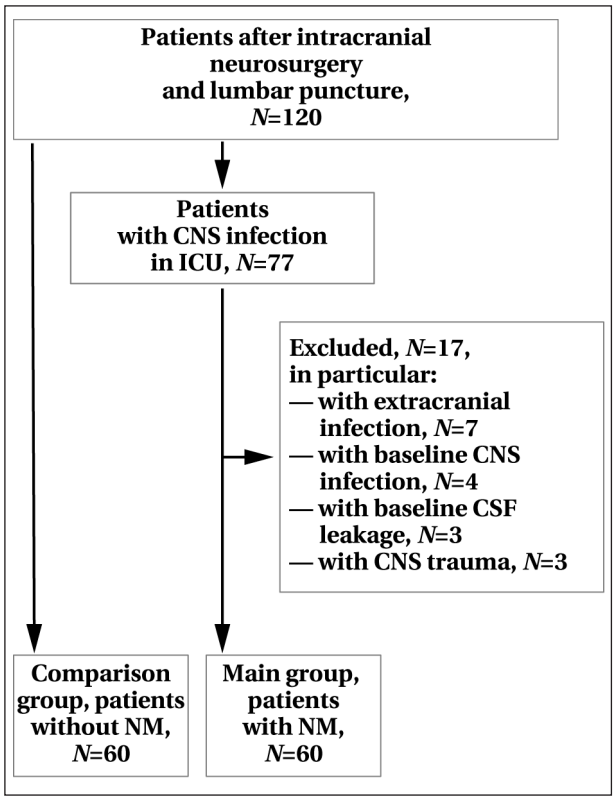

Fig. 1. Patient selection algorithm.
Notes. ICU — intensive care unit; NM — nosocomial meningitis.

The US Centers for Disease Control and Prevention (CDC) and N. N. Burdenko National Medical Research Center for Neurosurgery criteria for NM diagnosis were used in the study.

The diagnosis was based on the opinions of a neurosurgeon, an anesthesiologist-reanimatologist, and a clinical pharmacologist, following conclusions based primarily on CDC criteria. Surgical procedure in the comparison group was protected by perioperative antimicrobial prophylaxis (lasting less than 24 hours), while in the main group, antibacterial therapy was administered in subjects with complications of extracranial infectious.

For statistical data processing, descriptive and analytical statistics were employed: the Shapiro–Wilk test was used to check the data distribution for normality and select the method for comparison of the studied groups. The t-test was used to estimate intergroup comparability for age, and the Pearson's chi-square test was employed for processing categorical variables. The standard two-sided test of significance was used with a critical threshold of α=0.05. All comparisons, including sensitivity and specificity assessment of the features, AUROC and paired comparisons, were carried out with the assumption of a two-sided alternative hypothesis.

When calculating p-values, we used the built-in methods of Python statistical libraries, which are focused on classical two-sided testing. Collected data was used for determining sensitivity and specificity of a number of criteria. Statistical processing included correlation analysis with calculation of Spearman coefficients, point-biserial correlation, plotting of ROC curves with ROC AUC analysis, and estimation of optimal thresholds for a number of key parameters (body temperature, CSF cell count, glucose and lactate, CSF/SGLU). For determining the optimal cut-off points of a diagnostic feature, the Youden index was calculated as a summary measure of ROC analysis, using the formula:

$$J = \text{Sensitivity} + \text{Specificity} - 1.$$

The optimal threshold was determined as the point corresponding to the maximum value of the Youden index, which allowed for a balanced accounting of both sensitivity and specificity. When plottig ROC curves, we additionally calculated 95% confidence intervals (CIs) for the AUC using the DeLong algorithm; when the covariance matrix was unstable, we used bootstrapping (2000 iterations).

The following software and libraries were used for data processing: VS Code, Python programming language, and the following libraries: Pandas, NumPy, SciPy (Scipy.stats), Sklearn.metrics, and Matplotlib.pyplot.

Results

Assessment of samples representativeness showed no significant statistical differences in age (P=0.947) and gender (P=1.000) in the groups (Table 1).

The following calculated sensitivity and specificity values were obtained in the course of external validation of the CDC and N. N. Burdenko NMRCN criteria in the analyzed cohort of patients:

- CDC criteria: sensitivity — 81.67%, specificity — 83.33%;
- N. N. Burdenko NMRCN criteria:
  — probable NM: sensitivity — 81.67%, specificity — 88.33%;
  — confirmed NM: sensitivity — 51.67%, specificity — 100%.

Obtained results show that the highest diagnostic accuracy is achieved when using the N. N. Burdenko NMRCN criteria for probable NM. Meanwhile, the criteria for confirmed NM feature high specificity but low sensitivity.

Individual criteria sensitivity and specificity analysis. Sensitivity and specificity were calculated for criteria from the CDC and N. N. Burdenko NMRCN systems (Table 2).

In CDC criteria, the highest sensitivity was found for CSF protein concentration of >0.33 g/L (83.6%), although with extremely low specificity of 21%, and the highest specificity was found for CSF culture (100%).

In N. N. Burdenko NMRCN criteria for probable NM, the highest sensitivity was found for CSF cytosis

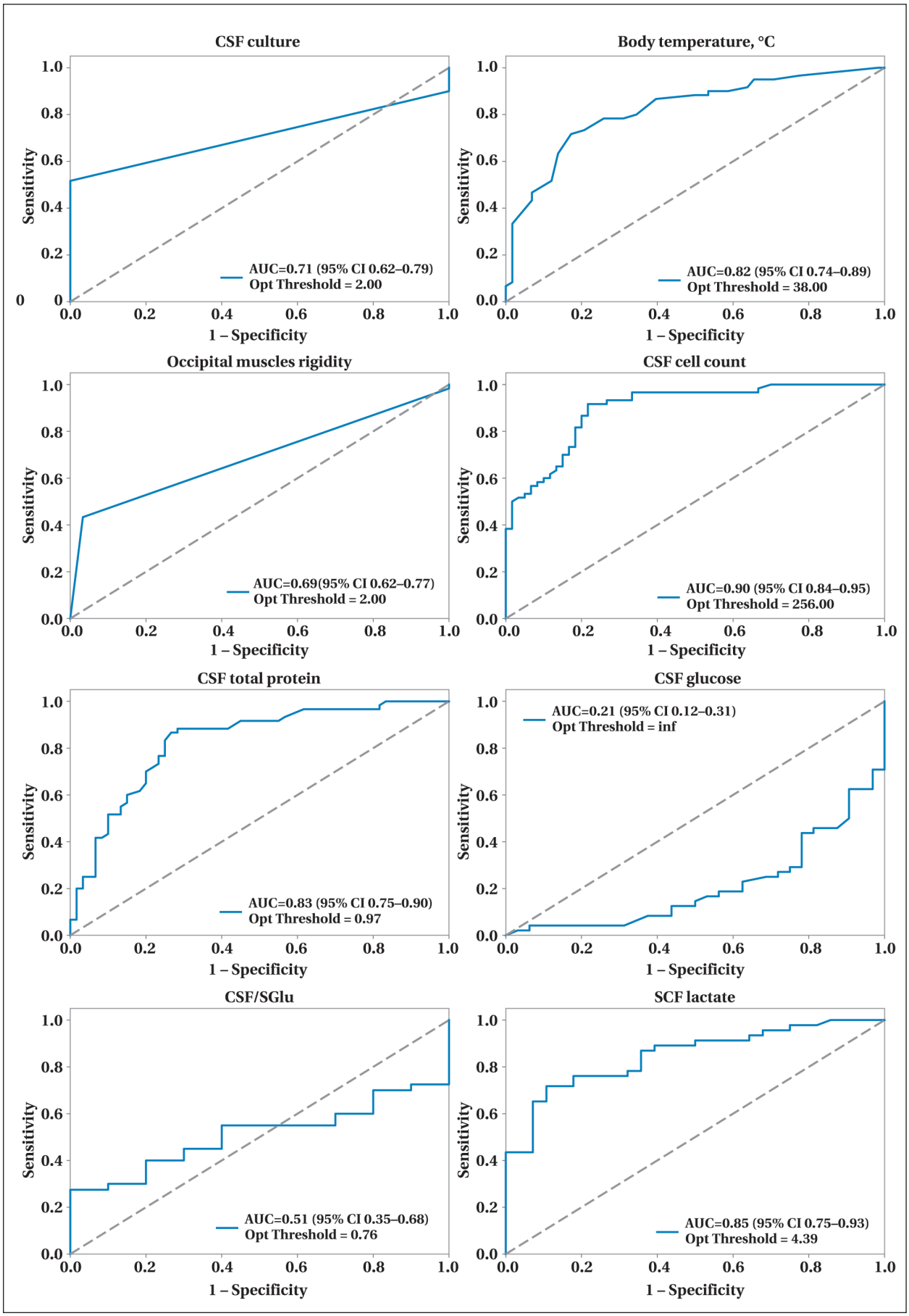

Fig. 2. ROC analysis of NM diagnostic criteria.

Table 2. Sensitivity and specificity of some diagnostic criteria.

Diagnostic criteria	Criteria	Sensitivity (%)	Specificity (%)	Accuracy (%)
CDC criteria	Positive CSF culture	69.2	100.0	79.6
	Body temperature >38°C	20.5	96.8	46.3
	Rigidity of the occipital muscles	53.6	92.6	66.8
	CSF cell count > 4 c/μl + > 50% of neutrophils	27, 5	58.2	37.9
	CSF protein > 0.33 г/л	83.6	21.5	62.6
	CSF glucose < 2.8 mmol/l	34.4	91.0	53.5
N. N. Burdenko NMRCN criteria for probable NM	Body temperature >38°C	20, 5	96.8	46.3
	Rigidity of the occipital muscles	53.6	92.6	66.8
	CSF cell count > 65	64.4	65.6	64.8
	CSF glucose < 2.6 mmol/l	29, 5	93.9	51.2
	CSF/SGLu ⩽ 0.45	29.2	96.8	52.0
	CSF lactate > 4.2 mmol/l	35.7	95.2	55.8
N. N. Burdenko NMRCN criteria for confirmed NM	Positive CSF culture	69.2	100.0	79.6
	Body temperature >38°C	20.5	96.8	46.3
	Rigidity of the occipital muscles	53.6	92.6	66.8
	CSF cell count > 65	95.2	51.1	80.3
	CSF glucose < 2.6 mmol/l	60.3	81.7	67.5
	CSF/SGLu ⩽ 0.45	61.3	90.4	71.1
	CSF lactate > 4.2 mmol/l	67.7	92.3	76.0

> 65 cells/μL (64.4%), and the highest specificity — for CSF glucose < 2.6 mmol/L (93.9%) and CSF/SGLU < 0.45 (96.8%). For confirmed NM, the maximum sensitivity was established for CSF cytosis > 65 cells/μL — 95.2%, although with 51% specificity. The highest specificity (92.3%) was found for CSF lactate > 4.2 mmol/L.

ROC-analysis. The selected cut-off points were used to compare different NM diagnostic criteria, and were not used for clinical stratification of patients.

The plotted ROC curves are presented in Fig. 2.

To assess the accuracy of the diagnostic criteria, the AUC 95% CI was calculated. The increases in CSF cytosis (AUC=0.9; 95% CI 0.84–0.95), CSF lactate (AUC=0.85; 95% CI 0.75–0.93), CSF total protein (AUC=0.83; 95% CI 0.75–0.9), and body temperature (AUC=0.82; 95% CI 0.74–0.89) showed good diagnostic value, while diagnostic value of CSF culture (AUC=0.85; 95% CI 0.75–0.93) was satisfactory. The presence of occipital muscle rigidity (AUC=0.69; 95% CI 0.66–0.79) showed a low diagnostic value. The predictive diagnostic ability of CSF glucose concentration and CSF/SGLU ratio (AUC=0.35–0.37; 95% CI included values < 0.50) was low.

The AUC values are presented in Table 3.

Correlation analysis. The correlation matrix revealed statistically significant relationships between particular laboratory and clinical parameters (Fig. 3).

The following parameters demonstrated the highest positive point-biserial correlation with the presence of NM:

- Positive CSF culture (*rpb*=0.522);
- Occipital muscles rigidity (*rpb*=0.415);
- Increased body temperature (*rpb*=0.415);
- Elevated CSF lactate (*rpb*=0.329);
- Increased CSF neutrophils count (*rpb*=0.249).

A reverse point-biserial correlation was found, in particular, for the CSF/SGLU ratio (*rpb*=–0.132) and CSF lymphocyte count (*rpb*=–0.242) (Table 4).

Therefore, the most clinically significant signs of NM were: increased CSF cytosis, increased concentrations of CSF lactate and CSF total protein, and fever.

Selection of NM predictor values. In the course of correction analysis, the thresholds of key laboratory and clinical signs included in the N.N. Burdenko NMRCN diagnostic criteria were optimized. Due to insufficient sensitivity and specificity of some initial criteria, the optimal threshold values for body temperature, CSF cytosis, CSF glucose and lactate were calculated using selection on a grid of values (Grid-search) method. The following optimal criteria were obtained:

- temperature > 37.7°C;
- CSF cell count > 245 cells/μL;
- CSF glucose < 2.0 mmol/L;
- CSF lactate > 3, mmol/L.

Using a combination of thresholds of all four parameters within the criteria allowed us to achieve: sensitivity: 90.00% (54 out of 60 patients with NM met the established optimal criteria), specificity: 91.67% (5 out of 60 patients without NM did not meet these criteria).

Discussion

The difficulties in diagnosing NM are due to many factors, including emergence of reactive CSF changes after intracranial surgery, the so-called «aseptic meningitis», presence of ICU specific microbial flora, recognized as the most common cause of NM, and interference of pre-analytical factors [17]. Relying on positive CSF culture — the gold standard for diagnosis — for verification of NM is not always

Table 3. Roc AUC analysis of some NM predictors.

Criteria	AUC	AUC 95% CI	AUC evaluation	Optimal value
Increased CSF cell count	0.90	0.84–0.95	Good	256
CSF lactate	0.85	0.75–0.93	Good	4.39
Total CSF protein	0.83	0.75–0.9	Good	0.97
Body temperature >38°C	0.82	0.74–0.89	Good	38
CSF culture	0.71	0.62–0.79	Satisfactory	Positive
Occipital muscle rigidity	0.69	0.62–0.77	Weak	Positive

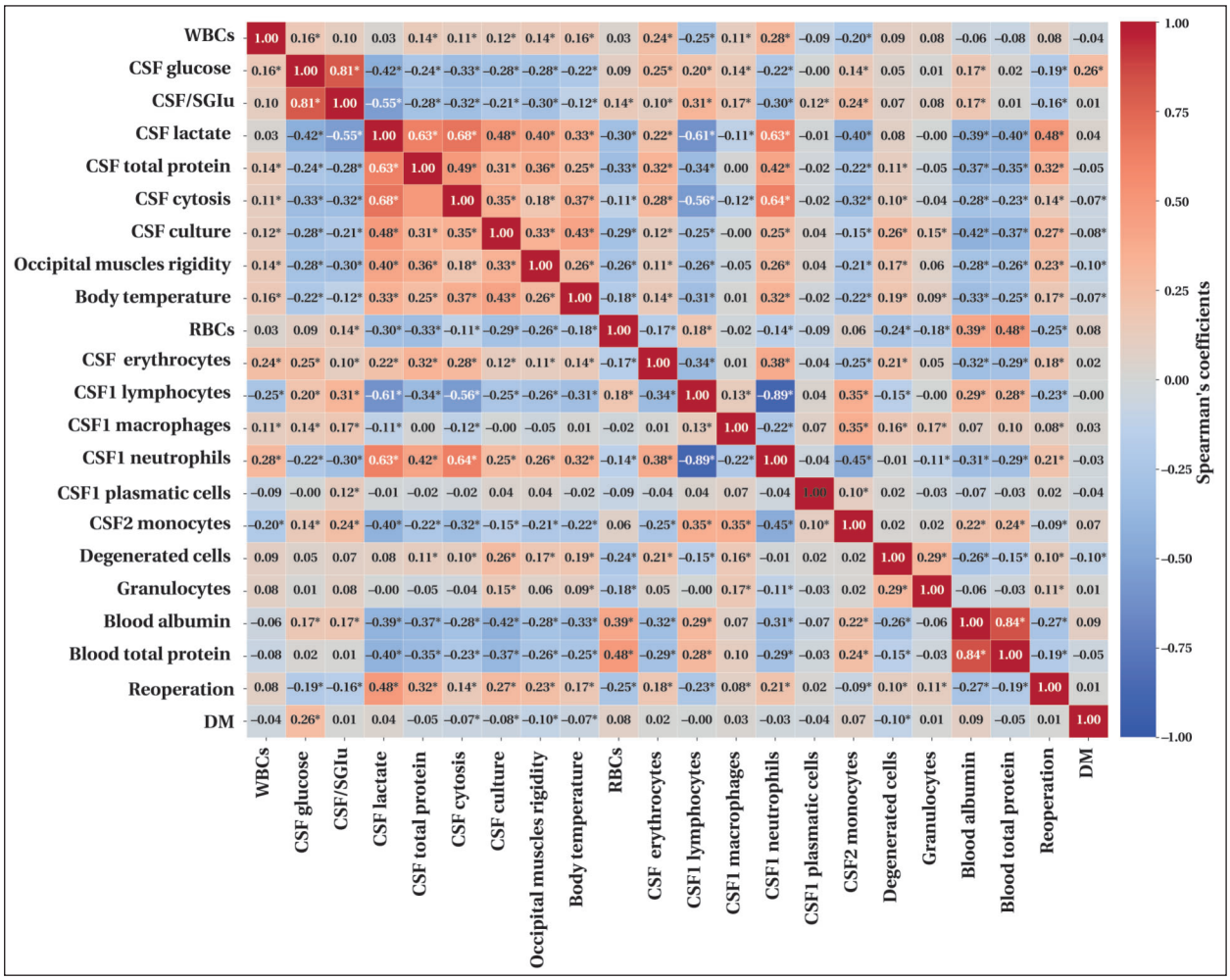

Fig. 3. Correlation matrix of clinical and laboratory parameters.
Note. Spearman's coefficients; * — $P<0.05$.

possible, as the condition necessitates initiation of antibiotic therapy within a limited timeframe, and because the culture growth can be suppressed by preceding antibiotic therapy or antibiotic prophylaxis [19]. These factors have led researchers to explore new ways to improve the diagnosis of NM.

Currently, the main indicators that should be considered in NM diagnosis have been identified, but their significance and diagnostic thresholds have not yet been definitively established [20]. According to our study, CSF cytosis and lactate showed the highest sensitivity among the laboratory data. In the absence of infection in the postoperative period, the interpretation of these parameters was complicated by a wide range of values. Different «cut-off points» for the diagnosis of NM have been described in available publications, ranging from 3.45 to 6 mmol/L for lactate concentration and from 4 to 1000 cells/μL for cytosis [21–25].

Good diagnostic significance was established for fever among clinical symptoms, and among laboratory findings — for increased CSF neutrophil count, CSF lactate and CSF total protein concentrations. Isolated decrease in CSF glucose and of CSF/SGlu ratio, traditionally used as markers of bacterial inflammation in the CNS, did not show statistical significance. It is possible that these deviations occurred because of glucose consumption by erythrocytes extravasated into cerebrospinal fluid. According to our observations, changes in

Table 4. Point–biserial correlation of clinical and laboratory parameters with the diagnosis of NM

Parameters	Point-biserial correlation coefficient rpb	*P*
CSF culture	0.522	0.0001
Occipital muscles rigidity	0.415	0.0001
Body temperature >38°C	0.415	0.0001
CSF lactate	0.329	0.0001
CSF neutrophil count	0.249	0.0001
Degenerated cell count	0.192	0.0001
WBCs	0.167	0.00030
CSF total protein	0.155	0.0001
CSF erythrocyte count	0.086	0.00982
Increased CSF cell count	0.079	0.01783
Re–operation	0.061	0.06503
CSF macrophage count	0.023	0.51205
Granulocyte count	–0.030	0.40659
CSF plasmatic cell count	–0.032	0.36858
Diabetes mellitus	–0.035	0.28835
CSF glucose	–0.055	0.17817
CSF/SGlu	–0.132	0.01007
CSF monocyte count	–0.143	0.00003
CSF lymphocyte count	–0.242	0.0001
Serum total protein	–0.250	0.00009
Serum albumin	–0.332	0.0001
RBCs	–0.347	0.0001

the glucose content of CSF in bacterial meningitis occur later than changes in other parameters.

High specificity of particular criteria (CSF culture, CSF/SGLU, and CSF lactate) allows to use them not only for confirmation, but also for ruling out the NM.

Study limitations. The study focused primarily on comparing diagnostic criteria rather than creating a definitive diagnostic model. Sensitivity, specificity, and AUROC were used for comparative analysis of existing clinical diagnostic thresholds rather than for determining new thresholds. Due to the limited number of patients, there was no objective method for selecting a comparison group. The sample size is planned to be expanded. This study was a pilot project.

Conclusion

The most clinically significant signs of NM are: elevated CSF lactate and CSF total protein, increase in CSF cell count, and fever. The «gold standard» for NM diagnosis, a positive CSF culture, showed a low sensitivity of 69.2%. When used in combination, the identified in the study threshold values of body temperature, cerebrospinal fluid (CSF) pleocytosis, CSF glucose, and CSF lactate have higher sensitivity and specificity versus previously used individual criteria.

References

1. *Corona-Nakamura A. L., Arias-Merino M. J., Ávila-Esparza E. I., Tolentino-Corona M. L., Cañedo-Castañeda C. C., Flores-Salinas H. E., Corona-Macías J. F., et al.* Ventriculitis due to multidrug-resistant gram-negative bacilli associated with external ventricular drain: evolution, treatment, and outcomes. *Front Neurol.* 2024; 15: 1384206.
DOI: 10.3389/fneur.2024.1384206. PMID: 38737346
2. *Курдюмова Н. В., Ершова О. Н., Савин И. А., Шифрин М. А., Данилов Г. В., Александрова И. А., Гаджиева О. А. с соавт.* Дренаж-ассоциированные менингиты у пациентов отделения нейрореанимации. Results пятилетнего проспективного наблюдения. *Вопросы нейрохирургии» имени Н. Н. Бурденко.* 2017; 81 (6): 56–63. 2. *Kurdyumova N. V., Ershova O. N., Savin I. A., Shifrin M. A., Danilov G. V., Aleksandrova I. A., Gadzhieva O. A., et al.* Drainage-associated meningitis in neurocritical care patients. The results of a five-year prospective study. *Burdenko's Journal of Neurosurgery = Zhurnal Voprosy Neirokhirurgii imeni N. N. Burdenko.* 2017; 81 (6): 56–63. (in Russ.).
DOI: 10.17116/neiro201781656-62.
3. *Siychan K., Piersiak M., Rubin J., Kozioł A., Tyliszczak M., Pawłowski M., Chojak R.* Regional and systemic complications following glioma resection: a systematic review and meta-analysis. *Neurosurg Rev.* 2025; 48 (1): 323.
DOI: 10.1007/s10143-025-03478-1. PMID: 40138052.
4. *Курдюмова Н. В., Усачев Д. Ю., Савин И. А., Ершова О. Н., Гаджиева О. А., Шифрин М. А., Данилов Г. В., с соавт.* Критерии лабораторной диагностики нозокомиального менингита у пациентов отделения реанимации и интенсивной терапии. Опыт пятилетнего проспективного наблюдения. *Вестник анестезиологии и реаниматологии.* 2021; 18 (5): 47–56. *Kurdyumova N. V., Usachev D.Yu., Savin I. A., Ershova O. N., Gadzhieva O. A., Shifrin M. A., Danilov G. V., et al.* Nosocomial meningitis laboratory criteria in ICU patients: 5-year surveillance. *Messenger of Anesthesiology and Resuscitation = Vestnik Anesthesiologii i Reanimatologii.* 2021; 18 (5): 47–56. (in Russ.).
DOI: 10.21292/2078-5658-2021-18-5-47-56.
5. *Chojak R., Koźba-Gosztyła M., Gaik M., Madej M., Majerska A., Soczyński O., Czapiga B.* Meningitis after elective intracranial surgery: a systematic review and meta-analysis of prevalence. *Eur J Med Res.* 2023; 28 (1): 184.
DOI: 10.1186/s40001-023-01141-3. PMID: 37291583.
6. *Zeggay A., Patry I., Chirouze C., Bouiller K.* Characteristics and outcomes of cerebrospinal fluid shunt and drain-associated infections. *Infect Dis Now.* 2023; 53 (3): 104665.
DOI: 10.1016/j.idnow.2023.104665. PMID: 36736666.
7. *Ramanan M., Shorr A., Lipman J.* Ventriculitis: infection or inflammation. *Antibiotics (Basel).* 2021; 10 (10): 1246.
DOI: 10.3390/antibiotics10101246. PMID: 34680826.
8. *Repplinger S., Jacquier H., Verret A., Berçot B., Munier A. L., Le Dorze M., Sonneville R., et al. The* Ventriculostomy-related infection score: an antibiotic stewardship tool in ventriculostomy-related infections. *Neurosurgery.* 2024; 97 (1): 223–233.
DOI: 10.1227/neu.0000000000003300.
PMID: 39636125.
9. *Bloch K., Hasbun R.* Central nervous system infections associated with neurologic devices. *Curr Opin Infect Dis.* 2021; 34 (3): 238–244.
DOI: 10.1097/QCO.0000000000000723.
PMID: 33741795.
10. *Zheng G., Shi Y., Sun J., Wang S., Qian L., Lv H., Zhang G., et al.* Clinical characteristics and predictors of mortality of patients with post-neurosurgical meningitis- a 900-cases cohort study. *Infect Drug Resist.* 2024; 17: 4853–4863.
DOI: 10.2147/IDR.S491379. PMID: 39524980.
11. Identifying Healthcare-associated Infections (HAI) for NHSN Surveillance. https://www.cdc.gov/nhsn/PDFs/pscManual/2PSC_IdentifyingHAIs_NHSNcurrent.pdf.
12. *Tunkel A. R., Hasbun R., Bhimraj A., Byers K., Kaplan S. L., Scheld W. M., van de Beek D., et al.* 2017 Infectious Diseases Society of America's clinical practice guidelines for healthcare-associated ventriculitis and meningitis. *Clin Infect Dis.* 2017; 64 (6): e34–e65.
DOI: 10.1093/cid/ciw861. PMID: 28203777.
13. *Bir R., Lackner P., Pfausler B., Schmutzhard E.* Nosocomial ventriculitis and meningitis in neurocritical care patients *J Neurol.* 2008; 255 (11): 1617–1624.
DOI: 10.1007/s00415-008-0059-8. PMID: 19156484.
14. *Mounier R., Lobo D., Cook F., Fratani A., Attias A., Martin M., Chedevergne K., et al.* Clinical, biological, and microbiological pattern associated with ventriculostomy-related infection: a retrospective longitudinal study. *Acta Neurochir (Wien).* 2015; 157 (12): 2209–2217.
DOI: 10.1007/s00701-015-2574-6. PMID: 26363898.
15. *Hasbun R.* Central nervous system device infections. *Curr Infect Dis Rep.* 2016; 18 (11): 34.
DOI: 10.1007/s11908-016-0541-x. PMID: 27686676.
16. *Karvouniaris M., Brotis A., Tsiakos K., Palli E., Koulenti D.* Current perspectives on the diagnosis and management of healthcare-associated ventriculitis and meningitis. *Infect Drug Resist.* 2022; 15: 697–721.
DOI: 10.2147/IDR.S326456. PMID: 35250284.
17. *Bedholm M., Blixt J., Glimåker M., Ternhag A., Hedlund J., Nelson D. W.* Cerebrospinal fluid cell count variability is a major confounding factor in external ventricular drain-associated infection surveillance diagnostics: a prospective observational study. *Crit Care.* 2021; 25 (1): 291.
DOI: 10.1186/s13054-021-03715-1 PMID: 34380543.
18. *Panic H., Gjurasin B., Santini M., Kutlesa M., Papic N.* Etiology and outcomes of healthcare-associated meningitis and ventriculitis- a single center cohort study. *Infect Dis Rep.* 2022; 14 (3): 420–427.
DOI: 10.3390/idr14030045. PMID: 35735755.
19. *Rogers T., Sok K., Erickson T., Aguilera E., Wootton S. H., Murray K. O., Hasbun R.* Impact of antibiotic therapy in the microbiological yield of healthcare-associated ventriculitis and meningitis. *Open Forum Infect Dis.* 2019; 6 (3): ofz050.
DOI: 10.1093/ofid/ofz050 PMID: 30899767.
20. *Djukic M., Lange P., Erbguth F., Nau R.* Spatial and temporal variation of routine parameters: pitfalls

in the cerebrospinal fluid analysis in central nervous system infections. *J Neuroinflammation*. 2022; 19 (1): 174.
DOI: 10.1186/s12974-022-02538-3. PMID: 35794632.

21. *Huy N. T., Thao N. T., Diep D. T., Kikuchi M., Zamora J., Hirayama K.* Cerebrospinal fluid lactate concentration to distinguish bacterial from aseptic meningitis: a systemic review and meta-analysis. *Crit Care*. 2010; 14 (6): R240.
DOI: 10.1186/cc9395. PMID: 21194480.
22. *Xiao X., Zhang Y., Zhang L., Kang P., Ji N.* The diagnostic value of cerebrospinal fluid lactate for post-neurosurgical bacterial meningitis: a meta-analysis. *BMC Infect Dis*. 2016; 16 (1): 483.
DOI: 10.1186/s12879-016-1818-2. PMID: 27618955.
23. *Wang Q., Wang Y., Yang Y., Kong Y., Peng Y.* The value of elevated cerebrospinal fluid lactate concentrations in post-neurosurgical bacterial meningitis. *BMC Neurol*. 2023; 23 (1): 377.
DOI: 10.1186/s12883-023-03428-8. PMID: 37864165.
24. *Dorresteijn K. R. I. S., Verheul R. J., Ponjee G. A. E., Tewarie R. N., Müller,M. C. A., van de Beek D., Brouwer M. C., et al.* Diagnostic accuracy of clinical signs and biochemical parameters for external ventricular CSF catheter-associated infection. *Neurol Clin Pract*. 2022; 12 (4): 298–306.
DOI: 10.1212/CPJ.0000000000200059.
PMID: 36382125.
25. *Bao M. Y., Xie H. T., Gao P., Mao X., Li Z.Y., Wang W. H., Sopheak S., et al.* Current diagnosis and potential obstacles for post-neurosurgical bacterial meningitis. *Eur Rev Med Pharmacol Sci*. 2022; 26 (17): 6351–6360.
DOI: 10.26355/eurrev_202209_29661.
PMID: 36111937.

Received 24.06.2025
Accepted 02.10.2025

https://doi.org/10.15360/1813-9779-2025-5-2525

Neuroprotective Properties of Inhaled Argon-Oxygen Mixture after Photochemically Induced Ischemic Stroke

Ekaterina A. Boeva[1]*, Maxim V. Sutormin[1], Artem N. Kuzovlev[1], Maxim A. Lyubomudrov[1], Victor V. Moroz[1], Natalia I. Usoltseva[1], Oleg A. Grebenchikov[1]

[1] V. A. Negovsky Research Institute of General Reanimatology, Federal Research and Clinical Center of Intensive Care Medicine and Rehabilitology, 25 Petrovka Str., Bldg. 2, 107031 Moscow, Russia
[2] M. F. Vladimirsky Moscow Regional Research Clinical Institute 61/2 Shchepkin Str., 129110 Moscow, Russia

For citation: *Anastasia M. Tynterova, Ekaterina M. Moiseeva, Matvey S. Khoymov, Natalya N. Shusharina.* Predictive Markers of Functional Outcome in Subtypes of Ischemic Stroke. *Obshchaya Reanimatologiya = General Reanimatology.* 2025; 21 (5): 35–43. https://doi.org/10.15360/1813-9779-2025-5-2525 [In Russ. and Engl.]

***Correspondence to:** Ekaterina A. Boeva, eboeva@fnkcrr.ru

Summary

The aim of this study was to investigate the effects of three 60-minute inhalations of an argon-oxygen gas mixture (Ar 70%/O_2 30%) on the severity of neurological deficits, brain lesion volume, inflammatory and cellular responses, and cytokine levels in rats after photochemically induced ischemic stroke.

Materials and Methods. The experiment was performed in 21 male Wistar rats (250–300 g) randomly assigned to three groups: (1) ischemia + N_2 70%/O_2 30% inhalation (ischemia group, *N*=10); (2) ischemia + Ar 70%/O_2 30% inhalation (ischemia + iAr group, *N*=8); and (3) sham-operated animals (sham group, *N*=3). Neurological status was assessed over 14 days using the limb placement test. On day 14 post-ischemia, animals underwent magnetic resonance imaging (MRI), histological and immunohistochemical analyses, and RT-PCR using RNA extracted from the liquid homogenate of the entire brain to evaluate the relative levels of IL-1β, IL-6, and TNF mRNAs.

Results. Significant differences in limb placement test scores were observed between ischemia and ischemia + iAr groups on day 3 (7.3 [5.3; 10.4] vs. 9.9 [10.2; 13.2], *P*=0.045) and day 7 (8.0 [7.3; 9.2] vs. 10.0 [9.0; 11.5], *P*=0.027). MRI showed a significantly smaller ischemia volume in the ischemia + iAr group compared to the ischemia group (12.5 [8.5; 17.4] mm³ vs. 21.0 [17.5; 22.68] mm³, *P*=0.01). Pro-inflammatory cytokine levels were significantly lower following argon-oxygen inhalation: IL-1β — 205 [175.5; 247.5] in the Ischemia + iAr group vs. 328.5 [299; 347.5] in the Ischemia group (*P*=0.001); TNF — 110.5 [93.5; 113] vs. 149.5 [126.5; 176.5], respectively (*P*=0.001).

Conclusion. Repeated 60 min inhalation of argon-oxygen mixture (Ar 70%/O_2 30%) after photochemically induced ischemic stroke significantly reduces neurological impairment, modulates pro-inflammatory cytokine levels, and affects inflammatory and cellular responses.

Keywords: argon; ischemia; neuroprotection; photochemically induced stroke

Conflict of interest. The authors declare no conflict of interest.

Information about the authors/Информация об авторах:
Ekaterina A. Boeva/Екатерина Александровна Боева: http://orcid.org/0000-0002-0422-5018
Maxim V. Sutormin/Максим Викторович Сутормин: http://orcid.org/0009-0001-5563-0363
Artem N. Kuzovlev/Артем Николаевич Кузовлев: https://orcid.org/0000-0002-5930-0118
Maxim A. Lyubomudrov/Максим Алексеевич Любомудров: https://orcid.org/0000-0002-1735-592X
Victor V. Moroz/Виктор Васильевич Мороз: https://orcid.org/0000-0002-5030-5457
Natalia I. Usoltseva/Наталья Ивановна Усольцева: http://orcid.org/0000-0002-7269-6444
Oleg A. Grebenchikov/Олег Александрович Гребенчиков: https://orcid.org/0000-0001-9045-6017

Introduction

Stroke is a significant cause of morbidity and mortality. Multitudinous studies of stroke have been conducted, however, therapeutic options for patients remain limited [1]. Extensive research of ischemic stroke pathogenesis has shown that neuronal damage is caused by neuronal death, oxidative stress, and diverse immune responses [2–4]. The repair of neuronal damage caused by ischemic stroke involves various molecular pathways. Neuronal survival provides the stability and completeness of brain functions, and neuronal loss directly leads to neurological deficits [5–10]. Therefore, ensuring the protection and regeneration of neurons is a crucial step in effective recovering from neurological deficits. In addition, cellular responses involving expression of pro-inflammatory mediators provide the base for ischemic tissue damage [7, 8, 10]. It is widely recognized that targeted activation of microglia and resident immune cells of the central nervous system can inhibit damage and promote recovery after stroke. Excessive activation of the phagocytic phenotype of microglia leads to exacerbation of brain damage due to phagocytosis of still viable cells. Mi-

croglia with a phagocytic phenotype releases pro-inflammatory cytokines, which also exacerbates the damage. At the same time, microglia of the restorative phenotype release trophic and anti-inflammatory factors. This indicates that microglia are characterized by great heterogeneity [7, 8, 10]. Cellular reactions involving expression of pro-inflammatory mediators at the blood-endothelium interface, such as adhesion molecules, cytokines, chemokines, and leukocytes, significantly contribute to the pathogenesis of tissue damage in ischemic stroke [11, 13, 14]. Interleukins also play an important role in the development of ischemic stroke [11]. Interleukins are the cytokines. to regulate and mediate inflammatory and immune responses, and hematopoiesis [12].They play a crucial role in the processes of information transfer, activation and regulation of immune cells, mediating the activation, proliferation, and differentiation of T and B cells, as well as the cellular responses involving expression of pro-inflammatory mediators [11–13]. In particular, IL-1β stimulates activation of microglia, the main effector cells in cellular response, leading to secondary brain damage through stimulation of secretion and release of potentially neurotoxic molecules, such as TNF-α and iNOS [11–15].

The development of neuroprotective compounds is an urgent task for modern science. Argon represents one of promising candidate molecules as a potential neuroprotector [16–18].

The results of studies of various neuroprotective agents are contradictory. The potency of neuroprotective effect depends on the model used, the exposure time, and the anesthetic agent itself [16–18]. In this regard, the aim of this study was to establish whether an argon-oxygen mixture has a neuroprotective effect after three 60-minute inhalations following a photo-induced ischemic stroke, as well as to find out how the proposed inhalation technique affects the cellular response of the brain.

Material and Methods

The experiments were conducted on male Wistar rats weighing 250–300 g (*N*=21). Eight hours before the experiment, the animals were deprived of food, but they still had access to water. The study protocol was approved by the Local Ethics Committee of the Federal Scientific and Clinical Center for Intensive Care Medicine and Rehabilitology (No. 3/22/3 dated December 14, 2022). All experiments were conducted in accordance with Directive 2010/63/EU of the European Parliament and of the Council of the European Union on the protection of animals used in scientific research.

The rats were randomly assigned to three groups depending on the interventions:

— the control group included animals with ischemia receiving inhalation with a gas mixture of N_2 70%/O_2 30% (ischemia group, *N*=10);

— the experimental group included animals with ischemia and inhalation of Ar 70%/O_2 30% gas mixture (ischemia + iAr group, *N*=8);

— the sham-operated group included animals without ischemia and no anesthesia and gas inhalation (SO group, *N*=3).

Modeling of photo-induced ischemic stroke. The stroke model was reproduced using the standard method [19], and 6% chloral hydrate (300 mg/kg, intraperitoneal) was used as the anesthetic agent. Approximately 42±16 minutes after the onset of the stroke, when the animal regained consciousness and restored its thermoregulation, it was anesthetized (paracetamol 50 mg/kg, subcutaneously) and placed in the chamber. A fresh gas mixture was constantly supplied to the chamber at a flow rate of 3 L/min (at least 0.5 L/min per animal): for the Ischemia group, oxygen-air (O_2 30%), and for the Ischemia + iAr group, Ar 70%/O_2 30%. Standard wood shavings on chamber bottom were used for drainage of liquids. The animal remained in the chamber for 60 minutes. After this period, the animal's overall condition (alertness and mobility) was assessed, the animal was re-anesthetized with paracetamol (50 mg/kg, subcutaneously) and placed in a cage with access to water and food. O_2 and CO_2 levels in the chamber were continuously monitored throughout the experiment, using a multi-gas sensor from InertGas Medical LLC. After 24 hours, the rats were again exposed to inhalation for 60 minutes, the next procedure was performed 72 hours after the start of the experiment. The study used a gas mixture produced by AKELA-N LLC, Khimki, Russia.

Assessment of neurological status. In this study the Limb Placement Test (LPT) was used, following a protocol based on M. De Rieck et al. methodology [20], modified by Y. Yolkkonen et al. [21].

Assessment of brain damage. Brain MRI using a 7 T magnetic field and a 105 mT/m gradient system (BioSpec 70/30, Bruker, Germany) was performed in animals 14 days after induction of stroke. Anesthesia was provided with isoflurane (1.5–2 vol %). A standard rat brain imaging protocol was used, including T2-weighted images. Spin echo-based (RARE) pulse sequences (PS) were used with the following parameters: TR=6000 ms, TE=63.9 ms, slice thickness 0.8 mm, slice spacing step 0.8 mm, 256×384 matrix, resolution 0.164×0.164 mm/pixel. The scanning time for one animal was approximately 25 min. To analyze the extent of brain damage, we used graphical image analysis in the ImageJ program (National Institutes of Health image software, Bethesda, MD, USA). For this purpose, the area of intact tissue in the healthy (S1) and damaged (S2) hemispheres was determined separately, and the area of damage was calculated using the formula $\Sigma S = S1 - S2$, where ΣS is the area of damage on one section (mm^2). The volume of brain damage was calculated using the formula $V = \Sigma Sn \times d$, where d is the slice thickness

(0.8 mm), and ΣSn is the sum of brain damage areas on all sections (mm²).

Histological and immunohistochemical examination. For histological analysis on the 14th day after stroke brain samples were extracted from rats immediately after euthanasia (decapitation under chloral hydrate anesthesia) and fixed in 10% buffered formalin for 24 hours and then processed using standard paraffin techniques. Frontal sections 4 µm thick were stained with hematoxylin and eosin and Nissl's stain. Morphometric analysis was performed after creating digital images using a Nikon Eclipse Ni-U microscope (Japan) with ×4, ×10, ×20, ×40 lenses and a DS-RI2 camera. Measurements were performed using the NIS-Elements BR software from Nikon (Japan), analyzing morphological changes and determining the area of damage in the infarct zone and penumbra.

The sections were then deparaffinized in xylene and rehydrated through a series of ethanol solutions. High-temperature antigen retrieval was performed in a citrate buffer with a pH of 6 (Target Retrieval Solution, DAKO, Denmark). The cooled sections were washed three times in a phosphate buffer (PBS IHC Wash Buffer + Tween, Cell Marque, USA) for 5 minutes. Endogenous peroxidase was blocked with 3% hydrogen peroxide for 10 min, and Protein Block Serum-free (Abcam, UK) was used for 30 min to prevent non-specific antibody binding. The sections were then incubated at 37°C for one hour with one of following primary antibodies: rabbit Iba-1 (ab153696, 1:500) for microglia, Rabbit NeuN (ab177487, 1:200) for neurons, Anti-Caspase-3 (ab13847, 1:100) for apoptosis, and rabbit anti-Von Willebrand factor (ab 9378, 1:200) for angiogenesis, all diluted in Antibody Diluent (ab64211 Abcam, Great Britain). Secondary goat anti-rabbit/mouse antibodies Dako REAL EnVision Detection System (DAB Dako Antibody Diluent) or ImmPACT® Vector® Red Substrate Kit, Alkaline Phosphatase (AP) (SK-5105) were then employed as recommended by the manufacturer. The sections were stained with hematoxylin for 1–2 min, then sequentially dehydrated in 70, 96, and 100% alcohol, and cleared twice in xylene.

Extraction of RNA from animal brain tissue. RNA was extracted using the RNeasy MiniKit (QIAGEN, USA) according to the manufacturer's instructions. The entire brain of an animal weighing 25 mg was ground in liquid nitrogen using a pestle and mortar. 600 µL of RLT buffer (QIAGEN, USA) was added to the resulting homogenate, and was homogenized using a syringe with a 0.8 mm needle. The resulting lysate was centrifuged for 3 min at 16100 g, then, the supernatant was transferred to a new tube. 450 µl of 96% ethanol was added to it, and the solution was applied to the RNeasy column. To purify the RNA, the column was washed with 700 µl of RW1 buffer and 500 µl of RPE buffer twice. Elution was performed using 50 µl of RNase-free water. The eluted RNA was precipitated with the addition of sodium acetate (1/10 volume of 3M solution) and 96% ethanol (2.5 volumes), and then dissolved in 30 µl of deionized water without RNAs.

Reverse transcription and real-time PCR. Reverse transcription was performed using the SuperScript III kit from ThermoScientific (USA). A mixture of oligo (dT)18 (500 µg/ml) and 50 ng of random primers was prepared in a 1:1 ratio (1 µl), and 2 µg of total RNA, 1 µl of deoxyribonucleotide mixture (10 µM), and MQ were added to a volume of 12 µl. The mixture was heated at 65°C for 6 min and cooled on ice. Then, 4 µl of 5x-buffer, 2 µl of 0.1M DTT, 1 µl of reverse transcriptase (20 units), and 1 µl of MQ were added. The mixture was incubated at room temperature for 10 minutes to anneal the random primers, then at 43°C for 50 minutes, after which the reaction was terminated by heating to 70°C for 15 minutes for enzyme inactivation.

The Beacon Designer program was used to select primers for PCR, and the appropriate primer pairs were selected for analysis (Table 1). According to the conditions specified in Table 2, real-time PCR was performed in a BioRad iCycler amplifier (USA) with a mixture of the following composition: Mixture B (intercalating dye Eva Green + recessive dye ROX + Taq Pol + 25mM dNTP + buffer (provided by Sintol) — 10 µl, primers (mixture of 10 µM forward and reverse primers — 0.5 µl, MQ — 9.5 µl, reverse transcription product — 5 µl). During statistical processing the expression analysis results were normalized to the expression of the 18S rRNA gene. Statistical analysis was performed using GraphPad Prizm 8.0 software. The normality of variable distribution in the samples was assessed using the Shapiro–Wilk test. In the case of normal distribution, the data were presented as the mean value and standard deviation; in the case of non-normal distribution, the data were presented as the median and interquartile range *Me* [*Q1; Q3*]. The nonparametric Mann-Whitney *U* test was used to assess the difference between two groups in the presence of at least one sample with a non-normal distribution. To compare more than two groups, the Kruskal–Wallis test was used with a post hoc analysis using Dunn's criterion. In this case, the adjustment for multiple comparisons (Dunn's multiple comparisons test) was taken into account. A two-tailed significance level was used in all tests. Differences were considered statistically significant at $P<0.05$.

Results and Discussion

The limb placement test (LPT). No animals were withdrawn from the study for 14 days and no humane endpoint was reached. There were no lethal outcomes. When comparing the experimental groups with the SO group, the total LPT scores at each stage of the study were lower in the experimental

groups. Statistically significant differences were obtained between the Ischemia group and the Ischemia + iAr group on day 3 (7.2 [5.2; 10.5] vs 10.0 [9.7; 13.2], *P*=0.045) and day 7 (8.0 [7.3; 9.2] vs 10.0 [9.0; 11.5], *P*=0.027) (Fig. 1).

MRI examination of the brain. Based on MRI findings, the average volume of damage in the Ischemia + iAr group and the Ischemia group was 12.5 [8.5; 17.4] mm³ and 21.0 [17.5; 22.68] mm³, respectively. Statistically significant differences were found between the groups (*P*=0.01) (Fig. 2).

Histochemical assessment of ischemic brain damage. Nissl staining showed that the lesions were distinct and clearly demarcated from the surrounding area of the ischemic focus. The underlying white matter was partially affected. The newly formed barrier in the form of a glial scar was more definite in the Ischemia + iAr group. Also in the Ischemia + iAr group, full-blooded capillaries with endotheliocytes were identified, as well as abundant fibroblasts in the cellular infiltration zone. In the Ischemia group, there were practically no capillaries, and heterogeneous neurons (dark, with a hyperchromic nucleus, displaced nucleus and/or nucleolus) were identified in the penumbra zone (Fig. 3, *a*). A significantly smaller average width of the penumbra was found in the Ischemia + iAr group (*P*=0.039).

Immunohistochemical analysis of histological sections of the brain. According to the literature, NeuN can be located both in the nuclei of neurons and in the cytoplasm [22, 23]. NeuN-positive cells were found in the area of ischemic damage in both groups. However, in the penumbra zone, the number of NeuN-positive cells was significantly higher in the Ischemia + iAr group (Ischemia group 43 [35; 46], vs. Ischemia + iAr group 60 [51; 73], *P*=0.042) (Fig. 3, *d*). Outside the ischemic lesion, the number of NeuN-positive cells was also significantly higher in the Is-

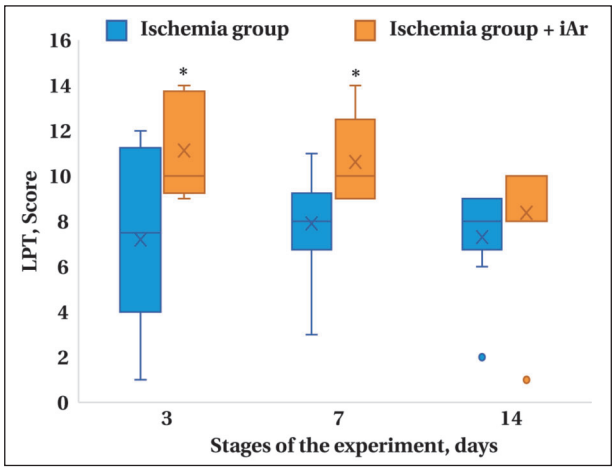

Fig. 1. LPT test. LPT test results on days 3,7, and 14 after ischemia modeling.
Note. * — statistically significant differences between the Ischemia and Ischemia + iAr groups. Data are presented as medians and quartiles [25%; 75%]. The ANOVA test was used to compare three or more groups.

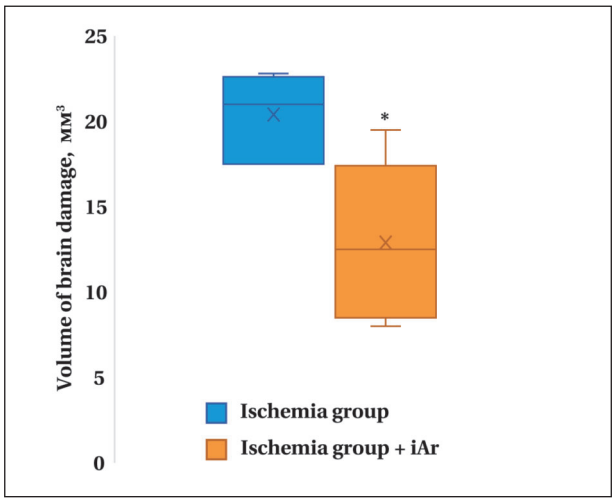

Fig. 2. Volume of brain damage on the 14th day of observation.
Note. Data are presented as medians and quartiles [25%; 75%]. * — statistically significant differences between groups.

Table 1. Sequences and main characteristics of primers used for real-time PCR.

Gene	Organism	Primer sequences (forward and reverse), 5'–3'	Annealing temperature, °C
18SrRNA	Rat	GACAGGATTGACAGATTGAT	56
		TTATCGGAATTAACCAGACAA	
TNF	Rat	TTATCTACTCCCAGGTTCT	56
		TGGTATGAAATGGCAAATC	
IL-1beta	Rat	AGAACATAAGCCAACAAGT	56
		ACACAGGACAGGTATAGAT	
IL-6	Rat	TGATTGTATGAACAGCGATGATG	58
		CCAGAAGACCAGAGCAGATT	

Table 2. Real time PCR protocol.

Period	Time	Temperature, °C	Number of cycles
Initiation	5 min	95	1
Denaturation	1 min	95	45
Denaturation	20 s	See Table 1	
Elongation	20 s	72	
	1 min	72	1
Obtaining the melting curve	30 s	Every 30 s the temperature increases by 0.5°C	45

chemia + iAr group, i. g. 250 [215; 353] cells in the Ischemia + iAr group vs 150 [45; 200] cells in the Ischemia group (P=0.043). Iba1 is a marker of microglia/macrophages [24–26]. A larger area occupied by Iba-1-positive cells was found in the Ischemia group compared to the Ischemia + iAr group (P=0.037). We could not differentiate these cells from systemic macrophages (Fig. 3, *b*). The area of vWF-positive staining in the Ischemia + iAr group was statistically significantly greater than in the control group, 0.23 [0.20; 0.29] vs. 0.15 [0.14; 0.18] (P=0.034). Quantitative analysis of Cas-3-positive cells showed a decrease in Cas-3-positive cells count in the Ischemia + iAr group compared to the Ischemia group, but the differences were not significant (Fig. 3, *c*).

Assessment of IL-1β, IL-6, and TNF mRNA content in the brain. Table 2 shows (real-time PCR data for IL-1β mRNA, IL-6 mRNA, and TNF mRNA in the rat brain homogenates after photo-induced brain ischemia modeling and treatment with Argox. The study revealed that the relative amount of IL-1β mRNA and TNF mRNA was significantly lower after exposure to an argon-oxygen mixture. Analysis of relative IL-6 mRNA amounts showed no significant difference between the groups. For the first time, it was shown that three 60-minute inhalations of an argon-oxygen mixture (Ar 70%/O_2 30%) after ischemic stroke exhibit neuroprotective properties due to their effect on cellular response. The model of ischemic stroke induced via occlusion of the middle cerebral artery is the most commonly used in experimental studies, but this method has limitations [1]. The photochemical thrombosis method is a relatively simple, reproducible model with minimal limitations and complications [27].

The only potential target for neuroprotective agents is the penumbra zone, involving cell response within and around it [28–30]. Our study showed that three 60-minute inhalations of argon-oxygen mixture in a photo-induced ischemic stroke model leads to a significant reduction in neurological deficit, a decrease in the volume of damage according to MRI findings, and a decrease in the average width of the penumbra according to histological findings. There are few studies that investigated the effect of argon-oxygen mixture on the models of photo-induced ischemic stroke using the immunohistochemical method. In this study, the effect of argon-oxygen mixture on microglia, neurons, apoptotic processes and angiogenesis processes was evaluated.

During a stroke or traumatic brain injury, massive neurons death occurs, partly caused by apoptotic processes. In oxygen and glucose deficiency, apoptosis pathways are activated, leading to widespread disruption of the nervous tissue structure and function. The extent of neuronal damage during ischemia is a crucial factor in determining the outcome. Oxidative stress, excitotoxicity, and cellular responses contribute to neuronal damage [28]. It was shown that the activity of apoptosis processes significantly decreases after exposure to an argon-oxygen mixture, as indicated by the dynamics of neuronal caspase-3 (Cas-3) content. Microglia plays a crucial role in cell proliferation and formation of glial scars after ischemic damage. It is also a source of pro- and anti-inflammatory agents in the brain [31]. Iba-1 staining was used to study microglia, as iba-1 is a marker for microglia/macrophages [9, 10].

Published studies [9, 10] report that the number of Iba-1+ cells peaked 4 days after ischemia and remained high after 8 days. A statistically significant decrease in the density of Iba-1-positive cells in the Ischemia + iAr group was shown, which suggests that microglia activity is reduced by the end of the second week after exposure to the argon-oxygen mixture. This is also supported by the statistically significant low level of Cas-3-positive cells. Identification of the type of macrophages seems to be very challenging. Microglia activation and increased capacity for phagocytosis occur in the first 24 hours after a stroke [9, 10].

Subsequently, it remains difficult to discern the identified macrophages as systemic, as the ischemic process leads to breakdown of the blood-brain barrier and release of macrophages from the vascular system [9, 10]. Specific neuronal markers, such as neuron-specific enolase, neurofilament proteins, and calbindin are used to differentiate neurons from glial cells in brain sections. NeuN protein is a splicing regulator. In this study, the number of NeuN-positive cells was significantly higher in the group receiving argon-oxygen inhalation. These data may indicate a greater number of preserved neurons in the damaged and the penumbra area, however, we cannot appreciate the functionality of these neurons.

Fahlenkamp et al. demonstrated that argon affects microglia activation in an in vitro model of LPS-induced inflammation in microglia cell cultures [31–33]. The results of these studies showed that argon suppresses the expression of the pro-inflammatory IL-1β gene. Another group of authors using a model of oxygen-glucose deprivation in cortical neuronal cell cultures showed that argon exposure reduces neuronal cell death by decreasing the expression of pro-inflammatory cytokines TNF-α and IL-6 [33]. Interleukins play a reversing role in ischemic damage by transmitting information, activating, and regulating immune cells. They also affect the activation, proliferation, and differentiation of T and B cells, as well as the activity of cellular responses that involve the expression of pro-inflammatory mediators [11]. In this study, the use of argon resulted in a statistically significant reduction in the expression of IL-1β and TNF-α genes. IL-1

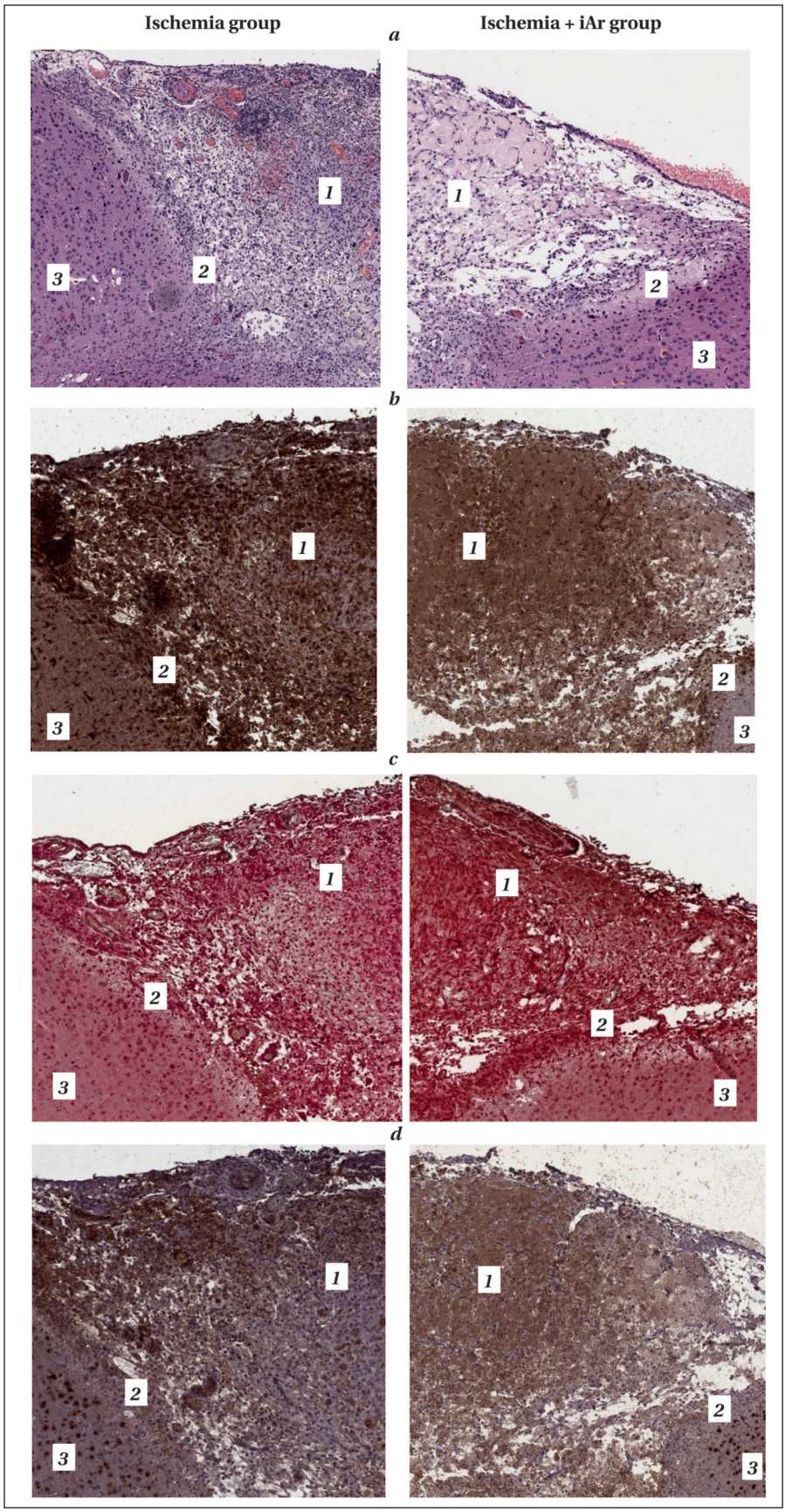

Fig. 3. Representative images of histological micro-preparations of rat brain.
Note. *1* — lesion; *2* — penumbra; *3* — undamaged tissue. *a* — stained with hematoxylin and eosin, ×20 magnification; *b* — Iba-1 staining, ×20 magnification; *c* — combined staining for von Willebrand factor (vWf): cells are stained red and caspase-3 (Cas-3) is stained brown; *d* — NeuN-positive cells.

can cause neurotoxicity indirectly through its action on vascular endothelium, promoting the recruitment of leukocytes, particularly neutrophils, which damage the neurovascular unit by releasing MMPs and reactive oxygen species (ROS) [11]. However, in the subacute and chronic phases after stroke, some effects of IL-1 may be beneficial. For example, IL-1 promotes glial scar formation and enhances angiogenesis, thereby contributing to recovery after ischemic stroke [11]. IL-1β is a member of the IL-1 family. Given that the expression level of the IL-1β gene was found to be above the normal values, its positive effect on the formation of scar tissue and new capillaries can be assumed, as evidenced by the large area of vWF-positive staining in the Ischemia + iAr group.

However, on the other hand, some studies have shown that IL-1β can influence the activation of the PI3K/AKT pathway, resulting in the production of IL-6 and other cytokines that affect ischemic areas and exacerbate the damage, activating apoptosis processes [11]. Nonetheless, when compared with the Ischemia group, the expression of the IL-1β gene was statistically significantly lower after exposure to the argon-oxygen mixture, indicating that its apoptotic effect was weaker than that of the oxygen-nitrogen mixture, as evidenced by the low number of Cas-3 positive cells in the Ischemia + iAr group. The results of this study showed that the IL-6 gene expression levels in the Ischemia + iAr group did not differ significantly from that in the Ischemia group. Some studies have shown that IL-6 favors neuronal survival in the central nervous system by reducing excitotoxic and NMDA-mediated damage to neurons, and by protecting neurons from apoptosis [12]. IL-6 demonstrates a dual effect in ischemic stroke, acting as a factor in the acute stage and as a neurotrophic mediator in the subacute and chronic phase [11, 12, 34, 35]. Thus, the argon-oxygen mixture in the model of photo-induced ischemic stroke reduces the severity of neurological deficit, decreases the lesion size according to MRI findings, reduces the expression level of pro-inflammatory cytokine genes, and also affects the cellular response according to histological and immunohistochemical findings.

Limitations of the study. One of the main limitations of the study was the use of chloral hydrate as an anesthetic during the ischemic stroke modeling stage because of limited choice of anesthetics as allowed by a local law. Other limitations include the relatively small number of animals in the groups, especially in the sham-operated group, which reduced the statistical power in several comparisons. Additionally, the study did not include a functional analysis of neuronal circuit preservation or an assessment of behavioral cognitive functions to further confirm the effectiveness of argon-oxygen therapy in a pre-clinical setting.

Conclusion

Three 60-minute inhalations of an argon-oxygen mixture (Ar 70%/O_2 30%) reduced the severity of neurological deficits in animals after ischemic stroke by influencing the cellular responses in the lesion and penumbra.

References

1. *Острова И. В., Бабкина А. С., Любомудров М. А., Гречко А. В., Голубев А. М.* Применение фотохимического тромбоза для моделирования ишемического инсульта (обзор). *Общая реаниматология*. 2023; 19 (3): 54–65. *Ostrova I. V., Babkina A. S., Lyubomudrov M. A., Grechko A. V., Golubev A. M.* Photochemically induced thrombosis as a model of ischemic stroke (review). *General Reanimatology = Obshchaya Reanimatologiya*. 2023; 19 (3): 54–65. (in Russ.&Eng.).
DOI: 10.15360/1813-9779-2023-3-54-65.
2. *Cipriani R., Domerq M., Martín A., Matute C.* Role of microglia in stroke. *Adv Neurobiol*. 2024; 37: 405–422.
DOI: 10.1007/978-3-031-55529-9_23. PMID: 39207705.
3. *Bitar L., Puig B., Oertner T. G., Dénes Á., Magnus T.* Changes in neuroimmunological synapses during cerebral ischemia. *Transl Stroke Res*. 2024.
DOI: 10.1007/s12975-024-01286-1. PMID: 39103660.
4. *Grinchevskaya L. R., Salikhova D. I., Silachev D. N., Goldshtein D. V.* Neural and glial regulation of angiogenesis in CNS in ischemic stroke. *Bull Exp Biol Med*. 2024.
DOI: 10.1007/s10517-024-06219-4. PMID: 39266920.
5. *Hakon J., Quattromani M. J., Sjölund C., Talhada D., Kim B., Moyanova S., Mastroiacovo F., et al.* Inhibiting metabotropic glutamate receptor 5 after stroke restores brain function and connectivity. *Brain*. 2024; 4; 147 (1): 186–200.
DOI: 10.1093/brain/awad293. PMID: 37656990.
6. *Takahashi S.* Metabolic contribution and cerebral blood flow regulation by astrocytes in the neurovascular unit. *Cells*. 2022; 11 (5): 813.
DOI: 10.3390/cells11050813. PMID: 35269435.
7. *Pinto M. J., Ragozzino D., Bessis A., Audinat E.* Microglial modulation of synaptic maturation, activity, and plasticity. *Adv Neurobiol*. 2024; 37: 209–219.
DOI: 10.1007/978-3-031-55529-9_12. PMID: 39207694.
8. *Guffart E., Prinz M.* Evolution of microglia. *Adv Neurobiol*. 2024; 37: 39–51.
DOI: 10.1007/978-3-031-55529-9_3. PMID: 39207685.
9. *Knezic A., Budusan E., Saez N. J., Broughton B. R.S., Rash L. D., King G. F, Widdop R. E., et al.* Hi1a improves sensorimotor deficit following endothelin-1-induced stroke in rats but does not improve functional outcomes following filament-induced stroke in mice. *ACS Pharmacol Transl Sci*. 2024; 7 (4): 1043–1054.
DOI: 10.1021/acsptsci.3c00328. PMID: 38638162.
10. *Jia J., Yang L., Chen Y., Zheng L., Chen Y., Xu Y., Zhang M.* The role of microglial phagocytosis in ischemic stroke. *Front Immunol*. 2022; 12: 790201.
DOI: 10.3389/fimmu.2021.790201. PMID: 35082781.
11. *Zhu H., Hu S., Li Y., Sun Y., Xiong X., Hu X., Chen J., et al.* Interleukins and ischemic stroke. *Front Immunol*. 2022; 13: 828447. DOI: 10.3389/fimmu.2022.828447. PMID: 35173738.
12. *Yuan S., Lin A., He Q.Q., Burgess S., Larsson S. C.* Circulating interleukins in relation to coronary artery disease, atrial fibrillation and ischemic stroke and its subtypes: a two-sample Mendelian randomization study. *Int J Cardiol*. 2020; 313: 99–104.
DOI: 10.1016/j.ijcard.2020.03.053. PMID: 32223966.
13. *Kong X., Gong Z., Zhang L., Sun X., Ou Z., Xu B., Huang J., et al.* JAK2/STAT3 signaling mediates IL-6-inhibited neurogenesis of neural stem cells through DNA demethylation/methylation. *Brain Behav Immun*. 2019; 79: 159–173.
DOI: 10.1016/j.bbi.2019.01.027.
14. *Jurcau A., Ardelean A. I.* Oxidative stress in ischemia/reperfusion injuries following acute ischemic stroke. *Biomedicines*. 2022; 10 (3): 574.
DOI: 10.3390/biomedicines10030574.
PMID: 35327376.
15. *Zhu H., Jian Z., Zhong Y., Ye Y., Zhang Y., Hu X., Pu B., et al.* Janus kinase inhibition ameliorates ischemic stroke injury and neuroinflammation through reducing NLRP3 inflammasome activation *via* JAK2/STAT3 pathway inhibition. *Front Immunol*. 2021; 12: 714943. DOI: 10.3389/fimmu.2021.714943. PMID: 34367186.
16. *Боева Е. А., Гребенчиков О. А.* Органопротективные свойств аргона (обзор). *Общая реаниматология*. 2022; 18 (5): 44–59. *Boeva E. A., Grebenchikov O. A.* Organoprotective properties of argon (review). *General Reanimatology = Obshchaya Reanimatologiya*. 2022; 18 (5): 44–59. (in Russ.&Eng.).
DOI: 10.15360/1813-9779-2022-5-44-59.
17. *Боева Е. А., Силачев Д. Н., Якупова Э. И., Милованова М. А., Варнакова Л. А., Калабушев С. Н., Денисов С. О., с соавт.* Изучение нейропротективного эффекта ингаляции аргон-кислородной смеси после фотоиндуцированного ишемического инсульта. *Общая реаниматология*. 2023; 19 (3): 46–53. *Boeva E. A., Silachev D. N., Yakupova E. I., Milovanova M. A., Varnakova L. A., Kalabushev S. N., Denisov S. O. et al.* Experimental study of neuroprotective properties of inhaled argon-oxygen mixture in a photoinduced ischemic stroke model. *General Reanimatology = Obshchaya Reanimatologiya*. 2023; 19 (3): 46–53. (in Russ.&Eng.).
DOI: 10.15360/1813-9779-2023-3-46-53.
18. *Бочарников А. Д., Боева Е. А., Милованова М. А., Антонова В. В., Якупова Э. И., Гречко А. В.* Оценка нейропротективных свойств анестетиков на моделях повреждения мозга. *Общая реаниматология*. 2024; 20 (2): 65–69. *Bocharnikov A. D., Boeva E. A., Milovanova M. A., Antonova V. V., Yakupova E. I., Grechko A. V.* Neuroprotection by anesthetics in brain injury models. *General Reanimatology = Obshchaya Reanimatologiya*. 2024; 20 (2): 65–69. (in Russ.&Eng).
DOI: 10.15360/1813-9779-2024-2-65-69.
19. *Silachev D. N., Uchevatkin A. A., Pirogov Y. A., Zorov D. B., Isaev N. K.* Comparative evaluation of two methods for studies of experimental focal ischemia: magnetic resonance tomography and triphenyltetrazoleum detection of brain injuries. *Bull Exp Biol Med*. 2009; 147 (2); 269–272.
DOI: 10.1007/s10517-009-0489-z.
20. *De Ryck M., Van Reempts J., Borgers M., Wauquier A., Janssen P. A.* Photochemical stroke model: flunarizine prevents sensorimotor deficits after neocortical infarcts in rats. *Stroke*. 1989; 20 (10); 1383–1390.
DOI: 10.1161/01.str.20.10.1383.
21. *Jolkkonen J., Puurunen K., Rantakömi S., Härkönen A., Haapalinna A., Sivenius J.* Behavioral effects of the

alpha (2)-adrenoceptor antagonist, atipamezole, after focal cerebral ischemia in rats. *Eur J Pharmacol.* 2000; 400 (2–3); 211–219.
DOI: 10.1016/s0014-2999 (00)00409-x.

22. *Anderson M. B., Das S., Miller K. E.* Subcellular localization of neuronal nuclei (NeuN) antigen in size and calcitonin gene-related peptide (CGRP) populations of dorsal root ganglion (DRG) neurons during acute peripheral inflammation. *Neurosci Lett.* 2021; 760: 135974. DOI: 10.1016/j.neulet.2021.135974.
23. *Zhu X., Yi Z., Li R., Wang C., Zhu W., Ma M., Lu J., Li P.* Constructing a transient ischemia attack model utilizing flexible spatial targeting photothrombosis with real-time blood flow imaging feedback. *Int J Mol Sci.* 2024; 25 (14): 7557.
DOI: 10.3390/ijms25147557. PMID: 39062800.
24. *Villa-González M., Rubio M., Martín-López G., Mallavibarrena P. R., Vallés-Saiz L., Vivien D., Wandosell F., et al.* Pharmacological inhibition of mTORC1 reduces neural death and damage volume after MCAO by modulating microglial reactivity. *Biol Direct.* 2024; 19 (1): 26.
DOI: 10.1186/s13062-024-00470-5. PMID: 38582839.
25. *Koukalova L., Chmelova M., Amlerova Z., Vargova L.* Out of the core: the impact of focal ischemia in regions beyond the penumbra. *Front Cell Neurosci.* 2024; 18: 1336886.
DOI: 10.3389/fncel.2024.1336886. PMID: 38504666.
26. *Chiang P. T., Tsai H. H., Yen R. F., Tsai Y. C., Wu C.H., Chiu C. H., Tsai L. K. in vivo* detection of poststroke cerebral cell proliferation in rodents and humans. *Ann Clin Transl Neurol.* 2024; 11 (2): 497–507.
DOI: 10.1002/acn3.51972.
27. *Chen W., Zhang Y., Yin M., Cheng Z., Li D., Luo X., Liu X., et al.* Circular R. N.A circPRDX3 mediates neuronal survival apoptosis in ischemic stroke by targeting miR-641 and NPR3. *Brain Res.* 2022; 1797: 148114. DOI: 10.1016/j.brainres.2022.148114.
28. *Kanemura Y., Yamamoto A., Katsuma A., Fukusumi H., Shofuda T., Kanematsu D., Handa Y., et al.* Human-induced pluripotent stem cell-derived neural progenitor cells showed neuronal differentiation, neurite extension, and formation of synaptic structures in rodent ischemic stroke brains. *Cells.* 2024; 13 (8): 671.
DOI: 10.3390/cells13080671. PMID: 38667286.
29. *Boyle B. R., Berghella A. P., Blanco-Suarez E.* Astrocyte regulation of neuronal function and survival in stroke pathophysiology. *Adv Neurobiol.* 2024; 39: 233–267.
DOI: 10.1007/978-3-031-64839-7_10. PMID: 39190078.
30. *Krenzlin H., Wesp D. M.A., Korinek A. A.E., Ubbens H., Volland J., Masomi-Bornwasser J., Weber K. J., et al.* Effects of argon in the acute phase of subarachnoid hemorrhage in an endovascular perforation model in rats. *Neurocrit Care.* 2024.
DOI: 10.1007/s12028-024-02090-3. PMID: 39174846.
31. *Moulson A. J., Squair J. W., Franklin R. J.M., Tetzlaff W., Assinck P.* Diversity of reactive astrogliosis in CNS pathology: heterogeneity or plasticity? *Front Cell Neurosci.* 2021; 15: 703810.
DOI: 10.3389/fncel.2021.703810. PMID: 34381334.
32. *Takamatsu H., Tatsumi M., Nitta S., Ichise R., Muramatsu K.,. Iida M., Nishimura S., et al.* Time courses of progress to the chronic stage of middle cerebral artery occlusion models in rats. *Exp Brain Res.* 2002; 146 (1): 95–102.
DOI: 10.1007/s00221-002-1147-0. PMID: 12192583.
33. *Qin C., Zhou L. Q., Ma X.T., Hu Z.W., Yang S., Chen M., Bosco D. B., et al.* Dual functions of microglia in ischemic stroke. *Neurosci Bull.* 2019; 35 (5): 921–933.
DOI: 10.1007/s12264-019-00388-3.
34. *Силкин В. В., Ершов В. И., Бурдаков В. В., Бирюкова Т. В., Бредихин А. Ю., Лозинская Т. Ю.* Математическое моделирование тяжелого ишемического инсульта с полиорганной недостаточностью: ретроспективное наблюдательное исследование. *Вестник интенсивной терапии имени А. И. Салтанова.* 2023; (1): 91–100. *Silkin V. V., Yershov V. I., Burdakov V. V., Biryukova T. V., Bredikhin A.Yu., Lozinskaya T.Yu.* Mathematical modeling of severe ischemic stroke with multiple organ failure: a retrospective observational study. *Ann Crit Care = Vestnik Intensivnoy Terapii im A. I. Saltanova.* 2023; (1): 91–100. (in Russ.).
DOI: 10.21320/1818-474X-2023-1-91-100.
35. *Авидзба А. Р., Саскин В. А., Киров М. Ю.* Гемодинамика и реперфузионная терапия при ишемическом инсульте: друзья или враги? *Анестезиология и реаниматология.* 2024; (2): 91–96. *Avidzba A. R., Saskin V. A., Kirov M. Y.* Hemodynamics and reperfusion in ischemic stroke: friends or foes? *Russ J Anesthesiol.Reanimatol = Anesteziologiya i Reanimatologiya.* 2024; (2): 91–96.
DOI: 10.17116/anaesthesiology202402191.

Received 07.11.2024
Accepted 29.04.2025
Online first 03.06.2025

https://doi.org/10.15360/1813-9779-2025-5-2528

Neuroprotective Potential of Lithium Chloride in a Model of Traumatic Brain Injury

Denis T. Sharikadze, Mikhail V. Gabitov*, Ivan V. Redkin, Artem N. Kuzovlev, Viktor V. Moroz

V. A. Negovsky Research Institute of General Reanimatology,
Federal Research and Clinical Center of Intensive Care Medicine and Rehabilitology,
25 Petrovka Str., Bldg. 2, 107031 Moscow, Russia

For citation: *Denis T. Sharikadze, Mikhail V. Gabitov, Ivan V. Redkin, Artem N. Kuzovlev, Viktor V. Moroz.* Neuroprotective Potential of Lithium Chloride in a Model of Traumatic Brain Injury. *Obshchaya Reanimatologiya = General Reanimatology.* 2025; 21 (5): 44–50. https://doi.org/10.15360/1813-9779-2025-5-2528 [In Russ. and Engl.]

***Correspondence to:** Mikhail V. Gabitov, gabitovmv@gmail.com

Summary

Aim: to investigate the neuroprotective properties of lithium chloride in a rat model of open traumatic brain injury (OTBI).

Materials and Methods. An open traumatic brain injury (OTBI) model was induced using the D. M. Feeney method. The study included 40 male Wistar rats divided into four groups: sham-operated animals (sham, *N*=10); an OTBI control group (control, *N*=10); a group receiving lithium chloride at a dose of 1.5 mmol/kg after OTBI (OTBI + lithium 63 mg/kg, *N*=10); and a group receiving lithium chloride at a dose of 0.5 mmol/kg after OTBI (OTBI + lithium 21 mg/kg, *N*=10). Cognitive and neurological functions were assessed using the Morris water maze and the forelimb placing test. Brain lesion volume was assessed by magnetic resonance imaging (MRI) on day 14 post-injury.

Results. Lithium chloride at 63 mg/kg administered 60 minutes after OTBI reduced brain lesion volume by 41.5% compared to the control group (*P*=0.001), while the 21 mg/kg dose reduced lesion volume by 27.5% (*P*=0.001). Lithium chloride at 63 mg/kg improved cognitive performance by 71% compared to the control group (P=0.009); the 21 mg/kg dose resulted in a 65% improvement (*P*=0.010).

Conclusion. Lithium chloride at doses of 21 mg/kg and 63 mg/kg has neuroprotective properties, significantly reduces brain lesion volume (as confirmed by MRI), alleviates neurological deficits, and thereby improves cognitive function in animals after OTBI.

Keywords: lithium; open traumatic brain injury; rat TBI model; lithium treatment

Conflict of interest. The authors declare no conflict of interest.

Information about the authors/Информация об авторах:
Denis T. Sharikadze/Денис Тамазович Шарикадзе: https://orcid.org/0000-0002-7288-4170
Mikhail V. Gabitov/Михаил Валерьевич Габитов: http://orcid.org/0009-0005-9615-6118
Ivan V. Redkin/Иван Валерьевич Редкин: http://orcid.org/0000-0001-7008-2038
Artem N. Kuzovlev/Артем Николаевич Кузовлев: http://orcid.org/0000-0002-5930-0118
Viktor V. Moroz/Виктор Васильевич Мороз: AuthorID (РИНЦ) 168246

Introduction

Trauma stays as unconquered challenge that affects overall morbidity. According to statistics, traumatic brain injury (TBI) ranks among the leading causes of death among the working-age population, which underscores the relevance of this issue for public health [1–6]. It is important to note that TBI results from various incidents, including traffic accidents, domestic injuries, and extreme sports injuries. Today, this remains relevant for both adults and children [7–9]. TBI is not just a disruption of brain functional integrity resulting from an external mechanical force. It is a complex and multifaceted pathophysiological processes involving many biochemical and cellular changes. Excitotoxicity is a pathophysiological term that explains the cause of neuronal damage and death due to action of neurotransmitters capable of hyperactivating NMDA and AMPA receptors. Today, several excitotoxins are known, such as glutamate, N-methyl-D-aspartate (NMDA), α-amino-methyl-isoxazole propionate (AMPA), kainate, and quisqualate. The resulting mitochondrial dysfunction is an important aspect of limiting the energy resources of cells, which exacerbates existing damage. In addition, oxidative stress, DNA damage, apoptosis, and neuronal death are part of a complex chain of secondary pathological processes that occur in TBI [10–18]. 76 billion is the current estimate of the average number of neurons in the human brain [19]. According to the latest published data, the number of glial cells is actually less than the number of neurons, resulting in the glial cell/neuron ratio of less than 1:1, rather than 10:1, as was incorrectly assumed for about 150 years [20]. The main goal of neuroprotection is to intervene in the pathological cascade, prevent cell death, and expand the boundaries of the «therapeutic window» for intensive care. As V. A. Negovsky, who considered it necessary to study such situations, wrote «when an organism protects itself from de-

struction», ... «forcing nature to respond, to find material evidence of this self-defense of the organism, the self-defense that developed in the process of animal evolution represents a big, but apparently worthwhile undertaking for the cause of revival!» [21].

Recent studies have shown the positive effect of lithium in preventing cell death from oxidative stress, its neuroprotective effects in a model of ischemic stroke, and its cardioprotective properties *in vivo* [22–24]. According to latest research, lithium is known to influence many pathological cascades and neuronal responses of the central nervous system, such as the Wnt signaling pathway, glycogen synthase kinase 3 (GSK-3), brain-derived neurotrophic factor (BDNF), mammalian target of rapamycin (mTOR), and glutamate receptors (GluR) [25–28]. Numerous studies demonstrated neuroprotective properties of lithium. This has been confirmed in experimental studies on rodents, *in vitro* cell cultures, and *in vivo* earthworms [29–31]. Lithium chloride has a protective effect in traumatic brain injuries and contributes to increased lifespan in animals under experimental conditions [32–36]. Lithium was initially used in gastroenterology but later found widespread acceptance in psychiatry. Today, interest in this drug continues to grow due to its antiviral effect and potential usefulness in treatment of conditions such as diabetes, obesity, osteoporosis, and sarcopenia [37, 38].

Lithium chloride is an inhibitor of GSK-3b, causing anti-apoptotic effects. Lithium prevents cell death from oxidative stress, its cardioprotective properties have been proven in an experimental model of myocardial infarction *in vivo*, and its neuroprotective effects in a model of ischemic stroke in rats. Thus, it can be assumed that lithium affects biological processes such as excitotoxicity, oxidative stress, and on-site neuronal cell death. A recent study found that the use of lithium chloride in safe doses (21 mg/kg and 63 mg/kg) immediately after modeling focal ischemia in rats contributed to a significant reduction in both the stroke focus and perifocal edema [39]. In addition, the content of p-GSK-3b in the ischemia zone significantly exceeded that in the control group when LiCl was used at the specified doses. The few existing studies analyzing the neuroprotective properties of lithium in TBI show promising results. It is important to note that in most experimental studies lithium salts were administered over a long period of time before TBI was simulated. This observation raises the question of the potential effectiveness of lithium when administered later, which could apparently lead to progress in the treatment of post-traumatic conditions. The aim of the study was to investigate the neuroprotective properties of lithium chloride in a model of open TBI (OTBI) in rats.

Material and Methods

Laboratory animals were kept in a vivarium at a temperature of 18–22°C, with humidity in individually ventilated cages ranging from 30 to 70%. The standard daily rhythm was 09.00–21.00, in accordance with GOST 33215-2014. The diet for laboratory rats included granulated complete feed and purified tap water, which was supplied ad libitum through nipple drinkers. Experimental studies were conducted in accordance with the guidelines for working with laboratory animals in preclinical studies (Recommendations of the European Economic Commission No. 33 of November 14,2023); European Union Directive on the Protection of Animals Used for Scientific Purposes 2010/63/EU, Article 14, paragraph 3; Federal Law No. 61-FZ of April 12, 2010 «On the Circulation of medicinal Products». The research protocol was approved by the Local Ethics Committee of the Federal Research and Clinical Center of Intensive Care Medicine and Rehabilitology No. 3/21/7 dated May 27, 2021. OTBI was simulated using D. M. Feeney weight drop injury model [40]. Intraperitoneal anesthesia with chloral hydrate at a dose of 300 mg/kg was used in all animals engaged in the experiment. The study included sexually mature male Wistar rats weighing 250–350 g (*N*=40), divided into 4 groups:

1. Sham — operated animals, that underwent anesthesia and preparatory measures with the application of a burr hole (SO, *N*=10).

2. A control group of animals that received a single intravenous injection of 0.9% sodium chloride solution at a dose of 1.5 ml/kg into a tail vein 60 minutes after OTBI modelling (Control, *N*=10).

3. Animals that received a single intravenous injection of 4.2% lithium chloride solution at a dose of 63 mg/kg into the tail vein 60 minutes after OTBI modelling (OTBI + Lithium 63 mg/kg, *N*=10).

4. Animals that received a single intravenous injection of 4.2% lithium chloride solution at a dose of 21 mg/kg into the tail vein 60 minutes after OTBI modelling (OTBI + Lithium 21 mg/kg, *N*=10).

Modeling of OTBI under general anesthesia. Preparation of the surgical field: the skin on the rat's head was carefully shaved and treated with an antiseptic (0.05% chlorhexidine solution); to ensure surgical access, the animal was fixed in a stereotactic frame, the head was secured and an incision was made in the skin. Cranial trepanation: using a 5 mm diameter drill cutter, an opening was created in the parietal and frontal areas of the skull above the left hemisphere (in the sensorimotor cortex area). The coordinates for trepanation were determined stereotaxically: 2.5 mm lateral to the sagittal suture and 1.5 mm caudal to the bregma. Induction of OTBI: the impact device for injury was placed strictly above the dura mater. The drop height of the impact

was 10 cm, and its weight was 50 g. Postoperative procedures: in the immediate postoperative period, the skin of the rat's head was sutured with Vicril 4–0 thread, and the intervention area was treated with a 5% solution of brilliant green. Waking period: the body temperature of laboratory animals was maintained at 37± 0.5°C using an electric heating pad. For postoperative pain relief, paracetamol was administered subcutaneously at a dose of 50 mg/kg.

Assessment of the neurological and cognitive status of laboratory animals in the post-traumatic period. Neurological deficits in laboratory animals were studied on the 7th day after modelling OTBI using the forelimb placing test. During the experimental study, scores were calculated and recorded in the logbook: 2 scores — the animal performed the test normally; 1 score — the animal performed the task with a delay of more than 2 seconds or incorrectly; 0 scores — the rat completely failed the test. The scores were summed for the analysis of the functional study [41]. The Morris water maze test was developed by Richard Morris in 1984 as a method for assessing cognitive functions such as spatial reasoning and navigation [42]. During the experimental work, the training of animals began on the 10th day after OTBI, and was continued over 4 days, during which the rats performed four attempts per day, each lasting at least 120 seconds. Testing of laboratory animals was carried out on the 14th day after OTBI modelling. The control parameters included several ratings, such as learning ability (the duration of the hidden platform search during each experiment), time entering the platform area, total time in the maze, and number of visits to the studied sector.

Assessment of the extent of brain damage in rats after OTBI. MRI of the rat brain (magnetic field 7 Tesla, gradient power 105 mT/m, Germany, BioSpec) was performed on the 14th day after OTBI. Pulse sequences are RARE (English: rapid acquisition with refocused echoes): repetition time 6000 ms, echo time 63.9 ms, slice thickness 0.8 mm, interval 0.8 mm, resolution 0.164×0.164 mm/pixel. The degree of brain damage was assessed using ImageJ software (National Institutes of Health image software, Bethesda, MD, USA). To calculate the brain lesion volume, the formula was used: $V=\Sigma Sn \times d$, where d is the thickness of the section, ΣSn is the total area of damage on 5 sections. Inhalation anesthesia with 1.5–2 vol.% isoflurane was used for rat brain MRI. Statistical analysis of experimental data was performed using GraphPad Software Prism (version 9.0.2; website www.graphpad.com, USA). The normality of data distribution was checked using the Shapiro–Wilk test. If the sample distribution differed from the normal, nonparametric criteria were used, the Mann–Whitney *U*-test for comparing continuous variables between two independent samples, when comparing more than two groups (for example, when assessing neurological deficit based on the forelimb placing test) — the Kruskal–Wallis test with Dunn's multiple comparisons. The results were presented in the form of medians and differences between the third and first quartiles, i. e. the interquartile range: *Me* — Median, *Q1* — first quartile, *Q3* — third quartile. Critical two-tailed *P*-value of less than 0.05 was considered statistically significant.

Results

MRI data revealed that the brain lesion volume in rats in the control group and the OTBI + Lithium 63 mg/kg group was 35.0 mm³ and 20.5 mm³, respectively (Table 1, Fig. 1). The statistical significance of the differences between the groups was *P*=0.001. Morphometric analysis of magnetic resonance imaging data revealed that the brain lesion volume in rats in the control group and the OTBI + Lithium 21 mg/kg group was 35.0 mm³ and 25.5 mm³, respectively (Fig. 2, Table 1). Assessment of neurological deficit based on the forelimb placing test yielded 7 scores in the control group, which was statistically significantly lower than in the sham-operated group (Table 2). Assessment of OTBI + Lithium 63 mg/kg group data totaled 11 scores, which is statistically significantly higher than in the control group (Table 2). In the OTBI + Lithium 21 mg/kg the score equaled 10, which was also statistically significantly higher than in the control group (Table 2). Cognitive functions in rats were studied on the 14th day after OTBI in the group of sham- operated animals (n=10), the control group (*N*=10), the group of OTBI + Lithium 63 mg/kg (*N*=10) and OTBI + Lithium 21 mg/kg (*N*=10). Morris water maze functional testing showed, that the latent period for finding the platform in sham-operated animals was 8 s [7–10], while in the control group it was more than twice as long — 17 s [15–19] (*P*=0.001), which indicated a significant deterioration in learning and spatial navigation ability in animals after traumatic brain injury. In the OTBI + Lithium 63 mg/kg group the latent period for finding the platform was 12 s [10–15] (*P*=0.009), which was statistically significantly lower than in the control group. In the OTBI + Lithium

Table 1. The brain lesion volume in rats in the study groups according to MRI findings on the 14th day of follow-up

Group	Brain lesion volume, mm³	*P*, significance relative to the	
		SO	Control
SO, *N*=10	12.0 [8.0–14.5]	—	<0.001
Control, *N*=10	35.0 [30–36]	<0.001	—
OTBI + Lithium 63 mg/kg, *N*=10	20.5 [17–22.5]	0.010	0.001
OTBI + Lithium 21 mg/kg, *N*=10	25.5 [21–29.5]	0.011	0.032

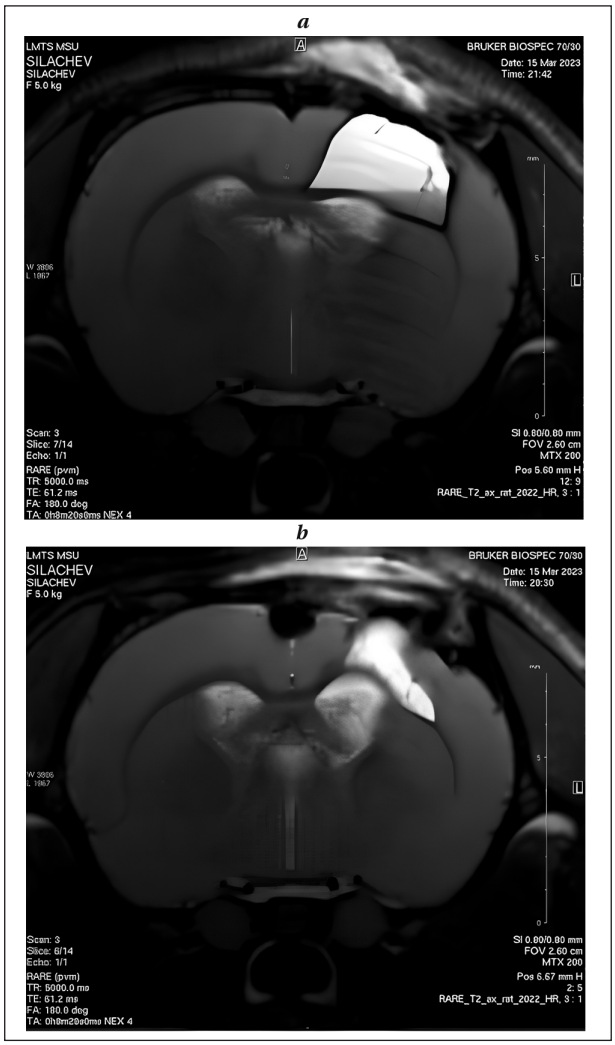

Fig. 1. MRI of the brain contusion area in rats on the 14th day after OTBI in the Control group *(a)* and OTBI + Lithium 63 mg/kg *(b)*.

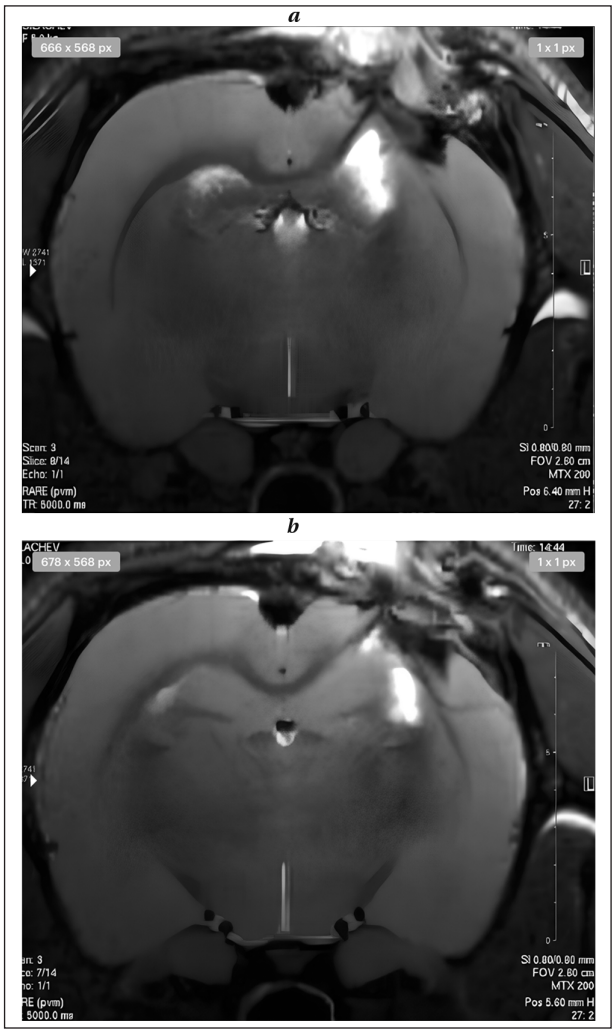

Fig. 2. MRI of the brain contusion area in rats on the 14th day after OTBI in the Control group *(a)* and OTBI + Lithium 21 mg/kg *(b)*.

21 mg/kg group, the latent period equaled 11 s [10–15] (P=0.011), which was also statistically significantly lower than in the control group. There were no removals from the study, no complications, no cases of reaching a humane endpoint and no deaths during all 14 days of the experiment. Animals were euthanized per study protocol by overdose of anesthetic (6% chloral hydrate solution).

Discussion

To study the potential neuroprotective properties of lithium chloride, a high reproducibility model was chosen. The basis for this study was the hypothesis that lithium has neuroprotective properties in a rat model of OTBI. The use of lithium chloride at a dose of 63 mg/kg 60 minutes after modelling OTBI reduced the brain lesion volume by 41.5% compared to the control group (P=0.001), while lithium chloride at a dose of 21 mg/kg, administered at the same time interval, reduced the brain lesion volume by 27.5% compared to the control group (P=0.001). Modeling of OTBI predictably caused neurological deficits in laboratory animals, and the use of lithium chloride at a dose of 63 mg/kg after 60 minutes statistically significantly reduced neurological deficits by 60% (P=0.010). Lithium chloride at a dose of 21 mg/kg also significantly changed the neurological status of rats by 43% (P=0.022). In a study by Yu Fengshan et al. on a model of traumatic brain injury in mice, lithium

Table 2. Assessment of neurological deficit using the forelimb placing test on the 7th day after OTBI.

Group	Neurological deficit, scores	*P*, significance relative to the	
		SO	Control
SO, *N*=10	14	—	<0.001
Control, *N*=10	7 [6–9]	<0.001	—
OTBI + Lithium 63 mg/kg, *n*=10	11 [9–12]	0.004	0.010
OTBI + Lithium 21 mg/kg, *n*=10	10 [9–11]	0.021	0.022

chloride was administered 15 minutes after injury. Comparable data were obtained [43], but the dose of the drug was twice as high. Thus, lithium at doses of 2.0 and 3.0 mmol/kg statistically significantly reduced the extent of brain damage 3 days after simulating traumatic brain injury. Treatment of laboratory animals with lithium chloride at a dose of 63 mg/kg statistically significantly improved the cognitive functions of rats by 71% compared to control animals (P=0.009), and in the group treated with lithium chloride at a dose of 21 mg/kg neurological parameters improved significantly by 65% (P=0.010). The results confirm our hypothesis about the neuroprotective properties of lithium chloride when administered late in conditions simulating OTBI. In a study by Zu-Fu Zhu et al., comparable data were obtained: lithium administration reduced edema and neurodegeneration in the hippocampus, improved memory and spatial learning after OTBI. However, unlike our study, lithium was administered daily for 2 weeks prior to TBI modelling [44]. In discussing the scientific and experimental work carried out, we would like to emphasize that the neuroprotective potential of lithium chloride in doses 0.5 mmol/kg and 1.5 mmol/kg 60 minutes after modelling OTBI was actioned, which was confirmed by the results of functional assessment of neurological deficits and cognitive functions of rats on the 7th and 14th day of the post-traumatic period.

Conclusion

Lithium chloride at doses of 21 mg/kg and 63 mg/kg has neuroprotective properties, reducing the brain lesion volume as shown by MRI, reducing neurological deficit and improving cognitive functions in rats. We believe that the results of our study indicate the need for further experimental research of the neuroprotective properties of lithium chloride in modeling traumatic brain injuries in laboratory animals, with an emphasis on identifying signaling pathways and molecular mechanisms of its action.

References

1. *Ключевский В. В., Литвинов И. И.* Практическая травматология: руководство для врачей. М.: Практическая медицина. 2020: 400. *Klyuchevsky V. V., Litvinov I. I.* Practical traumatology: physician's guide. Moscow: *Practical medicine = Prakticheskaya Meditsina*. 2020: 400. (in Russ.). ISBN 978-5-98811-610-3.
2. *Kaur P., Sharma S.* Recent advances in pathophysiology of traumatic brain injury. *Curr. Neuropharmacol.* 2018; 16 (8): 1224–1238. DOI: 10.2174/1570159X15666170613083606. PMID: 28606040.
3. *Сабиров Д.М, Росстальная А. Л., Махмудов М. А.* Эпидемиологические особенности черепно-мозгового травматизма. *Вестник экстренной медицины.* 2019; 12 (2): 2–3. 2. *Sabirov D. M., Rosstalnaya A. L., Makhmudov M. A.* Epidemiological features of cranial injury traumatism. *Bulletin of Emergency Medicine = Vestnik Ekstrennoy Meditsiny*. 2019; 12 (2): 2–3. (in Russ.).
4. *Аханов Г. Ж., Утеулиев Е. С., Дюсембеков Е. К., Нурбакыт А. Н., Попова Т. В.* Клинико-эпидемиологические аспекты черепно-мозговой травмы. *Вестник Казахского Национального медицинского университета.* 2018; 3: 113–116. *Akhanov G. Zh., Uteuliev E. S., Dyusembekov E. K., Nurbakyt A. N., Popova T. V.* Clinical and epidemiological aspects of traumatic brain injury. *Bulletin of the Kazakh National Medical University = Vestnik Kazakhskogo Natsionalnogo Meditsinskogo Universiteta*. 2018; 3: 113–116.
5. *Гаибов С. С.-Х., Захарчук Е. В., Воробьев Д. П.* Эпидемиология черепно-мозговой травмы у детей в условиях интенсивной урбанизации. *Российский педиатрический журнал*. 2020; 23 (3): 178–182. *Gaibov S. S.-Kh., Zakharchuk E. V., Vorobyev D. P.* Epidemiology of traumatic brain injury in children under dynamic urbanization conditions. *Russian Pediatric Journal = Rossiyskiy Pediatricheskiy Zhurnal*. 2020; 23 (3): 178–182. (in Russ.). DOI: 10.18821/1560-9561-2020-23-3-178-182.
6. *Рассказова В. Н., Кику П. Ф., Богданова В. Д., Волкова М. В., Палладова Л. М., Сухова А. В.* Актуальные проблемы детского травматизма и его профилактики. *Здравоохранение Российской Федерации.* 2022; 66 (2): 138–144. *Rasskazova V. N., Kiku P. F., Bogdanova V. D., Volkova M. V., Palladova L. M., Sukhova A. V.* Actual problems of childhood injuries and its prevention. *Healthcare of the Russian Federation = Zdravookhrneniye Rossiskoy Federatsii*. 2022; 66 (2): 138–144. (in Russ.). DOI: 10.47470/0044-197X-2022-66-2-138-144.
7. *Mira R. G., Lira M., Cerpa W.* Traumatic brain injury: mechanisms of glial response. *Front Physiol*. 2021; 22 (12): 740939. DOI: 10.3389/fphys.2021.740939. PMID: 34744783.
8. *Волков Е. В., Гандылян К. С., Карпов С. М., Елисеева Е. В.* Нейрофизиологические, цереброваскулярные и иммунологические аспекты формирования травматической болезни головного мозга у детей с сочетанной черепно-лицевой травмой. Ставрополь: СтГМУ. 2017: 107. *Volkov E. V., Gandylyan K. S., Karpov S. M., Eliseeva E. V.* Neurophysiological, cerebrovascular and immunological aspects of traumatic brain disease development in children with combined craniofacial trauma. Stavropol: StSMU. 2017: 107. (in Russ.). ISBN 978-5-89822-496-7.
9. *Немкова С. А.* Современные подходы к диагностике и лечению последствий черепно-мозговой травмы у детей и подростков. *Журнал неврологии и психиатрии имени С. С. Корсакова.* 2022; 122 (6): 20–29. *Nemkova S. A.* Modern approaches to the diagnosis and treatment of the consequences of traumatic brain injury in children and adolescents. *S.S. Korsakov Journal of Neurology and Psychiatry = Zhurnal Nevrologii i Psikhiatrii imeni S. S. Korsakova*. 2022; 122 (6): 20–29. (in Russ.). DOI: 10.17116/jnevro202212206120.
10. *Пиголкин Ю. И., Дубровин И. А., Леонов С. В., Горностаев Д. В.* Черепно-мозговая травма. Механогенез, морфология и судебно-медицинская оценка. М. 2018: 231. *Pigolkin Yu. I., Dubrovin I. A., Leonov S. V., Gornostaev D. V.* Traumatic brain injury. Mechanogenesis, morphology and forensic medical assessment. M. 2018: 231. (in Russ.). ISBN 978-5-534-12625-9.
11. *Усачёв Д. Ю., Лихтерман Л. Б., Кравчук А. Д., Охлопков В. А.* Нейрохирургия. Национальное руководство. Том II. Черепно-мозговая травма. М.: ФГАУ «Национальный медицинский исследовательский центр нейрохирургии им. акад. Н. Н. Бурденко» Министерства здравоохранения РФ. 2022: 30–59. *Usachev D. Yu., Likhterman L. B., Kravchuk A. D., Okhlopkov V. A.* Neurosurgery. National gidelines. Volume I. I. Traumatic brain injury. Moscow: FSAU «National Medical Research Center of Neurosurgery named after Academician N. N. Burdenko» of the Ministry of Health of the Russian Federation. 2022: 30–59. (in Russ.).
12. *Баранич А. И., Сычев А. А., Савин И. А., Полупан А. А., Ошоров А. В., Потапов А. А.* Коагулопатия, ассоциированная с острым периодом черепно-мозговой травмы. *Общая реаниматология.* 2020; 16 (1): 27–34. *Baranich A. I., Sychev A. A., Savin I. A., Polupan A. A., Oshorov A. V., Potapov A. A.* Coagulopathy associated in the acute phase of traumatic brain injury. *General Reanimatology = Obshchaya Reanimatologiya*. 2020; 16 (1): 27–34. (in Russ&Eng.). DOI: 10.15360/1813-9779-2020-1-27-34.
13. *Порядин Г. В.* Патофизиология: общая нозология и типовые патологические процессы. М. Медицинское информационное агентство. 2022: 247. *Poryadin G. V.* Pathophysiology: general nosology and typical pathological processes. M. Medical Information Agency. 2022: 247. (in Russ.). ISBN 978-5-9986-0472-0.
14. *Новицкий В. В., Кубатиев А. А., Пузырев В. П. Уразова О. И.* Патофизиология: учебник. М.: ГЭОТАР-Медиа. 2022: 591. *Novitsky V. V., Kubatiev A. A., Puzyrev V. P., Urazova O. I.* Pathophysiology: textbook. Moscow: GEOTAR-Media. 2022: 591. (in Russ.). ISBN 978-5-9704-6880-7.
15. *Саввина И. А., Баратов Б. И., Красненкова М. Б.* Патофизиология и интенсивная терапия тяжелой черепно-мозговой травмы: учебное пособие. СПб: Альгиз. 2019: 52. *Savvina I. A., Baratov B. I., Krasnenkova M. B.* Pathophysiology and intensive care of severe traumatic brain injury: a textbook. St. Petersburg: Algiz. 2019: 52. ISBN: 978–5-6044213-1-4.
16. *Берковиц А.* Клиническая патофизиология: проще не бывает. СПб: Диалект. 2021: 416. *Berkowitz A.* Clinical pathophysiology: it couldn't be simpler. SPb: Dialect. 2021: 416. ISBN 978-5-907203-96-9.
17. *Sussman E. S., Pendharkar A. V., Ho A. L., Ghajar J.* Mild traumatic brain injury and concussion: terminology and classification. *Handb Clin Neurol*. 2018; 158: 21–24. DOI: 10.1016/B978-0-444-63954-7.00003-3. PMID: 30482349.
18. *Беляевский А. Д., Лебедева Е. А., Белоусова М. Е.* Цитокины, оксидантный стресс и антиоксидантная защита при изолированной и сочетанной черепно-мозговой травме. *Общая реаниматология*. 2009; 5 (6): 36–39. *Belyaevsky A. D., Lebedeva E. A., Belousova M. Ye.* Cytokines, oxidative stress and antioxidant defense in isolated and concomitant brain injury. *General Reanimatology = Obshchaya Reanimatologiya*. 2009; 5 (6): 36–39. (in Russ.&Eng.). DOI: 10.15360/1813-9779-2009-6-36.
19. *Azevedo F. A. C., Andrade-Moraes C. H., Curado M. R., Oliveira-Pinto A. V., Guimarães D. M., Szczupak D., Gomes B. V., et al.* Automatic isotropic fractionation for large-scale quantitative cell analysis of nervous tissue. *J Neurosci Methods*. 2013; 212 (1): 72–78. DOI: 10.1016/j.jneumeth.2012.09.015. PMID: 23017980.
20. *Bartheld C. S., Bahney J., Herculano-Houzel S. J.* The search for true numbers of neurons and glial cells in the human brain: a review of 150 years of cell counting. *J Comp Neurol*. 2016; 524 (18): 3865–3895. DOI: 10.1002/cne.24040. PMID: 27187682.
21. *Заржецкий Ю. В., Волков А. В.* Некоторые вопросы патогенеза и терапии терминальных и постреанимационных состояний (экспериментальные исследования). *Общая реаниматология*. 2012; 8 (4): 55–58. *Zarzhetsky Yu.V., Volkov A. V.* Some problems of the pathogenesis and therapy of terminal and postresuscitation conditions

(experimental studies). *General Reanimatology = Obshchaya Reanimatologiya*. 2012; 8 (4): 55–58. (in Russ.&Eng.). DOI: 10.15360/1813-9779-2012-4-55.

22. *Мороз В. В., Силачев Д. Н., Плотников Е. Ю., Зорова Л. Д., Певзнер И. Б., Гребенчиков О. А., Лихванцев В. В.* Механизмы повреждения и защиты клетки при ишемии/реперфузии и экспериментальное обоснование применения препаратов на основе лития в анестезиологии. *Общая реаниматология*. 2013; 9 (1): 63–66. *Moroz V. V., Silachev D. N., Plotnikov E.Yu., Zorova L. D., Pevzner I. B., Grebenchikov O. A., Likhvantsev V. V.* Mechanisms of cell damage and protection in ischemia/reperfusion and experimental rationale for the use of lithium-based preparations in anesthesiology. *General Reanimatology = Obshchaya Reanimatologiya* 2013; 9 (1): 63–66. (in Russ.&Eng.). DOI: 10.15360/1813-9779-2013-1-63.
23. *Гребенчиков О. А., Черпаков Р. А., Евсеев А. К., Ершов А. В., Кузовлев А. Н., Лончинский П. А., Петриков С. С., соавт.* Влияние хлорида лития на летальность и неврологический дефицит при ишемическом инсульте у крыс. *Журнал им. Н.В. Склифосовского «Неотложная медицинская помощь»*. 2021; 10 (4): 676–686. *Grebenchikov O. A., Cherpakov R. A., Evseyev A. K., Ershov A. V., Kuzovlev A. N., Lonchinsky P. A., Petrikov S. S., et al.* Lithium chloride effect on mortality and neurological deficits in the model of ischemic stroke in rats. *Russian Sklifosovsky Journal «Emergency Medical Care» = Zhurnal im. N.V. Sklifosovskogo «Neotlozhnaya Meditsinskaya Pomoshch»*. 2021; 10 (4): 676–686. (in Russ.). DOI: 10.23934/2223-9022-2021-10-4-676-686b.
24. *Гребенчиков О. А., Лобанов А. В., Шайхутдинова Э. Р., Кузовлев А. Н., Ершов А. В.* Кардиопротекторные свойства хлорида лития на модели инфаркта миокарда у крыс. *Патология кровообращения и кардиохирургия*. 2019; 23 (2): 43–49. *Grebenchikov O. A., Lobanov A. V., Shaikhutdinova E. R., Kuzovlev A. N., Yershov A. V.* Cardioprotective properties of lithium chloride on a model of myocardial infarction in rats. *Pathology of Blood Circulation and Cardiac Surgery = Patologiya Krovoobrashcheniya i Kardiokhirurgiya*. 2019; 23 (2): 43–49. (in Russ.). DOI: 10.21688/1681-3472-2019-2-43-49.
25. *Junde Z., Tingting L., Lu Z., Shan C., Dan Y., Yizhen Z.* Lithium chloride promotes neural functional recovery after local cerebral ischaemia injury in rats through Wnt signalling pathway activation. *Folia Morphol (Warsz)*. 2023; 82 (3): 519–532. DOI: 10.5603/FM.a2022.0068. PMID: 35916382.
26. *Pan H.-Y., Valapala M.* Regulation of autophagy by the glycogen synthase kinase-3 (GSK-3) signaling pathway. *Int J Mol Sci*. 2022; 23 (3): 1709. DOI: 10.3390/ijms23031709. PMID: 35163631.
27. *Lu K.-T., Cheng N.-C., Wu, C.-Y. Yang Y.-L.* NKCC1-mediated traumatic brain injury-induced brain edema and neuron death via Raf/MEK/MAPK cascade. *Crit Care Med*. 2008; 36 (3): 917–922. DOI: 10.1097/ccm.0b013e31816590c4. PMID: 18431281.
28. *Xiao Y., Fan M., Jin W., Li W.A., Jia Y., Dong Y., Jiang X., et al.* Lithium chloride ameliorated spatial cognitive impairment through activating mTOR phosphorylation and inhibiting excessive autophagy in the repeated cerebral ischemia-reperfusion mouse model. *Exper Ther Med*. 2020; 20 (5): 109. DOI: 10.3892/etm.2020.9237. PMID: 32989388.
29. *Chen B., Zhang M., Ji M., Zhang D., Chen B., Gong W., Li X., et al.* The neuroprotective mechanism of lithium after ischaemic stroke. *Commun Biol*. 2022; 5 (1): 105. DOI: 10.1038/s42003-022-03051-2. PMID: 35115638.
30. *Barbisan F., Azzolin V. F., Teixeira C. F. Mastella M. H., Ribeiro E. E., do Prado-Lima P. A. S., Praia R. S., et al.* Xanthine-catechin mixture enhances lithium-induced anti-inflammatory response in activated macrophages in vitro. *Biomed Res Int*. 2017; 2017: 4151594. DOI: 10.1155/2017/4151594. PMID: 29250539.
31. *Mastella M. H., Roggia I., Turra B. O., Bonotto N. C. A., Teixeira C. F., Pulcinelli D. L. F., Meira G. M., et al.* The protective effect of lithium against rotenone may be evolutionarily conserved: evidence from eisenia fetida, a primitive animal with a ganglionic brain. *Neurochem Res*. 2023; 48 (12): 3538–3559. DOI: 10.1007/s11064-023-04001-y. PMID: 37526866.
32. *Araldi E., Jutzeler C. R., Ristow M.* Lithium treatment extends human lifespan: findings from the UK Biobank. *Aging (Albany N. Y.)*. 2023; 15 (2): 421–440. DOI: 10.18632/aging.206118. PMID: 36640269.
33. *Zhu Z.-F, Wang Q.-G., Han B.-J., William C. P.* Neuroprotective effect and cognitive outcome of chronic lithium on traumatic brain injury in mice. *Brain Res Bull*. 2010; 83 (5): 272–277. DOI: 10.1016/j.brainresbull.2010.07.008. PMID: 20638460.
34. *Dash P. K., Johnson D., Clark J., Orsi S. A., Zhang M., Zhao J., Grill R. J., et al.* Involvement of the glycogen synthase kinase-3 signaling pathway in TBI pathology and neurocognitive outcome. *PLoS One*. 2011; 6 (9): e24648.
35. *Yu F., Zhang Y., Chuang D.-M.* Lithium reduces BACE1 overexpression, β amyloid accumulation, and spatial learning deficits in mice with traumatic brain injury. *J Neurotrauma*. 2012; 29 (13): 2342–2351. DOI: 10.1089/neu.2012.2449. PMID: 18589444.
36. *Carlson S. W., Dixon C. E.* Lithium improves dopamine neurotransmission and increases dopaminergic protein abundance in the striatum after traumatic brain injury. *J Neurotrauma*. 2018; 35 (23): 2827–2836. DOI: 10.1089/neu.2017.5509. PMID: 29699444.
37. *Delangre E., Pommier G., Tolu S., Uzan B., Bailbe D., Movassat J.* Lithium treatment mitigates the diabetogenic effects of chronic cortico-therapy. *Biomed Pharmacother*. 2023; 164: 114895. DOI: 10.1016/j.biopha.2023.114895. PMID: 37224758.
38. *Li B., Wang W., Huang Y., Han L., Li J., Zheng N., Wu Z., et al.* Lithium treatment promotes the activation of primordial follicles through PI3K/Akt signaling. *Biol Reprod*. 2022; 107 (4): 1059–1071. DOI: 10.1093/biolre/ioac150. PMID: 35871551.
39. *Черпаков Р. А., Гребенчиков О. А.* Влияние концентрации хлорида лития на его нейропротекторные свойства при ишемическом инсульте у крыс. *Общая реаниматология*. 2021; 17 (5): 101–110. *Cherpakov R. A., Grebenchikov O. A.* Effect of lithium chloride concentration on its neuroprotective properties in ischemic stroke in rats. *General Reanimatology = Obshchaya Reanimatologiya*. 2021; 17 (5): 101–110. (in Russ.&Eng.). DOI: 10.15360/1813-9779-2021-5-101-110.
40. *Feeney D. M., Boyeson M. G., Linn R. T., Murray H. M., Dail W. G.* Responses to cortical injury: I. Methodology and local effects of contusions in the rat. *Brain Res*. 1981; 211 (1): 67–77. DOI: 10.1016/0006-8993 (81)90067-6. PMID: 7225844.
41. *Jolkkonen J., Puurunen K., Rantakömi S., Härkönen A., Haapalinna A., Sivenius J.* Behavioral effects of the α2-adrenoceptor antagonist, atipamezole, after focal cerebral ischemia in rats. *Eur J Pharmacol*. 2000; 400 (2–3): 211–219. DOI: 10.1016/s0014-2999 (00)00409-x. PMID: 10988336.
42. *Morris R. G. M.* Spatial localization does not require the presence of local cues. *Learning and Motivation*. 1981; 12 (2): 239–260. DOI: 10.1016/0023-9690 (81)90020-5.
43. *Yu F., Wang Z., Tchantchou F., Chiu C.-T., Zhang Y., Chuang D.-M.* Lithium ameliorates neurodegeneration, suppresses neuroinflammation, and improves behavioral performance in a mouse model of traumatic brain injury. *J Neurotrauma*. 2012; 29 (2): 362–374. DOI: 10.1089/neu.2011.1942. PMID: 21895523.
44. *Zhu Z.-F, Wang Q.-G., Han B.-J., William C. P.* Neuroprotective effect and cognitive outcome of chronic lithium on traumatic brain injury in mice. *Brain Res Bull*. 2010; 83 (5): 272–277. DOI: 10.1016/j.brainresbull.2010.07.008. PMID: 20638460.

Received 07.11.2024
Accepted 29.04.2025
Online first 03.08.2025

https://doi.org/10.15360/1813-9779-2025-5-2570

Neuroprotective Effect of Pharmacological Preconditioning with Dicholine Succinate in Experimental Ischemic Stroke in Rats

Igor A. Pomytkin[1]*, Marat A. Magomedov[2], Anna G. Demchenko[3], Maxim V. Balyazin[3,4], NikolayV. Shishkin[5], Rostislav A. Cherpakov[5]*, Vladimir N. Karkishchenko[1]

[1] Scientific Center for Biomedical Technologies, Federal Medical and Biological Agency, Svetlye Gory village, bldg 1, 143442 Krasnogorsk District, Moscow Region, Russia
[2] N.I. Pirogov City Clinical Hospital № 1, Moscow City Health Department, 8 Leninsky Ave., 119049 Moscow, Russia
[3] Academician Bochkov Medical Genetics Research Center 1 Moskvorechye Str., 115478 Moscow, Russia
[4] Scientific and Educational Resource Center for Cellular Technologies, Patrice Lumumba Peoples Friendship University of Russia, 6 Miklukho-Maclaya Str., 117198 Moscow, Russia
[5] Federal Research and Clinical Center of Intensive Care Medicine and Rehabilitology, 25 Petrovka Str., Bldg. 2, 107031 Moscow, Russia

For citation: *Igor A. Pomytkin, Marat A. Magomedov, Anna G. Demchenko, Maxim V. Balyazin, NikolayV. Shishkin, Rostislav A. Cherpakov, Vladimir N. Karkishchenko.* Neuroprotective Effect of Pharmacological Preconditioning with Dicholine Succinate in Experimental Ischemic Stroke in Rats. *Obshchaya Reanimatologiya = General Reanimatology.* 2025; 21 (5): 51–58. https://doi.org/10.15360/1813-9779-2025-5-2570 [In Russ. and Engl.]

***Correspondence to:** Igor A. Pomytkin, ipomytkin@mail.ru; Rostislav A. Cherpakov, rcherpakov@fnkcrr.ru

Summary

Ischemic stroke is currently considered as one of the most pressing public health issues. Despite the differences in underlying mechanisms of ischemic and ischemic-reperfusion damage to the nervous tissue, the ultimate percentage of disability depends on intervention effects on the penumbra zone. Dicholine succinate (DCS), a neuronal insulin-sensitizer, is a promising pharmacological agent for management and prevention of stroke consequences.

The aim of the study was to investigate the effect of pharmacological preconditioning with DCS on brain cell death in experimental ischemic stroke in rats.

Materials and methods. Ischemic stroke in rats (*N*=16) was modeled by injecting the vasoconstrictor endothelin-1 (ET-1) into the striatum. The effect of pharmacological preconditioning with DCS as the active substance was evaluated by measuring the area of brain infarction in brain sections stained with cresyl violet. The effect of DCS on glycolysis and oxidative phosphorylation in primary cultures of rat cerebellum cells was assessed by measuring the rate of extracellular acidification and the rate of oxygen uptake, respectively.

Results. DCS administration in the preconditioning mode for 7 days, once a day orally, at a dose of 50 mg/kg, reduces the maximum area of the brain infarction zone by 34% ($P<0.05$) compared to the control in the subsequent experimental ischemic stroke induced by ET-1 administration. Three-day incubation of rat cerebellum primary culture with 50 μM DCS does not affect the basal levels of glycolysis ($P=0.916$) and cellular respiration ($P=0.8346$), but increases cellular glycolytic reserve by 70.0% ($P<0.0001$) compared to the control.

Conclusion. For the first time, the neuroprotective effect of pharmacological preconditioning with the neuronal insulin-sensitizer DCS in ischemic stroke has been shown. Mechanism of DCS action associates with an increase in the glycolytic reserve of brain cells, i.e., with increased ability of preconditioned cells to produce ATP and lactate via glycolysis in case of acutely compromised oxidative phosphorylation.

Keywords: ischemic stroke; pharmacological preconditioning; dicholine succinate; neuroprotection; endothelin-1; rats; glycolysis; oxidative phosphorylation

Conflict of interest. The authors declare no conflict of interest.

Information about the authors/Информация об авторах:
Igor A. Pomytkin/Игорь Анатольевич Помыткин: https://orcid.org/0000-0002-8426-3371
Marat A. Magomedov/Марат Адессович Магомедов: https://orcid.org/0000-0002-1972-7336
Anna G. Demchenko/Анна Григорьевна Демченко: https://orcid.org/0000-0002-4460-7627
Maxim V. Balyazin/Максим Витальевич Балясин: https://orcid.org/0000-0002-3097-344X
Nikolay V. Shishkin/Николай Владимирович Шишкин: https://orcid.org/0009-0001-1621-4148
Rostislav A. Cherpakov/Ростислав Александрович Черпаков: https://orcid.org/0000-0002-0514-2177
Vladimir N. Karkishchenko/Владимир Николаевич Каркищенко: https://orcid.org/0000-0001-7145-0314

Introduction

Ischemic stroke is the main cause of disability in Russia and remains the third leading cause of death and disability worldwide [1]. Compromised blood supply due to embolism, thrombosis, or constriction of cerebral arteries leads to hypoxia, decrease of ATP and phosphocreatine levels, anoxic depolarization of neuronal membranes, release of glutamate, and development of glutamate excitotoxicity. Increased production of reactive oxygen species and inflammatory response of microglia after clot dissolution causes brain cells death and expansion of necrotic zone [2]. Even though the primacy of protecting neurons in the acute phase of stroke is evident, there is still no pharmacological solution to this problem, and successful preclinical trials of more than 1,000 candidate substances failed to prove reliable neuroprotection in clinical practice [3, 4]. Some success in this area was achieved after discovery of ischemic preconditioning, demonstrating reduced cell death in ischemic incident after a brief episode of non-lethal ischemia [5, 6].

The protective effect of ischemic preconditioning includes adaptation of cell metabolism to hypoxia, in particular, switching to increased anaerobic glycolysis as a source of ATP and partial shutdown of energy-consuming processes [7]. Activation of hypoxia-inducible factor 1 (HIF-1), which regulates the transcription of more than 700 genes, including genes for erythropoietin (EPO), vascular endothelial growth factor (VEGF), glycolytic enzymes, and the glucose transporter GLUT1, plays a central role in adaptation to ischemia [8, 9]. Insulin is a known alternative activator of HIF-1 under normoxic conditions [10]. Both insulin and hypoxia induce the transcription of common target genes that collectively promote adaptation to hypoxia/ischemia, including EPO, VEGF, GLUT1 genes, and glycolytic enzymes [11–16]. Additionally, there is limited evidence of insulin preconditioning effect. For example, intracerebroventricular insulin administration reduced hippocampal CA3 neuronal death in Mongolian gerbils in a subsequent episode of transient cerebral ischemia compared to placebo [17].

Based on these findings, preconditioning with agents that improve insulin signaling in the brain may represent a new approach to protecting neurons in ischemic stroke.

Dicholin succinate (DCS) is a salt of choline and succinic acid (Fig. 1, *a*) displaying features of neuronal insulin-sensitizer with the ability to increase phosphorylation of the insulin receptor in neurons in response to low suboptimal concentrations of insulin [18]. DCS prevents cognitive decline in rats under experimental chronic cerebral hypo-perfusion [18, 19].

Pretreatment with DCS significantly reduces the depletion rate of ATP macroergic bonds and phosphocreatine in the brain during subsequent episodes of global ischemia, as demonstrated using ^{31}P NMR *in vivo* [20]. However, the question of whether neuronal preconditioning with DCS can reduce brain cell death in ischemic stroke remains open.

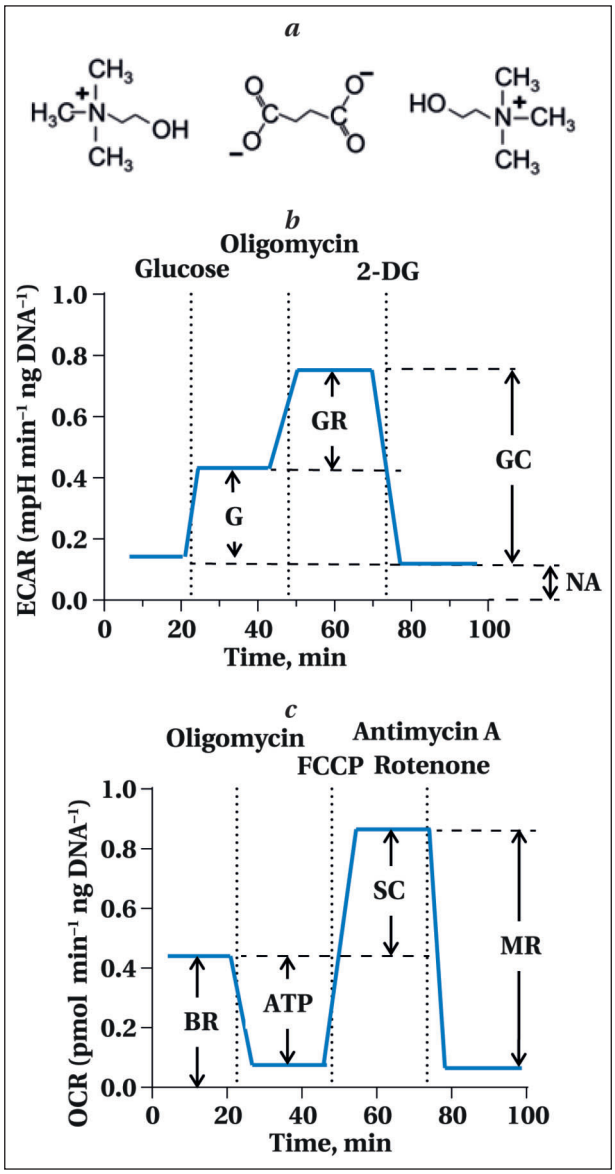

Fig. 1. Scheme for assessing the effect of DCS (*a*); on glycolysis indicators in the glycolytic stress test (*b*); and on oxidative metabolism indicators in the mitochondrial stress test (*c*).

The aim of this study was to investigate the effect of pharmacological preconditioning with DCS on brain cell death in experimental ischemic stroke in rats.

Material and Methods

Sigma-Aldrich (Merck, USA) materials were used in the study.

Modeling of ischemic stroke. Experiments were performed on male Wistar rats, weighing 200–250 g, obtained from the «Stolbovaya» branch

of the Federal State Budgetary Scientific Institution National Center for Biomedical Technologies (FSBSI NCBT) of the Federal Medical and Biological Agency (FMBA) of Russia, Moscow region. The animals were fed with standard granulated laboratory animal complete feed (extruded) PC-120 in accordance with GOST R 51849-2001 R.5. Tap water was provided ad libitum to all animals. The animals were kept in a controlled environment with air temperature of 18–22°C, a relative humidity of 60–70%, and indoor lighting with a 12/12 cycle.

The experiments were conducted in accordance with the «Principles of Good Laboratory Practice (GLP)», decree No. 202 of the Board of the Eurasian Economic Commission dated November 26, 2019, «On Approval of the Guidelines for Preclinical Safety Studies for Clinical Research and Drug Registration». All experiments were approved by the Bioethics Commission of the FSBSI NCBT, FMBA of Russia (Protocol No. 8 dated February 6, 2024).

16 animals were divided into two groups. Group 1 received normal saline (control), and Group 2 — DCS orally at a dose of 50 mg/kg in 1 ml of water through a gastric tube for 7 days before stroke induction. One day after the last administration of saline or DCS, rats were anesthetized with 2.0% isoflurane in a 70/30 volume ratio of nitrous oxide/oxygen, placed on a stereotactic frame, and maintained under 1–1.5% isoflurane anesthesia for the remainder of the procedure. The body temperature was monitored by a rectal probe, and normothermia was maintained with a heated blanket. A small hole was drilled in the skull. To induce ischemic brain damage, 1 µL of saline containing 25 pmol of endothelin-1 (ET-1) was injected into the left striatum for 2 minutes using a glass capillary needle (tip <50 µm). The following coordinates were used for stereotactic injections: anteriorly from the Bregma +1.0 mm, laterally +3.0 mm and +4.5 mm deep from the brain surface. 24 hours after ET-1 administration, rats were subjected to deep anesthesia and transcardial perfusion with heparinized saline followed by fixation with formalin solution. The brain was quickly extracted and frozen in isopentane cooled on dry ice. The striatum was divided into sections on a cryostat (20 µm thick sections) at 80 µm intervals. All sections were stained with cresyl violet. The area of the largest infarction zone was recorded.

Cerebellum cell culture. The cerebellum of 5–7 day-old Wistar rats was placed in a cold HBSS solution v/v with Ca^{2+}/Mg^{2+} and 1 mM sodium pyruvate, 10 mM Hepes, and was minced and incubated in a 0.5% trypsin-HBSS solution v/v Ca^{2+}/Mg^{2+} at 37°C for 15 minutes. The resulting cell suspension was washed twice with a cold HBSS solution and centrifuged at 1700 rpm for 3 minutes at +4°C. The precipitate was resuspended in standard Neurobasal Medium supplemented with B-27 Supplement (50X), 2 mM GlutaMax, 20 mM KCl, 100 units/mL of penicillin, and 100 µ/mL of streptomycin. Cells were seeded at a concentration of 1×10^5 cells per well in a standard 24-well Seahorse XF 24 plate pre-coated with polyethyleneimine, and cultivated at 37°C in the presence of 5% CO_2. Starting from the 7th day of incubation, 50 µM DCS or buffer (control) was added to the samples of the study group once a day for three consecutive days. 24 hours after the last DCS or buffer supplementation, cell metabolic activity was analyzed using the Seahorse XF 24 analyzer (Agilent Technologies) according to the manufacturer's instructions.

Assessment of metabolic activity. A standard protocol for the Seahorse glycolytic stress test (Aglient technologies) was used to assess the glycolytic activity of cells. The cells were previously washed twice with 500 µl Ng buffer (pH 7.4, 0.4 mM NaH_2PO_4, 3.5 mM KCl, 120 mM NaCl, 5 mM HEPES, GlutaMAX, 1.3 mM $CaCl_2$, 1 mM $MgCl_2$, 2 mM sodium pyruvate), then incubated with 500 µl Ng buffer for 40 minutes in a thermostat at 37°C without CO_2, after which the extracellular acidification rate (ECAR) was measured in accordance with the manufacturer's instructions. The basal level of glycolysis (G), glycolytic capacity (GC), glycolytic reserve (GR), and non-glycolytic acidification (NA) were measured by the sequential addition of glucose, oligomycin, and 2-deoxyglucose (2-DG), as shown in Fig. 1, *b*.

To assess oxidative phosphorylation, we used the standard mitochondrial stress test protocol (Seahorse Mito-stress test, Agilent technologies). The cells were previously washed twice with 500 µl Nm buffer (pH 7.4, 0.4 mM NaH_2PO_4, 3.5 mM KCl, 120 mM NaCl, 5 mM HEPES, GlutaMAX, 1.3 mM $CaCl_2$, 1 mM $MgCl_2$, 10 mM glucose), then incubated with 500 µl Nm buffer for 40 minutes in a thermostat at 37°C without CO_2, after which the oxygen consumption rate (OCR) was measured in accordance with the manufacturer's instructions. The basal respiratory rate (BR, basal respiration), maximal respiratory rate (MR, maximal respiration), ATP production (ATP), and spare capacity (SC) were measured by the sequential addition of oligomycin, protonophore FCCP, and antimycin A with rotenone, as shown in Fig. 1, *c*.

OCR and ECAR data were normalized by DNA. To do this, DNA was isolated from cells using the standard protocol the ReliaPrep™ gDNA Tissue (Promega) and quantified using the QuantiFluor® dsDNA fluorescent staining kit (Promega).

Statistical analysis was performed using the Student's unpaired two-way *t*-test, two-way analysis of variance (two-way ANOVA) with a posteriori Sidak's test for multiple comparisons between groups using GraphPad Prism v.8.3.0 software (San Diego, USA). The Shapiro–Wilk test was used to select parametric or nonparametric methods of statistical

analysis. The following symbols were used: *M* — mean, *m* — standard error, *n* — sample size, and *P* — achieved significance level. Differences were considered statistically significant at $P<0.05$.

Results

In order to find out whether pharmacological preconditioning using DCS as an active substance could affect the size of ischemic lesion in the brain after a subsequent episode of ischemia, male Wistar rats were administered DCS or saline orally once a day for 7 days. Ischemic stroke was induced by injection of a vasoconstrictor ET-1 into the striatum in 24 hours after the last administration of solutions. The infarct/ischemic lesion size was measured in brain sections obtained 24 hours after stroke induction (Fig. 2). Comparison of average values of greatest infarct sizes showed its' significant reduction by 34% after preconditioning with DCS ($P<0.05$) compared to the control.

Taken together, these results suggest that preconditioning with DCS may reduce brain cell death during subsequent episodes of ischemia.

In order to clarify whether the DCS neuroprotective effect is related to its effect on metabolism and, in particular, to glycolysis in brain cells, the primary culture of rat cerebellum cells was incubated for 3 days with added DCS or without it (control), after which extracellular acidification rate (ECAR) was measured in the presence of different additives (Fig. 3, *a*).

Glycolysis indicators expressed in ECAR units, such as the basic level of glycolysis (G), glycolytic capacity (GC), glycolytic reserve (GR) and non-glycolytic acidification of the medium (NA) are shown in Fig. 3, *b*. Two-way ANOVA revealed the presence of statistically significant differences between the groups by «glycolysis index» factor ($F_{3.157}=157.0$; $P<0.0001$), and the «DCS/control» factor ($F_{1.157}=52.28$; $P<0.0001$). A posteriori Sidak's test showed that DCS significantly increased glycolytic cell capacity by 50.5% ($P<0.0001$) and glycolytic reserve by 70.0% ($P<0.0001$) compared to the control, but did not affect basal glycolysis levels ($P=0.916$) or non-glycolytic acidification ($P=0.699$).

In order to find out whether DCS affects oxidative phosphorylation in brain cells, a primary culture of rat cerebellum cells was incubated for 3 days in the presence of DCS or without it (control), and then the oxygen consumption rate (OCR) was measured in the presence of the additives (Fig. 3, *b*). The oxidative metabolism parameters, such as the basal respiratory rate (BR), maximum respiratory rate (MR), ATP production (ATP), and spare respiratory capacity (SC), expressed in terms of OCR, are presented in Fig. 3, *c*. Two-way ANOVA revealed statistically significant differences between the groups in terms of the «oxidative metabolism index» ($F_{3,208}=249.0$; $P<0.0001$) and the «DCS/control» ($F_{1,208}=17.28$; $P<0.0001$). A posteriori Sidak's test showed that DCS significantly reduced the maximum respiratory rate by 19.4% ($P=0.0006$) and the spare respiratory capacity by 18.7% ($P=0.014$) compared to the control, but did

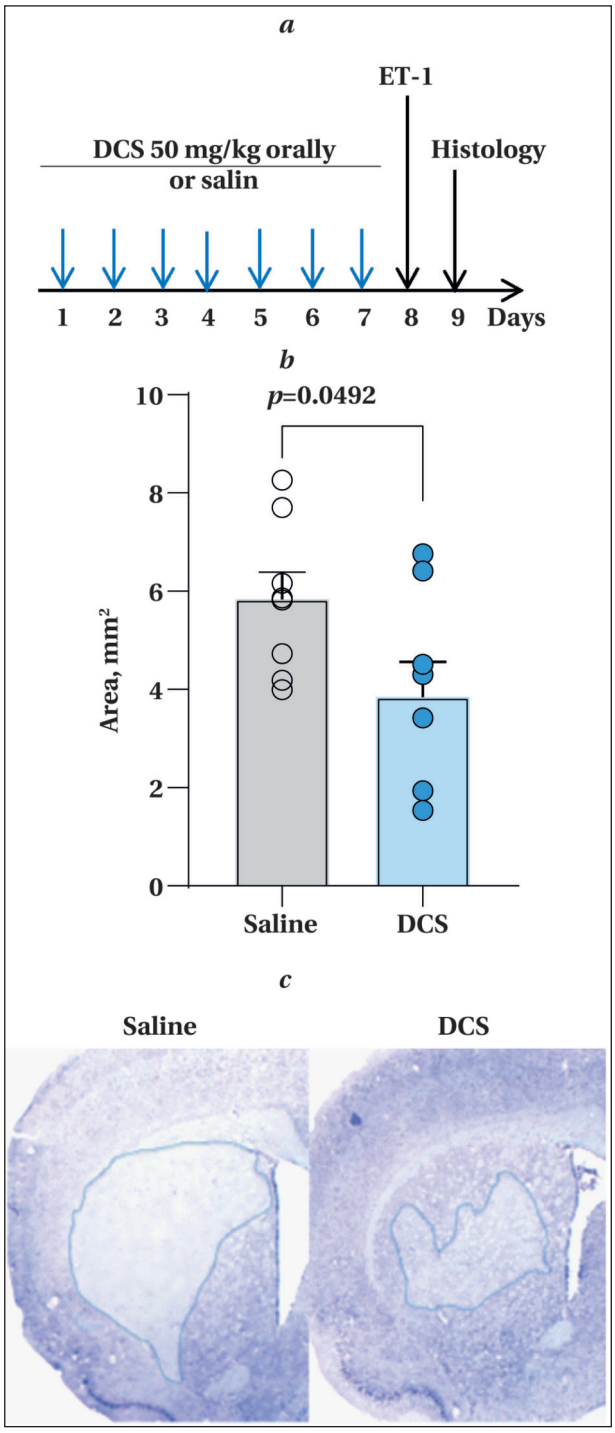

Fig. 2. The effects of pharmacological preconditioning using DCS as an active substance on the area and volume of the brain infarction zone in rats with stroke induced by ET-1 vasoconstrictor.

Note: *a* — experiment schedule; *b* — average areas of the maximum infarct zone, mm²; *c* — representative images of histological samples, stained with cresyl violet. The results were presented as *M*±*m* (*N*=8). * — $P<0.05$.

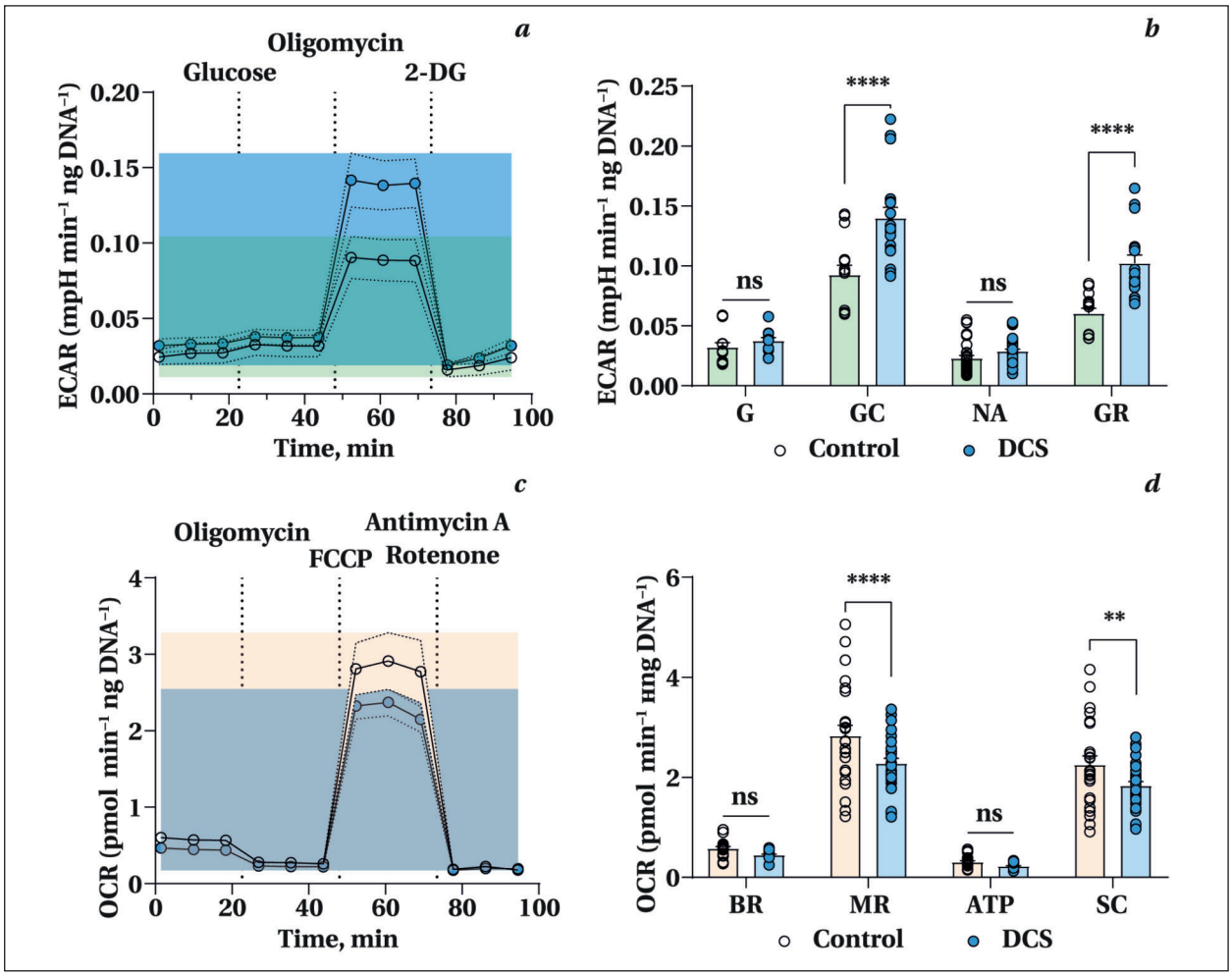

Fig. 3. DCS effect on glycolysis and oxidative metabolism in primary cultures of rat cerebellum cells, as analyzed by Seahorse.
Note. *a* — extracellular acidification rate (ECAR) in the presence of glucose, oligomycin, and 2-deoxyglucose (2-DG) additives; *b* — indicators of glycolysis: basal glycolysis level (G), glycolytic capacity (GC), glycolytic reserve (GR), and non-glycolytic acidification of the medium (NA); *c* — oxygen consumption rate (OCR) of cells in the presence of oligomycin, FCCP protonophore, and also rotenone and antimycin A, inhibitors of mitochondrial complexes I and III, respectively; *d* — indicators of oxidative metabolism – basal respiratory rate (BR), maximal respiratory rate (MR), ATP production (ATP) and spare capacity (SC). The results were presented as $M \pm m$ (N=15–30). ** — $P<0.01$; **** — $P<0.0001$; ns — not significant.

not affect the basal respiratory rate (P=0.8346) or ATP production (P=0.9596).

Taken together, these results show that pharmacological preconditioning using DCS builds up brain cells capacity to increase the rate of anaerobic conversion of glucose to lactate in milieu of acute oxidative phosphorylation deficiency, without affecting the baseline levels of glycolysis and oxidative metabolism.

Discussion

Pharmacological preconditioning is considered as an alternative to hypoxic preconditioning approach to protect brain cells under conditions of ischemia. As candidates for the role of pharmacological agents with a similar effect, compounds of different classes were investigated, including erythropoietin growth factor, volatile anesthetics (isoflurane), mitochondrial ATP-sensitive selective potassium channel opener diazoxide, iron chelator deferoxamine, opioids [21] and insulin [17]. In this study, it was shown that agents that improve insulin sensitivity (insulin sensitizers) can also be considered as potential neuroprotectors when used for preconditioning.

Dicholine succinate, a neuronal insulin sensitizer, is used as an active ingredient in a drug for treatment of ischemic stroke in the early recovery period [22, 23]. In this study, we demonstrated for the first time, that DCS administration to healthy animals for preconditioning was an effective way to reduce the size of brain infarct after subsequent episode of acute cerebrovascular accident.

The mechanism of DCS's preconditioning outcomes may be related to its metabolic effects. Although DCS did not affect the baseline levels of glycolysis and oxidative phosphorylation in the primary cell culture, it significantly increased the gly-

colytic reserve by 70%, which is the ability of cells to produce ATP after abrupt decrease in oxidative metabolism.

This effect appears to underlie the neuroprotective action of DCS and explains the results of one early study, in which administration of DCS to Wistar rats in the same preconditioning regimen significantly slowed down the decline rate of ATP and phosphocreatine levels in the brain during a subsequent episode of global ischemia induced by cardiac arrest [19]. In addition, DCS protective effect may be related to increased ability of cells to produce lactate, as lactate has neuroprotective properties in cerebral ischemia [24–27].

The decrease in maximum respiratory rates in preconditioned brain cells by an average of 19.4% can also be attributed to the protective effects of DCS, as the emergence of active oxygen metabolites, recognized as damaging factors in stroke [28], is directly related to increased oxygen consumption during the reperfusion phase.

Conclusion

For the first time, the results demonstrated neuroprotective effect of pharmacological preconditioning with the neural insulin-sensitizer dicholine succinate in ischemic stroke. Data show that DCS, when administered preventively, reduces the size of brain infarct in rats in a subsequent episode of ischemia, provoked by injection of vasoconstrictor endothelin-1 into the striatum. Mechanism of DCS action associates with an increase in the glycolytic reserve of brain cells, i. e., an increase in the ability of DCS-preconditioned cells to enhance production of ATP and lactate via glycolysis after abrupt reduction of oxidative phosphorylation.

References

1. *Feigin V. L., Brainin M., Norrving B., Martins S., Sacco R. L., Hacke W., Fisher M., et al.* World Stroke Organization (WSO): global stroke fact sheet 2022. *Int J Stroke.* 2022; 17 (1): 18–29. DOI: 10.1177/17474930211065917. PMID: 34986727.
2. *Гусев Е. И., Скворцова В. И.* Ишемия головного мозга. Москва: Медицина; 2001. 328 с. *Gusev E. I., Skvortsova V. I.* Cerebral ischemia. Moscow: Medicine; 2001. 328 p (in Russ.).
3. *O'Collins V. E., Macleod M. R., Donnan G. A., Horky L. L., van der Worp B. H., Howells D. W.* 1,026 experimental treatments in acute stroke. *Ann Neurol.* 2006; 59 (3): 467–477. DOI: 10.1002/ana.20741. PMID: 16453316.
4. *Lourbopoulos A., Mourouzis I., Xinaris C., Zerva N., Filippakis K., Pavlopoulos A., Pantos C.* Translational block in stroke: a constructive and «out-of-the-box» reappraisal. *Front Neurosci.* 2021; 15: 652403. DOI: 10.3389/fnins.2021.652403. PMID: 34054413.
5. *Murry C. E., Jennings R. B., Reimer K. A.* Preconditioning with ischemia: a delay of lethal cell injury in ischemic myocardium. *Circulation.* 1986; 74 (5): 1124–1136. DOI: 10.1161/01.CIR.74.5.1124. PMID: 3769170.
6. *Liu Y., Kato H., Nakata N., Kogure K.* Protection of rat hippocampus against ischemic neuronal damage by pretreatment with sublethal ischemia. *Brain Res.* 1992; 586 (1): 121–124. DOI: 10.1016/0006-8993 (92)91380-W. PMID: 1380876.
7. *Li S., Hafeez A., Noorulla F., Geng X.,Shao G., Ren C., Lu G., et al.* Preconditioning in neuroprotection: from hypoxia to ischemia. *Prog Neurobiol.* 2017; 157: 79–91. DOI: 10.1016/j.pneurobio.2017.01.001. PMID: 28110083.
8. *Dengler V. L., Galbraith M., Espinosa J. M.* Transcriptional regulation by hypoxia inducible factors. *Crit Rev Biochem Mol Biol.* 2014; 49 (1): 1–15. DOI: 10.3109/10409238.2013.838205. PMID: 24099156.
9. *Dong P., Li Q., Han H.* HIF-1α in cerebral ischemia (Review). *Mol Med Rep.* 2022; 25 (2): 41. DOI: 10.3892/mmr.2021.12557. PMID: 34878158.
10. *Zelzer E., Levy Y., Kahana C., Shilo B. Z., Rubinstein M., Cohen B.* Insulin induces transcription of target genes through the hypoxia-inducible factor HIF-1alpha/ARNT. *EMBO J.* 1998; 17 (17): 5085–5094. DOI: 10.1093/emboj/17.17.5085. PMID: 9724644.
11. *Pilkis S. J., Granner D. K.* Molecular physiology of the regulation of hepatic gluconeogenesis and glycolysis. *Annu Rev Physiol.* 1992; 54: 885–909. DOI: 10.1146/annurev.ph.54.030192.004321. PMID: 1562196.
12. *Taha C., Mitsumoto Y., Liu Z., Skolnik E. Y., Klip A.* The insulin-dependent biosynthesis of GLUT1 and GLUT3 glucose transporters in L6 muscle cells is mediated by distinct pathways. Roles of p21ras and pp7o S6 kinase. *J Biol Chem.* 1995; 270 (42): 24678–24681. DOI: 10.1074/jbc.270.42.24678. PMID: 7559581.
13. *Masuda S., Chikuma M., Sasaki R.* Insulin-like growth factors and insulin stimulate erythropoietin production in primary cultured astrocytes. *Brain Res.* 1997; 746 (1–2): 63–70. DOI: 10.1016/S0006-8993 (96)01186-9. PMID: 9037485.
14. *Miele C., Rochford J. J., Filippa N., Giorgetti-Peradi S., Van Obberghen E.* Insulin and insulin-like growth factor-I induce vascular endothelial growth factor mRNA expression via different signaling pathways. *J Biol Chem.* 2000; 275 (28): 21695–21702. DOI: 10.1074/jbc.M000805200. PMID: 10777488.
15. *Treins C., Giorgetti-Peraldi S., Murdaca J., Semenza G. L., Van Obberghen E.* Insulin stimulates hypoxia-inducible factor 1 through a phosphatidylinositol 3-kinase/target of rapamycin-dependent signaling pathway. *J Biol Chem.* 2002; 277 (31): 27975-27981. DOI: 10.1074/jbc.M204152200. PMID: 12032158.
16. *Stiehl D. P., Jelkmann W., Wenger R. H., Hellwig-Bürgel T.* Normoxic induction of the hypoxia-inducible factor 1alpha by insulin and interleukin-1beta involves the phosphatidylinositol 3-kinase pathway. *FEBS Lett.* 2002; 512 (1-3): 157–162. DOI: 10.1016/S0014-5793 (02)02247-0. PMID: 11852072.
17. *Russo V., Candeloro P., Malara N., Perozziello G., Iannone M., Scicchitano M., Mollace R., et al.* Key role of cytochrome C for apoptosis detection using Raman microimaging in an animal model of brain ischemia with insulin treatment. *Appl Spectrosc.* 2019; 73 (10): 1208–1217. DOI: 10.1177/0003702819858671. PMID: 31219322.
18. *Storozheva Z. I., Proshin A. T., Sherstnev V. V., Storozhevykh T., Senilova Y. E., Persyantseva N. A., Pinelis V. G., et al.* Dicholine salt of succinic acid, a neuronal insulin sensitizer, ameliorates cognitive deficits in rodent models of normal aging, chronic cerebral hypoperfusion, and beta-amyloid peptide-(25-35)-induced amnesia. *BMC Pharmacol.* 2008; 8: 1. DOI: 10.1186/1471-2210-8-1. PMID: 18215309.
19. *Pomytkin I. A., Semenova N. A.* Study of the effect of preconditioning with succinic acid salt of choline (1:2) on the disturbances of energy metabolism in the brain during ischemia by ^{31}P NMR *in vivo. Dokl Biochem Biophys.* 2005; 403: 289–292. DOI: 10.1007/s10628-005-0094-7. PMID: 16229144.
20. *Pomytkin I. A., Storozheva Z. I., Semenova N. A., Proshin A. T., Sherstnev V. V., Varfolomeev S. D.* Neuroprotective effect of choline succinate in rats with experimental chronic cerebral ischemia evaluated by cognitive ability tests. *Biol Bull.* 2007; 34 (2): 144–147.
21. *Esposito E., Desai R., Ji X., Lo E. H.* Pharmacologic pre- and postconditioning for stroke: Basic mechanisms and translational opportunity. *Brain Circ.* 2015; 1: 104–113. DOI: 10.4103/2394-8108.166380.
22. *Помыткин И. А., Писарев В. В., Меркулов М. Е., Кузнецова Е. Б., Салина Е. А., Малыгин А. Ю., Каркищенко Н. Н.* Results клинического исследования II фазы лекарственного репарата Дирекорд: рандомизированное, двойное слепое, плацебо-контролируемое, с параллельными группами, проспективное исследование по подбору оптимальной дозировки и изучению эффективности, безопасности и переносимости у пациентов с ишемическим инсультом в раннем восстановительном периоде. *Биомедицина.* 2023; 19 (3): 87–96. *Pomytkin I. A., Pisarev V. V., Merkulov M. E., Kuznetso-*

va E. B., Salina E. A., Malygin A.Yu., Karkishchenko N. N. Phase II of clinical trial of Direkord: randomized, double-blind, placebo-controlled, parallel group, and prospective study to select optimal dosage and to study the efficacy, safety, and tolerability in ischemic stroke patients in the early recovery period. *Biomedicine = Biomeditsina*. 2023; 19 (3): 87–96. (in Russ.).
DOI: 10.33647/2074-5982-19-3-87-96.

23. *Помыткин И. А., Писарев В. В., Меркулов М. Е., Лукиных Л. В., Моржухина М. В., Каркищенко Н. Н.* Результаты клинического исследования III фазы: многоцентровое рандомизированное двойное слепое плацебо-контролируемое в параллельных группах исследование эффективности и безопасности лекарственного препарата Директорд у пациентов с ишемическим инсультом в раннем восстановительном периоде. *Биомедицина*. 2023; 19 (4): 81–93. *Pomytkin I. A., Pisarev V. V., Merkulov M. E., Lukinykh L. V., Morzhukhina M. V., Karkischenko N. N.* Results of phase III clinical trial: a multicenter randomized, double-blind, placebo-controlled, parallel group study of the efficacy and safety of Direkord in ischemic stroke patients in early recovery period. *Biomedicine = Biomeditsina*. 2023; 19 (3): 87–96. (in Russ.).
DOI: 10.33647/2074-5982-19-4-81-93.
24. *Berthet C., Castillo X., Magistretti P. J., Hirt L.* New evidence of neuroprotection by lactate after transient focal cerebral ischaemia: extended benefit after intracerebroventricular injection and efficacy of intravenous administration. *Cerebrovasc Dis*. 2012; 34 (5–6): 329–335.
DOI: 10.1159/000343657. PMID: 23154656.
25. *Jourdain P., Rothenfusser K., Ben-Adiba C., Allaman I., Marquet P., Magistretti P. J.* Dual action of L-Lactate on the activity of NR2B-containing NMDA receptors: from potentiation to neuroprotection. *Sci Rep*. 2018; 8 (1): 13472.
DOI: 10.1038/s41598-018-31534-y. PMID: 30194439.
26. *Jourdain P., Allaman I., Rothenfusser K., Fiumelli H., Marquet P., Magistretti P. J.* L-Lactate protects neurons against excitotoxicity: implication of an ATP-mediated signaling cascade. *Sci Rep*. 2016; 6: 21250.
DOI: 10.1038/srep21250. PMID: 26893204.
27. *Cerina M., Levers M., Keller J. M., Frega M.* Neuroprotective role of lactate in a human *in vitro* model of the ischemic penumbra. *Sci Rep*. 2024; 14: 7973.
DOI: 10.1038/s41598-024-58669-5. PMID: 38575687.
28. *Sanderson T. H., Reynolds C. A., Kumar R., Przyklenk K. M.* Molecular mechanisms of ischemia-reperfusion injury in brain: pivotal role of the mitochondrial membrane potential in reactive oxygen species generation. *Mol Neurobiol*. 2013; 47 (1): 9–23.
DOI: 10.1007/s12035-012-8344-z. PMID: 23011809.

Received 16.04.2025
Accepted 09.09.2025
Online first 30.09.2025

https://doi.org/10.15360/1813-9779-2025-5-2598

The Role of Infectious Diseases of the Lower Respiratory Tract in the Pathogenesis of Ischemic Stroke (Review)

Anastasiya S. Babkina

V. A. Negovsky Research Institute of General Reanimatology,
Federal Research and Clinical Center of Intensive Care Medicine and Rehabilitology,
25 Petrovka Str., Bldg. 2, 107031 Moscow, Russia

For citation: *Anastasiya S. Babkina.* The Role of Infectious Diseases of the Lower Respiratory Tract in the Pathogenesis of Ischemic Stroke (Review). *Obshchaya Reanimatologiya = General Reanimatology.* 2025; 21 (5): 59–72. https://doi.org/10.15360/1813-9779-2025-5-2598 [In Russ. and Engl.]

***Correspondence to:** Anastasiya S. Babkina, ababkina@fnkcrr.ru

Summary

Objective: to clarify the pathogenesis of ischemic stroke in infectious diseases of the lower respiratory tract.

Material and methods. We searched the PubMed database for original research articles, clinical reports, review articles, editorials, commentaries, and short communications published before June 25, 2025. Additional studies that were not captured through the primary database search were analyzed after manually examining the reference lists of the selected articles. Articles were selected based on the relevance of the title and abstract to the purpose of this review. Data from 160 sources were included in the analysis.

Results. We have identified and analyzed in detail the mechanisms of ischemic stroke development in respiratory infections: activation of the coagulation system and disruption of natural anticoagulant and fibrinolytic mechanisms (1); interaction of the hemostasis system with innate immunity (2); the effect of infectious agents on the progression of atherosclerosis and the stability of the atherosclerotic plaque (3); the formation of thromboemboli in the pulmonary veins (4).

Conclusion. Both bacterial and viral infections can initiate a procoagulant state mediated by tissue factor, von Willebrand factor, platelet activation, neutrophil extracellular traps and decreased activity of endogenous anticoagulants. The infectious process localized in the lungs, characterized by damage to the pulmonary vascular endothelium, alveolocytes, intraalveolar fibrin deposition, edema, cellular infiltration, in concert with hemostasis alterations create conditions for the formation of thrombi in the pulmonary vessels. Thus, the pulmonary veins and venules can be a source of cerebral thromboembolism. This mechanism of thromboembolic stroke development largely explains causes of acute cerebrovascular events in patients with lower respiratory tract infection without cardiovascular risk factors. Another mechanism of ischemic stroke is associated with direct or indirect effects of pathogens on the stability of atherosclerotic plaques in cerebral vessels, which, together with systemic procoagulant imbalance, leads to the formation of atherothrombosis. Given the significant pathogenetic relationship between acute infectious lung diseases and thromboembolic and atherothrombotic strokes, clinical alertness regarding acute cerebrovascular events should be included in monitoring and management of such patients.

Key words: ischemic stroke; pneumonia; respiratory infection; atherosclerosis; thromboembolism; hemostasis; inflammation

Conflict of interest. The authors declare no conflict of interest.

Information about the authors/Информация об авторе:
Anastasia S. Babkina/Анастасия Сергеевна Бабкина: https://orcid.org/0000-0003-1780-9829

Introduction

Understanding the relationship between acute cerebrovascular accidents (CVA), one of the leading causes of death worldwide, and lower respiratory tract infections, the leading cause of death among infectious diseases, is of global public health significance. The hypothesis linking acute infectious diseases and stroke emerged in the late 19th century, based on the first works of P. Marie and S. Freud [1], devoted to the problem of stroke in children. In 1930, S. Collins et al. first noted a link between seasonal influenza activity and mortality from cardiovascular diseases [2]. Data on the increased risk of ischemic stroke and myocardial infarction in respiratory infections, obtained on the basis of an analysis of large patient databases [3–5], as well as a number of modern publications on ischemic stroke in children associated with a preceding bacterial or viral infection, confirm the previously formulated hypotheses [6–10]. Infection, particularly respiratory infection, has been considered as a trigger for ischemic stroke in both elderly and young patients and children [11–13].

The significance of this problem has become especially evident during the COVID-19 pandemic, which is confirmed by a large number of published clinical reports of acute cerebrovascular accidents in patients hospitalized with the diagnosis of COVID-19. According to A. E. Merkler et al., approximately 1.6% of patients admitted to the emergency department or hospitalized with COVID-19 experienced ischemic stroke, which was incidence

was significantly higher than in patients with influenza [14]. In contrast, a study by Ward et al. demonstrated a similar risk of ischemic stroke in COVID-19 and influenza [15]. According to W. Luo et al., the prevalence of ischemic stroke in COVID-19 was 2% [16]. Similar results were obtained by us when analyzing fatal COVID-19 cases based on autopsy reports [17–18]. However, it is necessary to take into account the high heterogeneity of studies published during the pandemic [19].

Various pathogenetic types of strokes have been described in patients with respiratory infections. Wang et al. showed a high risk of predominantly ischemic stroke (atherothrombotic and cardioembolic) in patients with a recent respiratory tract infection [20]. M. C. Zurrú et al. found that recent respiratory tract infections were significantly associated with atherothrombotic stroke [21]. According to A. Paganini-Hill et al., respiratory tract infection increases the risk of cardioembolic ischemic stroke, even in patients without cardiovascular risk factors [22]. It should be noted that cardioembolic stroke was not associated with infective endocarditis in the mentioned studies.

Despite a large number of studies, data on a direct causal relationship between stroke and respiratory infectious diseases remain contradictory to this day [23]. For example, in a study by T. G. Beach et al., aimed at comparing the frequencies of ischemic and hemorrhagic strokes in patients with pneumonia confirmed at autopsy and without pneumonia, similar risks of stroke were demonstrated for patients in both groups [24].

The mechanisms linking acute respiratory infections and stroke have not been fully addressed in many studies published on this topic. The lack of a clear understanding of the pathogenesis of this association was particularly noticeable in studies conducted during the COVID-19 period. Increased interest in the properties of the Sars-CoV-2 virus and the molecular mechanisms of COVID-19 complications, without regard to morphological and pathological studies, has led to a focus on the «cytokine storm» and the «unique» neuroinvasive and epitheliotropic properties of the virus, interpreting most findings as specific to COVID-19. However, most hypotheses regarding the pathogenesis of stroke in COVID-19 have already been described in the context of other respiratory infections and are not unique to this infection. The uncertainty and inconsistency of data regarding the causal relationship between ischemic stroke and respiratory infections are largely due to an insufficient understanding of the pathogenesis of thrombi or thromboemboli that cause cerebral vascular occlusion.

The aim of the review was to clarify the pathogenesis of ischemic stroke in infectious diseases of the lower respiratory tract.

Material and Methods

To identify studies relevant to the aim of the review, a literature search was conducted in PubMed using the combinations listed in Table 1. Additional sources not identified through the primary database search were analyzed after examining the reference lists of the selected articles.

Results

Based on data from 160 sources, the mechanisms of ischemic stroke development in respiratory infections were identified, requiring detailed consideration and systematization: 1) activation of the blood coagulation system and disruption of natural anticoagulant and fibrinolytic mechanisms; 2) interaction of the hemostasis system with innate immunity; 3) the impact of infectious agents on the progression of atherosclerosis and the stability of atherosclerotic plaque; 4) formation of thromboemboli in the pulmonary veins.

Activation of the blood coagulation system. The lungs are involved in the regulation of the hemostatic system in both physiological and pathological conditions [25]. In pneumonia, inflammation and hemostasis are components of the host's antibacterial defense. Disruption of natural anticoagulant and fibrinolytic mechanisms has been described in detail in acute respiratory distress syndrome (ARDS), severe pneumonia, and sepsis [26, 27]. Some studies indicate hemostatic disorders in patients with moderate and even mild lower respiratory tract diseases [28, 29]. In a study by Milbrandt et al. aimed at studying blood coagulation markers in patients with community-acquired pneumonia over time, it was shown that hemostatic disorders (changes in D-dimer and thrombin-antithrombin complex [TAT] levels) were observed and progressed both in patients with severe disease and in patients with mild, disease without complications [30].

Based on the clot waveform analysis data (CWA — clot waveform using a modified activated partial thromboplastin time (APTT) analysis based on continuous recording of changes in the optical density of the test sample, Tan et al. showed that bacterial infections lead to a general prothrombotic state, while common respiratory viral infections do not have a significant effect on CWA parameters [31]. Studies assessing the effect of lipopolysaccharide (LPS) on hemostasis have noted activation of the Hageman factor, an increase in the content of von Willebrand factor, an increase in the activity of plasminogen activator inhibitor, and a decrease in the activity of tissue plasminogen activator [32, 33]. Procoagulant imbalance in patients with community-acquired pneumonia was noted not only during the disease but also during convalescence [34].

Activation of the tissue factor-thrombin pathway. The role of tissue factor (TF) in the pathogenesis

of respiratory infectious diseases and ARDS is given special attention, since TF is one of the main initiators of procoagulant activity during tissue alteration and inflammation [35–37]. TF is a transmembrane glycoprotein expressed by fibroblasts, vascular smooth muscle cells, mononuclear cells, and endothelial cells [38–40]. Under physiological conditions, TF comes into contact with blood and circulating coagulation factors only after vascular damage [41, 42]. TF activates the blood coagulation factor F VII to F VIIa. The TF-FVIIa complex promotes the additional formation of FVIIa from FVII and activates coagulation factors X and IX [43]. TF-dependent coagulation generates thrombin and induces pleiotropic cellular effects of thrombin on platelets via protease-activated receptors (PARs) [44].

Morphological immunohistochemistry (IHC) studies showed intense TF staining in alveolar epithelial cells, alveolar macrophages, and hyaline membranes of the lungs of patients with ARDS. In contrast, weak TF expression was observed in the lungs of control patients [45]. Exposure of alveolar cell cultures to edema fluid from patients with ARDS was accompanied by a dose-dependent and time-dependent TF expression. TF production during pulmonary infection is suggested to be mediated by tumor necrosis factor α (TNF-α) and interleukin-1β (IL-1β) [46].

TF was detected in the bronchoalveolar lavage (BAL) of patients with bacterial pneumonia [47]. Experimental studies indicate that bacterial antigens, both gram-positive and gram-negative, can directly activate the coagulation system [48, 49]. Bronchoscopic instillation of lipoteichoic acid (LTC), the main component of the membrane of gram-positive bacteria, and instillation of lipopolysaccharide (LPS) in healthy volunteers were shown to induce procoagulant changes in the human bronchoalveolar space. The authors explained the identified features of LTC- and LPS-induced lung inflammation by the action of LTC and LPS on various toll-like receptors, TLR2 and TLR4, respectively. The release of soluble TF in BAL was noted upon exposure to both LTC and LPS. However, increased TF mRNA expression in alveolar macrophages was associated with LTC but not LPS exposure [50–52].

The role of TF in viral infections is supported by studies that have revealed TF expression during infection of various cell types, including pulmonary epithelial and endothelial cells and monocytes [53, 54]. Furthermore, TF expression in endothelial cells is induced by activation of TLR3 (toll-like receptor 3), a pattern recognition receptor that detects single-stranded RNA [55]. Angiotensin II can also induce TF expression in vascular smooth muscle cells and endothelial cells [56]. RNA viruses penetrate cellular endosomes, stimulate endosomal formation and activation of NADPH oxidase complexes through RNA-sensitive toll-like receptors, inducing TF expression [57]. On the one hand, initiation of the procoagulant cascade may promote thrombosis, and on the other hand, TF-dependent activation of coagulation is part of the host's innate immune response to viral infection, which helps prevent intrapulmonary hemorrhage, as evidenced by an increase in alveolar hemorrhage with a genetic decrease in TF in epithelial cells [56].

Increased TF expression in ARDS, pneumonia, and ventilator-induced lung injury is associated with hypercoagulation and thrombus formation in the pulmonary vascular bed, as well as interalveolar fibrin deposition [47, 58–60]. Given the data indicating an elevated level of circulating TF as a potential risk factor for the development of ischemic stroke [61], and also taking into account the role of circulating TF on monocytes and cellular TF-positive microvesicles in thrombus formation after rupture of atherosclerotic plaques [62], TF should be considered as a component of the pathogenesis of ischemic stroke in respiratory infections.

Violation of natural anticoagulant and fibrinolytic mechanisms. Endothelial cells play a key role in maintaining intravascular patency due to their anticoagulant properties. They provide a favorable environment for plasma anticoagulant proteins, including antithrombin, tissue factor inhibitor, and protein C. Infectious diseases impair the anticoagulant properties of endothelial cells. Endothelial cells synthesize heparan sulfate, a component of the glycocalyx, which binds and potentiates anticoagulant plasma proteins, including tissue factor pathway inhibitor (TFPI) and antithrombin [63]. Endothelial

Table. Word combinations used for the PubMed database search strategy .

Keyword combinations
((pneumonia) OR (respiratory infection)) AND (stroke)
((acute respiratory distress syndrome) OR (ARDS)) AND (stroke)
((pneumonia) OR (respiratory infection)) AND (embolic stroke)
(((infection respiratory) OR (pneumonia))) AND (coagulation)
(((infection respiratory) OR (pneumonia))) AND (hemostasis)
((platelets) AND (stroke)) AND (infection)
((pneumonia) OR (respiratory infection)) AND (atherosclerosis)
((pneumonia) OR (respiratory infection)) AND (biomarkers)
((pneumonia) OR (respiratory infection)) AND (pathogenesis) AND (thrombosis)
(thrombosis) OR (immunothrombosis) OR (immunothrombosis) OR ((thromboinflammation) AND (pneumonia))

cells also produce thrombomodulin, which, by binding to thrombin, converts it from a procoagulant to an anticoagulant, activating anticoagulant protein C [64]. Activated protein C (APC), together with cofactor protein S, inactivates factors FVa and FVIIIa. In addition, endothelial cells synthesize and release tissue plasminogen activator (tPA), potentiating plasmin-mediated fibrinolysis in the vascular bed [63, 65].

Tissue factor pathway inhibitor (TFPI) is a central endogenous regulator of TF-thrombin pathway activity. This glycoprotein is produced primarily by endothelial cells and platelets. TFPI directly inhibits factor Xa forming the Xa-TFPI complex, which subsequently inhibits the TFVIIa complex [43]. The highest amount of TFPI mRNA is reported to be expressed in the human lung, while the lowest is expressed in the brain [66]. In the lung, TFPI is localized along the alveolar septa and in the alveolar epithelium, suggesting that decreased TFPI activity may play a significant role in coagulation disorders in the context of lung injury [67, 68]. The exact physiological mechanisms responsible for the decreased TFPI activity observed during infections are unclear. One common hypothesis is that TFPI is cleaved by endogenous or pathogen-derived proteases. Cleavage of TFPI by leukocyte elastase has been described [69]. A study by T. H. Yun et al. presented a mechanism for proteolytic inactivation of TFPI by omptins, the outer membrane aspartyl proteases of gram-negative bacteria, which, according to the authors, contributes to increased pathogen virulence [70]. However, S. Massberg et al. consider local proteolysis of TFPI by serine proteases and extracellular nucleosomes as part of the host's antimicrobial defense, promoting compartmentalization of bacteria in blood vessels with a resulting decrease in tissue invasion [71–72].

Elevated TFPI levels have been found in the lavage fluid of patients with ARDS or pneumonia [73]. However, the relationship of increased TFPI levels and decreased TFPI activity with coagulation remains unclear. To examine the effects of endogenous TFPI levels on coagulation, inflammation, and bacterial growth during *S. pneumoniae* pneumonia, F. E. Van Den Boogaard et al. conducted studies in genetically modified TFPI-deficient mice and in wild-type mice administered with a neutralizing anti-TFPI antibody. The results of the study refuted a significant role for endogenous TFPI in the antibacterial, inflammatory, and procoagulant responses in pneumococcal pneumonia, as none of the low TFPI groups showed altered procoagulant responses in the lungs or plasma during pneumonia [68].

J. A. Bastarache et al. suggested that although alveolar epithelial cells produce TFPI, the amount of this endogenous protein is insufficient to block the increased procoagulant activity of TF during inflammation [67]. Data from other studies also indicate that the increased procoagulant activity observed in various lung diseases is not counterbalanced by TFPI [73, 74]. Of clinical significance is that the recombinant TFPI (rh-TFPI) showed no beneficial effect in patients with severe community-acquired pneumonia [75].

The role of plasma TFPI in the development of cardiovascular diseases has not been determined, despite the fact that in atherosclerotic plaques TFPI is localized together with TF, where it is believed to suppress TF activity [76].

Thrombomodulin (TM) is a transmembrane glycoprotein found primarily on endothelial cells, but also found in immune cells, vascular smooth muscle cells, keratinocytes, and alveolar epithelial cells of the lung. TM is a potent anticoagulant that binds to thrombin and then deactivates it, triggering the anticoagulant cascade [77]. Thrombin interacts with thrombomodulin (TM), thereby mediating the activation of protein C, which binds to the endothelial cell protein C receptor (EPCR) [78, 79]. Transcriptional expression of TM occurs in high amounts in the vessels of the heart, pancreas, and lungs, and to a lesser extent in the brain [66].

It has been shown that TM (sTM) increases in blood plasma in community-acquired pneumonia, COVID-19, and mycoplasma pneumonia, and that TM level examination has prognostic value [80–82]. The informative value of sTM in relation to thrombotic risk in patients with COVID-19 has been noted [83].

A study by A. W. Rijneveld et al. on mice with a mutation in the TM gene (TM pro/pro) was aimed at elucidating the pathogenetic role of TM in bacterial pneumonia. Bacterial pneumonia was associated with fibrin deposits in the lungs, inflammatory infiltrates, and an increase in thrombin-antithrombin complexes in bronchoalveolar lavage fluid in both TM pro/pro mice and mice without the mutation. This data, according to the authors, indicates that the ability of TM to generate APS does not play an important role in the pulmonary response to respiratory pathogens or LPS [84].

Based on studies showing high levels of soluble thrombomodulin in pulmonary inflammation, it can be assumed that the release of thrombomodulin from the cell surface contributes to protein C deficiency [60, 85].

Impaired production and/or activation of protein C is another potential mechanism leading to thrombosis in pneumonia [86]. Relative deficiency of APS may be due to increased consumption and enhanced degradation of protein C by neutrophil elastase [87]. It should be taken into account that, although some APS is detected in bronchoalveolar fluid, the lungs are capable of producing only a small amount [88]. Since the main synthesis of APS occurs in liver cells, a decrease in its content in blood plasma may be due to liver cell damage due to tissue hypoxia caused by respiratory failure [89].

Ware et al. showed that in patients with ARDS, plasma APC concentrations were reduced, while plasminogen activator inhibitor type 1 (PAI-1) levels were increased, compared to a control group of patients with cardiogenic pulmonary edema [90]. Low APC and high PAI-1 concentrations associated with increased mortality in patients with ARDS [91]. Relatively low protein C activity was noted in COVID-19 [92]. Increased APC expression was shown to enhance host defense during experimental pneumococcal pneumonia [93].

T. Won et al. studied the expression of TM and endothelial protein C receptor (EPCR) in the lungs, kidneys, and hearts of patients who died from COVID-19. A significant difference between the control group and the group of patients who died from COVID-19 was a decrease in the expression of TM and EPCR in the lungs [77].

In scientific literature, there is data on impaired fibrinolysis and decreased protein C activation as hemostatic risk factors for cerebral infarction. The findings of the case-control study by R. F. Macko et al. indicate that protein C dysfunction and endogenous fibrinolysis may contribute to an increased risk of cerebral infarction after a recent (⩽1 week) infection [94].

When analyzing hemostasis mechanisms in infectious diseases, genetic predisposition to thrombosis should be taken into account. Single nucleotide polymorphisms of protein C, factor V (e. g., the Leiden mutation), and plasminogen activator inhibitor-1 have been found to be associated with an increased risk of deep vein thrombosis, pulmonary embolism, acute myocardial infarction, and stroke [95]. Therefore, a personalized approach to assessing the risk of thrombotic complications of infectious respiratory diseases is necessary.

Interaction of the hemostasis system and innate immunity. Since the onset of the COVID-19 pandemic, the previously existing terms «thromboinflammation» and «immunothrombosis» have gained widespread popularity and prevalence. The first mentions of «thromboinflammation» date back to the 1990s in experimental studies on cerebral air embolism models. It has been suggested that damage to the cerebral vascular endothelium results from secondary reactions involving the interaction of air emboli with blood elements (platelets, leukocytes), fibrinogen, and the endothelium, leading to local fibrin accumulation, as well as platelet and leukocyte adhesion to the endothelium. Thus, to describe the process of thrombus formation with a pronounced cellular reaction, the authors used the term «thromboinflammation» [96].

Later, with the emergence of a large amount of evidence of the involvement of the immune system, in particular proteins of the complement system, in the process of thrombus formation, the preconditions arose for the introduction of a term encompassing the interaction of the immune system and hemostasis [97]. Thus, in 2013, the term «immunothrombosis» appeared [98]. These terms are most often used in studies devoted to the pathogenesis of pulmonary artery thrombosis in ARDS. However, the interaction of the hemostatic system and innate immunity is an integral component of thrombus formation, which was studied even before the appearance of the term «immunothrombosis» [99–102].

Neutrophil extracellular traps, von Willebrand factor, ADAMTS-13. The association of acute infections with an increased risk of thrombotic complications, including ischemic stroke, has recently been increasingly explained by mechanisms of innate immunity, in particular, special attention is paid to neutrophil extracellular traps (NETs) [103]. Neutrophils are known to kill invading microorganisms using two strategies: phagocytosis and degranulation [104]. In a study by O. Porembskaya et al., in rats with normal neutrophil counts and neutropenia, showed that no thrombi were detected in the pulmonary artery in animals with neutropenia. Neutropenia caused a significant decrease in the size of the thrombus in the inferior vena cava and slowed the transition from fresh fibrin to mature fibrin and connective tissue within the thrombus [105].

NETosis is one of the mechanisms of neutrophil involvement in thrombosis. Brinkmann et al. first reported NETosis as an antimicrobial strategy of neutrophils, through which a mesh-like structure of chromatin with histones and granular proteins is released from neutrophils into the extracellular space to capture and destroy bacteria and protect the host from infection [106].

S. Massberg et al. showed that serine proteases, neutrophil elastase and cathepsin G, promote coagulation and thrombus formation by inducing TF-factor XII-dependent coagulation and suppressing endogenous anticoagulants [71]. Extracellular DNA derived from NETs mediates thrombin generation in an FXII- or FXI-dependent pathway. Histones induce thrombin generation in platelet-rich plasma (PRP) by activating platelets through TLR2 and TLR4 [107]. Furthermore, histones, especially H4, directly interact with platelets and activate integrin α IIb β3 on the platelet surface, inducing subsequent fibrinogen-mediated platelet aggregation [108].

Uncontrolled NET formation can lead to endothelial cell damage indirectly through NET-associated proteases, defensins, and histones. Endothelial damage and the release of von Willebrand factor (VWF) from Weibel-Palade bodies contribute to thrombus formation.

VWF is produced and secreted by endothelial cells, megakaryocytes, and platelets. The majority of VWF (80–90%) in plasma is produced by endothelial cells. VWF recruits circulating platelets at

sites of vascular injury and mediates subsequent platelet activation and aggregation [109]. VWF activity is size-dependent. Ultra-large VWF multimers (UL — VWF), released by endothelial cells in response to endothelial-damaging factors, can spontaneously recruit excess circulating platelets and other blood cells, promoting thrombosis [110].

ADAMTS metalloprotease 13 (a disintegrin and metalloproteinase with thrombospondin type 1 motif, member 13) specifically cleaves the Tyr 1605- Met 1606 bond in the VWF domain A2 regulating the size and activity of VWF multimers, preventing thrombus formation [111]. VWF directly binds and immobilizes extracellular DNA released from leukocytes [112]. Since NETs and VWF are involved in the inflammatory process, the interaction between NETs and VWF may contribute to the development of thrombosis in infectious diseases. An increase in NETs reduces ADAMTS13 activity, promoting the formation of UL-VWF, which leads to the formation of a vicious circle [113].

NETs are very large structures and may contribute to thrombus stability similar to von Willebrand factor (VWF) and fibrin. In vitro studies have shown that NETs provide a thrombolytic-resistant scaffold for blood clots [114]. Individual DNA and histones have been shown to have a more pronounced procoagulant effect than intact NETs [115].

An increase in the VWF factor content in combination with a decrease in the ADAMTS-13 content in blood plasma has been observed in respiratory infectious diseases of both viral and bacterial etiology [34]. The imbalance between VWF and ADAMTS-13 is explained by a relative deficiency of ADAMTS-13 due to a significant increase in the VWF level [116]. Thus, in patients with COVID-19, such an imbalance led to the appearance of large VWF multimers, which was associated with a high thrombotic risk [117, 118]. The important role of VWF in the development of thrombosis in COVID-19 is confirmed by significantly more intense immunohistochemical (IHC) staining of VWF in the pulmonary vascular endothelium in patients with thrombotic complications than in patients without thrombotic complications [119].

Patients with hospital-acquired pneumonia also exhibit a procoagulant imbalance, in particular the VWF/ADAMTS13 ratio was higher in patients with pneumonia than in healthy study participants [34]. The ability of Streptococcus pneumoniae, the most common causative agent of pneumonia, to induce Weibel-Palade body exocytosis and the release of VWF and interleukin 8 (IL-8) from pulmonary endothelial cells has been reported [120]. *Staphylococcus aureus* infection has been shown to be associated with an increase in NETs and VWF content, as well as a decrease in ADAMTS13 activity [121]. Considering that patients with severe acute respiratory infections may require artificial ventilation (AV), which in itself is associated with many complications, including thrombotic ones [122, 123], it is necessary to take into account studies that have shown an increase in VWF expression in the endothelium of patients on mechanical ventilation [124].

The role of NETs was noted in the pathogenesis of cardiovascular diseases, in particular in the formation of atherosclerotic plaques, arterial and venous thrombosis, as well as in the development and progression of aneurysms [125]. A significant increase in NETs markers was found in plasma of patients with ischemic stroke [126].

Excess neutrophils and NETs are observed in almost all thrombi obtained from patients with ischemic stroke [127]. Experimental targeting of NETs with DNase I or Cl-amidine significantly inhibited arterial thrombosis and improved stroke outcome [128]. Experiments in In vitro studies have shown that the addition of extracellular DNA and histones to fibrin increases the thickness, rigidity and stability of the fibrin network, making thrombolysis more difficult [129].

A study by R. B. Patel et al. confirmed the role of VWF-ADAMTS13 imbalance in stroke severity in respiratory infections in an experimental setting. Thus, Vwf -/- deficient mice infected with *S. aureus* or SARS-CoV-2 showed a reduced number of infarcts and improved functional outcomes, while infected Adamts13 -/- deficient mice showed greater stroke severity [130]. A study in patients also confirmed the effect of SARS — CoV -2 infection preceding ischemic stroke on coagulation and NETosis biomarkers, leading to an imbalance in the VWF — ADAMTS 13 axis [131].

Platelet activation. The complex interaction between NETs and platelets, characterized by the ability of NET components to enhance platelet aggregation and activation, which, in turn, under certain conditions, can activate neutrophils to form NETs [132]. A wide range of functional Pattern Recognition Receptors (PRR) receptors are present on the platelet surface, including TLR and Fc receptors. In response to pathogen invasion, activated platelets release their granules containing various immunomodulatory and antimicrobial molecules that either promote the differentiation and activation of immune cells or can directly kill pathogens [133]. Platelets have been shown to interact with Gram-negative and Gram-positive bacteria. LPS enhances the platelet response through interaction with TLR4 [134].

M. Mirsaeidi et al. showed an independent association of thrombocytosis with increased length of hospital stay and mortality in patients with community-acquired pneumonia [135]. Increased platelet reactivity and activation compared to controls was noted in patients with viral respiratory infections, including COVID-19 [136, 137]. P. D. McMullen et al.

performed an immunohistochemical study of autopsy material from the lungs of patients who died from COVID-19, influenza, bacterial and fungal infections using antibodies to CD 61. Almost all samples showed an increase in the area of CD 61 IHC staining compared to control lung tissue. The area of CD 61 staining in COVID-19 infection was higher than in influenza, but still comparable to many other infectious diseases. The highest area of CD 61 staining was observed in cases of aspiration pneumonia, *Staphylococcus aureus* infection, and blastomycosis [138].

The role of infections in the development of atherothrombosis and atherosclerotic plaque instability. The hypothesis suggesting a pathogenetic link between infection and atherosclerosis has existed for quite some time. It is believed that both viral and bacterial pathogens may be associated with the development and progression of atherosclerosis, as well as with disruption of atherosclerotic plaque stability [139]. Given the high prevalence of atherosclerosis, understanding the mechanisms by which infection influences existing atherosclerotic vascular changes in patients is important. We previously showed that COVID-19 patients who died from ischemic stroke had severe cardiovascular comorbidity, in particular atherosclerosis and stenosis of the arteries of the base of the brain [17, 140].

The most compelling evidence for a link between atherosclerosis and infections is presented in relation to *Chlamydia pneumoniae*. R. Ezzahiri et al. described increased T-cell infiltration and atherosclerotic plaque progression in *Chlamydia pneumoniae* infected hypercholesterolemic mice [141]. Currently, plaque progression is not considered to be a continuous process. Therefore, it is proposed that repeated infections throughout life are associated with multiple episodes of increased T cell infiltration, which contributes to plaque composition remodeling. *Chlamydia pneumoniae* bacterial antigens persist in tissues and remain accessible to immunocompetent cells, which is accompanied by a cellular response for at least 4 weeks. T cell lines derived from carotid artery plaques showed antigen specificity for chlamydial antigens in approximately 50% of plaques [142]. A comparative study of the walls of the aorta, coronary, and basilar arteries revealed intra- and extracellular deposition of *Chlamydia pneumoniae* in unstable atherosclerotic plaques, which were characterized by infiltration of the cap and intima adjacent to the atheromatous core, and infiltration by mononuclear cells, primarily T cells. *Chlamydia pneumoniae* was not detected in the intima of unchanged areas of the vascular wall, and insignificant amounts were detected in stable atherosclerotic plaques [143].

Pneumonia caused by *Streptococcus pneumoniae* has been shown to alter plaque characteristics and promote aortic wall remodeling in hypercholesterolemic mice [144].

M. Boumegouas et al. demonstrated for the first time the binding of *Staphylococcus aureus* and *Pseudomonas aeruginosa* with cholesterol crystals, which partially reveals the mechanism of bacterial adhesion to atherosclerotic plaques and their destabilization [145]. It has been shown that the flagellar protein FlgE *Pseudomonas aeruginosa* induces lipid uptake by macrophages and proinflammatory responses mediated by ATP 5 B/NF — kB/AP-1 signaling [146].

B. B. Lanter et al. showed that bacteria form biofilm deposits in carotid artery plaques, which, when exposed to physiologically relevant levels of norepinephrine in the presence of transferrin, could disperse, releasing bacterial enzymes. The authors suggested that these enzymes may damage surrounding tissue and promote plaque rupture. Thus, this study demonstrates a potential link between infections, atherothrombosis, and conditions associated with elevated adrenaline [147].

The role of a local cross-reactive immune response in human atherosclerotic plaques cannot be ruled out. Cross-reaction with bacterial outer membrane proteins *Proteus mirabilis* and *Klebsiella pneumoniae*, a well as with transgelin, cytoskeletal protein involved in atherogenesis, has been described [148].

For some viruses, data have also been obtained substantiating their involvement in the pathogenesis of atherosclerosis and plaque destabilization. Neuraminidase, a group of enzymes that cleave sialic acid during virus release from the host cell, can induce desialylation of lipoproteins, increase the uptake of low-density lipoproteins, and thus contribute to the progression of atherosclerosis [149–151]. A mechanism for the destabilization of vulnerable atherosclerotic plaques in arteries has been described, mediated by increased expression of matrix metalloproteinase-13 (MMP-13) in influenza A [152].

Some studies attribute a significant role in vascular damage to infection of perivascular adipose tissue (PAT). Under physiological conditions, PAT has potent antiatherogenic properties mediated by its ability to secrete various biologically active factors involved in thermogenesis and fatty acid metabolism. In pathological conditions, steatocytes lose their thermogenic capacity and release adipokines, which induce endothelial dysfunction and inflammatory cell infiltration, contributing to the development of atherosclerosis [153, 154].

Influenza A mRNA levels in the aortic AF in mice were shown to be ~4–8 times higher than in the vessel wall. Infection also increased the number of Ly6Clow and Ly6Chigh monocytes in the vessel wall, followed by more intense monocyte infiltration into the AF [155].

Ischemic stroke due to pulmonary venous thromboembolism. The pathogenesis of thrombus

formation in the pulmonary arteries and veins during respiratory infections has been described in detail. Local pulmonary factors associated with damage to endothelial cells, alveolar cells, fibrin deposition, and pulmonary edema, coupled with systemic hemostatic disorders characteristic of lower respiratory tract infections, especially severe ones, contribute to thrombus formation in the pulmonary vascular bed. Pulmonary vein thrombosis can cause thromboembolic stroke. However, the link between infection and pulmonary vein thrombosis is often overlooked.

A number of clinical reports have been published on pulmonary vein thromboembolism in respiratory infections, including COVID-19 [156–159]. An analysis of thrombotic complications of COVID-19 revealed pulmonary vein thrombosis in 5.8% of deceased patients [18].

It is important to note that the pulmonary veins are the most proximal source of thromboembolism. Therefore, careful evaluation of the pulmonary veins should be performed in all cases of arterial thromboembolism [160]. Understanding this mechanism of thromboembolism is important for both clinicians and pathologists, especially in cases where the source of embolism cannot be determined.

Conclusion

The pathogenesis of ischemic stroke in acute lower respiratory tract infections is at the intersection of alteration, inflammation, immunopathological processes, and circulatory impairment. Based on a review of the literature, it is clear that both bacterial and viral infections, despite differences in their mechanisms of action on the immune system and hemostasis, can initiate a procoagulant state mediated by tissue factor, von Willebrand factor, platelet activation, neutrophil extracellular traps, and decreased activity of endogenous anticoagulants. An infectious process localized in the lungs, characterized by damage to the pulmonary vascular endothelium and alveolar cells, interalveolar fibrin accumulation, edema, and cellular infiltration, combined with hemostatic disorders, creates conditions conducive to thrombus formation in the pulmonary vessels. Thus, the pulmonary veins and venules may be a source of cerebral thromboembolism. This mechanism of thromboembolic stroke development largely explains cases of acute cerebrovascular accidents in patients with lower respiratory tract infections without cardiovascular risk factors. Another mechanism of ischemic stroke is associated with the direct or indirect effects of pathogens on the stability of atherosclerotic plaques in cerebral vessels, which, combined with procoagulant imbalance, leads to the development of atherothrombosis.

Understanding the mechanisms of ischemic stroke in respiratory infectious diseases is essential for developing targeted therapeutic strategies and improving patient outcomes. Clinical awareness of ischemic stroke in acute infectious lung diseases is essential for the management of these patients.

References

1. *Miller E. C., Elkind M. S. V.* Infection and stroke: an update on recent progress. *Curr Neurol Neurosci Rep.* 2016; 16 (1): 2. DOI: 10.1007/s11910-015-0602-9. PMID: 26677196.
2. *Collins S.* Excess mortality from causes other than influenza and pneumonia during influenza epidemics. *Public Health Rep.* 1932; 47: 2159–2189.
3. *Meier C. R., Jick S. S., Derby L. E., Vasilakis C., Jick H., Meier C., Jick S., et al.* Acute respiratory-tract infections and risk of first-time acute myocardial infarction. *Lancet.* 1998; 351 (9114): 1467–1471. DOI: 10.1016/S0140-6736 (97)11084-4. PMID: 9605802.
4. *Clayton T. C., Capps N. E., Stephens N.G., Wedzicha J. A., Meadw T. W.* Recent respiratory infection and the risk of myocardial infarction. *Heart.* 2005; 91 (12): 1601–1602. DOI: 10.1136/hrt.2004.046920. PMID: 16287745.
5. *Clayton T. C., Thompson M., Meade T. W.* Recent respiratory infection and risk of cardiovascular disease: case-control study through a general practice database. *Europ Heart J.* 2007; 29 (1): 96–103. DOI: 10.1093/eurheartj/ehm516. PMID: 18063596
6. *Fu M., Wong K. S., Lam W. W.M., Wong G. W. K.* Middle cerebral artery occlusion after recent mycoplasma pneumoniae infection. *J Neurol Sc.* 1998; 157 (1): 113–115. DOI: 10.1016/S0022-510X (98)00074-4. PMID: 9600687.
7. *Fullerton H. J., Hills N. K., Elkind M. S.V., Dowling M. M., Wintermark M., Glaser C. A., Tan M., et al.* Infection, vaccination, and childhood arterial ischemic stroke: Results of the VIPS study. *Neurol.* 2015; 85 (17): 1459–66. DOI: 10.1212/WNL.0000000000002065. PMID: 26423434.
8. *Amlie-Lefond C., Fullerton H.* Rashes, sniffles, and stroke: a role for infection in ischemic stroke of childhood. *Infect Disord Drug Targets.* 2010; 10 (2): 67–75. DOI: 10.2174/187152610790963465. PMID: 20166975.
9. *Kutleša M., Tešović G., Knezović I., Miše B., Višković K., Barišić N.* Ischemic stroke associated with adenoviral infection in a 4-year-old boy. *Wien Klin Wochenschr.* 2009; 121 (23–24): 776–779. DOI: 10.1007/s00508-009-1286-4. PMID: 20047116.
10. *Cao Q., Yang F., Zhang J., Liang H., Liu X., Wang H.* Features of childhood arterial ischemic stroke in China. *Fetal Pediatr Pathol.* 2019; 38 (4): 317–25. DOI: 10.1080/15513815.2019.1588438. PMID: 30890011.
11. *Grau A. J., Buggle F., Hacke W.* Infektionskrankheiten als ursache und risikofaktor für zerebrovaskuläre ischämien. [Infectious diseases as a cause and risk factor for cerebrovascular ischemia]. *Nervenarzt.* 1996; 67 (8): 639–649. DOI: 10.1007/s001150050036. PMID: 8805109.
12. *Grau A. J., Buggle F., Heindl S., Steichen-Wiehn C., Banerjee T., Maiwald M., Rohlfs M., et al.* Recent infection as a risk factor for cerebrovascular ischemia. *Stroke.* 1995; 26 (3): 373–379. DOI: 10.1161/01.STR.26.3.373. PMID: 7886709.
13. *Boehme A. K., Luna J., Kulick E. R., Kamel H., Elkind M. S. V.* Influenza-like illness as a trigger for ischemic stroke. *Ann Clin Transl Neurol.* 2018; 5 (4): 456–463. DOI: 10.1002/acn3.545. PMID: 29687022.
14. *Merkler A. E., Parikh N. S., Mir S., Gupta A., Kamel H., Lin E., Lantos J., et al.* Risk of ischemic stroke in patients with COVID-19 versus patients with influenza. *JAMA Neurol.* 2020. DOI: 10.1101/2020.05.18.20105494. PMID: 32614385.
15. *Ward A., Sarraju A., Lee D., Bhasin K., Gad S., Beetel R., Chang S., et al.* COVID-19 is associated with higher risk of venous thrombosis, but not arterial thrombosis, compared with influenza: Insights from a large US cohort. *PLoS ONE.* 2022; 17 (1): e0261786. DOI: 10.1371/journal.pone.0261786. PMID: 35020742.
16. *Luo W., Liu X., Bao K., Huang C.* Ischemic stroke associated with COVID-19: a systematic review and meta-analysis. *J Neurol.* 2022; 269 (4): 1731–40. DOI: 10.1007/s00415-021-10837-7. PMID: 34652503.
17. *Babkina A. S., Yadgarov M.Ya., Lyubomudrov M. A., Ostrova I. V., Volkov A. V., Kuzovlev A. N., Grechko A. V., et al.* Morphologic findings in the cerebral cortex in COVID-19: association of microglial changes with clinical and demographic variables. *Biomedicines.* 2023; 11 (5): 1407. DOI: 10.3390/biomedicines11051407. PMID: 37239078.
18. *Babkina A. S., Yadgarov M. Y., Volkov A. V., Kuzovlev A. N., Grechko A. V., Golubev A. M.* Spectrum of thrombotic complications in fatal cases of COVID-19: focus on pulmonary artery thrombosis in situ. *Viruses.* 2023; 15 (8): 1681. DOI: 10.3390/v15081681. PMID: 37632023.
19. *De Souza A. M. L. B., De Araújo E. F., Junior N. C., Raimundo A. C. S., Pereira A. C., De Castro Meneghim M.* Association between SARS-CoV-2 and stroke: perspectives from a metaumbrella-review. *BMC Neurol.* 2025; 25 (1): 97. DOI: 10.1186/s12883-025-04041-7. PMID: 40055630.
20. *Wang J. E.-H., Tsai S.-J., Wang Y.-P., Chen T.-J., Wang T.-J., Chen M.-H.* Bacterial pneumonia and stroke risk: a nationwide longitudinal follow-up study. *Curr Neurovasc Res.* 2023; 20 (5): 578–85. DOI: 10.2174/0115672026280736240108093755. PMID: 38288840.
21. *Zurrú M. C., Alonzo C., Brescacín L., Romano M., Cámera L. A., Waisman G., Cristiano E., et al.* Recent respiratory infection predicts atherothrombotic stroke: case–control study in a Buenos Aires healthcare system. *Stroke.* 2009; 40 (6): 1986–1990. DOI: 10.1161/STROKEAHA.108.535559. PMID: 19359651.
22. *Paganini-Hill A., Lozano E., Fischberg G., Barreto M. P., Rajamani K., Ameriso S. F., Heseltine P. N. R., et al.* Infection and risk of ischemic stroke: differences among stroke subtypes. *Stroke.* 2003; 34 (2): 452–457. DOI: 10.1161/01.STR.0000053451.28410.98. PMID: 12574559.
23. *Taylor L. D., Ameen O. S., Zaharie S.-D.* Complete clinicopathological case report of a young patient dying of COVID-19-related stroke. *Am J Forensic Med Pathol.* 2021; 42 (2): 160–163. DOI: 10.1097/PAF.0000000000000668.
24. *Beach T. G., Sue L. I., Intorcia A. J., Glass M. J., Walker J. E., Arce R., Nelson C. M., et al.* Acute brain ischemia, infarction and hemorrhage in subjects dying with or without autopsy-proven acute pneumonia *MedRxiv [Preprint.].* 2021: 22.21254139. DOI: 10.1101/2021.03.22.21254139. PMID: 33791728.
25. *Арипов А. Н., Каюмов У. К., Иноятова Ф. Х., Хидоятова М. Р.* Роль легких в системе гемостаза (обзор литературы). *Клиническая лабораторная диагностика.* 2021; 66 (7): 411–416. *Aripov A. N., Kayumov U. K., Inoyatova F. Kh., Khidoyatova M. R.* Role of lungs in the hemostasis system (review of literature). *Klin Lab Diagn.* 2021; 66 (7): 411–416. (in Russ.). DOI: 10.51620/0869-2084-2021-66-7-411-416. PMID: 34292683.
26. *Bos L. D. J., Ware L. B.* Acute respiratory distress syndrome: causes, pathophysiology, and phenotypes. *Lancet.* 2022; 400 (10358): 1145–56. DOI: 10.1016/S0140-6736 (22)01485-4. PMID: 36070787.
27. *Stroo I., Ding C., Novak A., Yang J., Roelofs J. J. T. H., Meijers J. C. M., Revenko A. S., et al.* Inhibition of the extrinsic or intrinsic coagulation pathway during pneumonia-derived sepsis. *Am J Physiol Lung Cell Mol Physiol.* 2018; 315 (5): L799–809. DOI: 10.1152/ajplung.00014.2018. PMID: 30136609.
28. *Horan J. T., Francis C. W., Falsey A. R., Kolassa J., Smith B. H., Hall W. J.* Prothrombotic changes in hemostatic parameters and C-reactive protein in the elderly with winter acute respiratory tract infections. *Thromb Haemost.* 2001; 85 (2): 245–249. PMID: 11246541.
29. *Van Wissen M., Keller T. T., Van Gorp E. C. M., Gerdes V. E. A., Meijers J. C. M., Van Doornum G. J. J., Büller H. R., et al.* Acute respiratory tract infection leads to procoagulant changes in human subjects. *J Thromb Haemost.* 2011; 9 (7): 1432–1434. DOI: 10.1111/j.1538-7836.2011.04340.x. PMID: 21605331.

30. *Milbrandt E. B., Reade M. C., Lee M., Shook S. L., Angus D. C., Kong L., et al., GenIMS Investigators.* Prevalence and significance of coagulation abnormalities in community-acquired pneumonia. *Mol Med.* 2009; 15 (11–12): 438–45. DOI: 10.2119/molmed.2009.00091. PMID: 19753144.
31. *Tan C. W., Wong W. H., Cheen M. H. H., Chu Y. M. H., Lim S. S., Ng L. C. K., Yeo D. G. D., et al.* Assessment of aPTT-based clot waveform analysis for the detection of haemostatic changes in different types of infections. *Sci Rep.* 2020; 10 (1): 14186. DOI: 10.1038/s41598-020-71063-1. PMID: 32843693.
32. *Gattinoni L., Chiumello D., Caironi P., Busana M., Romitti F., Brazzi L., Camporota L.* COVID-19 pneumonia: different respiratory treatments for different phenotypes? *Intensive Care Med.* 2020; 46 (6): 1099–1102. DOI: 10.1007/s00134-020-06033-2. PMID: 32291463.
33. *Mattila K. J., Valtonen V. V., Nieminen M. S., Asikainen S.* Role of infection as a risk factor for atherosclerosis, myocardial infarction, and stroke. *Clin Infect Dis.* 1998; 26 (3): 719–734. DOI: 10.1086/514570. PMID: 9524851.
34. *Tripodi A., Rossi S. C., Clerici M., Merati G., Scalambrino E., Mancini I., Baronciani L., et al.* Pro-coagulant imbalance in patients with community acquired pneumonia assessed on admission and one month after hospital discharge. *Clin Chem Lab Med (CCLM).* 2021; 59 (10): 1699–708. DOI: 10.1515/cclm-2021-0538. PMID: 34192831.
35. *Eilertsen K.-E., Østerud B.* Tissue factor: (patho)physiology and cellular biology. *Blood Coagul Fibrinolysis.* 2004; 15 (7): 521–38. DOI: 10.1097/00001721-200410000-00001. PMID: 15389118.
36. *Musher D. M., Rueda A. M., Kaka A. S., Mapara S. M.* The association between pneumococcal pneumonia and acute cardiac events. *Clin Infect Dis.* 2007; 45 (2): 158–65. DOI: 10.1086/518849. PMID: 17578773.
37. *Pieralli F., Vannucchi V., Nozzoli C., Augello G., Dentali F., De Marzi G., Uomo G., et al.* Acute cardiovascular events in patients with community acquired pneumonia: results from the observational prospective FADOI-ICECAP study. *BMC Infect Dis.* 2021; 21 (1): 116. DOI: 10.1186/s12879-021-05781-w. PMID: 33494707.
38. *Africano H. F., Serrano-Mayorga C. C., Ramirez-Valbuena P. C., Bustos I. G., Bastidas A., Vargas H. A., Gómez S., et al.* Major adverse cardiovascular events during invasive pneumococcal disease are serotype dependent. *Clin Infect Dis.* 2021; 72 (11): e711–9. DOI: 10.1093/cid/ciaa1427. PMID: 32964223.
39. *Guan X. R., Jiang L. X., Ma X. H.* Relationship between *Mycoplasma pneumoniae* infection and acute myocardial infarction. *Zhongguo Wei Zhong Bing Ji Jiu Yi Xue.* 2008; 20 (4): 236–237. (Chinese). PMID: 18419961.
40. *Momiyama Y., Ohmori R., Taniguchi H., Nakamura H., Ohsuzu F.* Association of mycoplasma pneumoniae infection with coronary artery disease and its interaction with chlamydial infection. *Atherosclerosis.* 2004; 176 (1): 139–144. DOI: 10.1016/j.atherosclerosis.2004.04.019. PMID: 15306186.
41. *Long B., Brady W. J., Koyfman A., Gottlieb M.* Cardiovascular complications in COVID-19. *Am J Emerg Med.* 2020; 38 (7): 1504–7. DOI: 10.1016/j.ajem.2020.04.048. PMID: 32317203.
42. *Del Prete A., Conway F., Della Rocca D. G., Biondi-Zoccai G., De Felice F., Musto C., Picichè M., et al.* COVID-19, acute mmyocardial injury, and infarction. *Card Electrophysiol Clin.* 2022; 14 (1): 29–39. DOI: 10.1016/j.ccep.2021.10.004. PMID: 35221083.
43. *Josů R. J., Williams A., Manuel A., Brown J. S., Chambers R. C.* Targeting coagulation activation in severe COVID-19 pneumonia: lessons from bacterial pneumonia and sepsis. *Eur Respir Rev.* 2020; 29 (157): 200240. DOI: 10.1183/16000617.0240-2020. PMID: 33004529.
44. *Coughlin S. R.* Thrombin signalling and protease-activated receptors. *Nature.* 2000; 407 (6801): 258–64. DOI: 10.1038/35025229. PMID: 11001069.
45. *Bastarache J. A., Wang L., Geiser T., Wang Z., Albertine K. H., Matthay M. A., Ware L. B.* The alveolar epithelium can initiate the extrinsic coagulation cascade through expression of tissue factor. *Thorax.* 2007; 62 (7): 608–16. DOI: 10.1136/thx.2006.063305. PMID: 17356058.
46. *Levi M., van der Poll T., Schultz M.* New insights into pathways that determine the link between infection and thrombosis. *Neth J Med.* 2012; 70 (3): 114–120. PMID: 22516575.
47. *Rijneveld A. W., Weijer S., Bresser P., Florquin S., Vlasuk G. P., Rote W. E., Spek C. A., et al.* Local activation of the tissue factor-factor VIIa pathway in patients with pneumonia and the effect of inhibition of this pathway in murine pneumococcal pneumonia. *Crit Care Med.* 2006; 34 (6): 1725–1730. DOI: 10.1097/01.CCM.0000218807.20570.C2. PMID: 16625114.
48. *Beutler B., Rietschel E. Th.* Innate immune sensing and its roots: the story of endotoxin. *Nat Rev Immunol.* 2003; 3 (2): 169–176. DOI: 10.1038/nri1004. PMID: 12563300.
49. *Weidenmaier C., Peschel A.* Teichoic acids and related cell-wall glycopolymers in gram-positive physiology and host interactions. *Nat Rev Microbiol.* 2008; 6 (4): 276–287. DOI: 10.1038/nrmicro1861. PMID: 18327271.
50. *Hoogerwerf J. J., De Vos A. F., Bresser P., Van Der Zee J. S., Pater J. M., De Boer A., Tanck M., et al.* Lung inflammation induced by lipoteichoic acid or lipopolysaccharide in humans. *Am J Respir Crit Care Med.* 2008; 178 (1): 34–41. DOI: 10.1164/rccm.200708-1261OC. PMID: 18403723.
51. *Hoogerwerf J. J., de Vos A. F., Levi M., Bresser P., van der Zee J. S., Draing C., von Aulock S., van der Poll T.* Activation of coagulation and inhibition of fibrinolysis in the human lung on bronchial instillation of lipoteichoic acid and lipopolysaccharide. *Crit Care Med.* 2009; 37 (2): 619-625. DOI: 10.1097/CCM.0b013e31819584f9. PMID: 19114879.
52. *Van der Poll T.* Tissue factor as an initiator of coagulation and inflammation in the lung. *Crit Care.* 2008; 12 Suppl 6 (Suppl 6): S3. DOI: 10.1186/cc7026. PMID: 19105796.
53. *Antoniak S., Mackman N.* Multiple roles of the coagulation protease cascade during virus infection. *Blood.* 2014; 123 (17): 2605–13. DOI: 10.1182/blood-2013-09-526277. PMID: 24632711.
54. *Antoniak S., Tatsumi K., Hisada Y., Milner J. J., Neidich S. D., Shaver C. M., Pawlinski R., et al.* Tissue factor deficiency increases alveolar hemorrhage and death in influenza A virus-infected mice. *J Thromb Haemost.* 2016; 14 (6): 1238–1248. DOI: 10.1111/jth.13307. PMID: 26947929.
55. *Shibamiya A., Hersemeyer K., Schmidt Wöll T., Sedding D., Daniel J.-M., Bauer S., Koyama T., et al.* A key role for toll-like receptor-3 in disrupting the hemostasis balance on endothelial cells. *Blood.* 2009; 113 (3): 714–722. DOI: 10.1182/blood-2008-02-137901. PMID: 18971420.
56. *Mackman N., Antoniak S., Wolberg A. S., Kasthuri R., Key N. S.* Coagulation abnormalities and thrombosis in patients infected with SARS-CoV-2 and other pandemic viruses. *Atheroscler Thromb Vasc Biol.* 2020; 40 (9): 2033–44. DOI: 10.1161/ATVBAHA.120.314514. PMID: 32657623.
57. *DiNicolantonio J. J., McCarty M.* Thrombotic complications of COVID-19 may reflect an upregulation of endothelial tissue factor expression that is contingent on activation of endosomal NADPH oxidase. *Open Heart.* 2020; 7 (1): e001337. DOI: 10.1136/openhrt-2020-001337. PMID: 32532805.
58. *Choi G., Schultz M. J., Van Till J. W. O., Bresser P., van der Zee J. S., Boermeester M. A., Levi M., et al.* Disturbed alveolar fibrin turnover during pneumonia is restricted to the site of infection. *Eur Respir J.* 2004; 24 (5): 786–9. DOI: 10.1183/09031936.04.00140703. PMID: 15516673.
59. *Bastarache J. A., Fremont R. D., Kropski J. A., Bossert F. R., Ware L. B.* Procoagulant alveolar microparticles in the lungs of patients with acute respiratory distress syndrome. *Am J Physiol Lung Cell Mol Physiol.* 2009; 297 (6): L1035–41. DOI: 10.1152/ajplung.00214.2009. PMID: 19700643.

60. *Choi G., Wolthuis E. K., Bresser P., Levi M., Van Der Poll T., Dzoljic M., Vroom M. B., et al.* Mechanical ventilation with lower tidal volumes and positive end-expiratory pressure prevents alveolar coagulation in patients without lung injury. *Anesthesiology*. 2006; 105 (4): 689–695. DOI: 10.1097/00000542-200610000-00013. PMID: 17006066.
61. *Iacoviello L., Di Castelnuovo A., De Curtis A., Agnoli C., Frasca G., Mattiello A., Matullo G., et al.* Circulating tissue factor levels and risk of stroke: findings from the EPICOR study. *Stroke*. 2015; 46 (6): 1501–7. DOI: 10.1161/STROKEAHA.115.008678. PMID: 25931463.
62. *Tatsumi K., Mackman N.* Tissue factor and atherothrombosis. *J Atheroscler Thromb*. 2015; 22 (6): 543–9. DOI: 10.5551/jat.30940. PMID: 26016513.
63. *Ito T., Kakuuchi M., Maruyama I.* Endotheliopathy in septic conditions: mechanistic insight into intravascular coagulation. *Crit Care*. 2021; 25 (1): 95. DOI: 10.1186/s13054-021-03524-6. PMID: 33685461.
64. *Ito T., Maruyama I.* Thrombomodulin: protectorate God of the vasculature in thrombosis and inflammation. *J Thromb Haemost*. 2011; 9: 168–73. DOI: 10.1111/j.1538-7836.2011.04319.x. PMID: 21781252.
65. *Urano T., Castellino F. J., Suzuki Y.* Regulation of plasminogen activation on cell surfaces and fibrin. *J Thromb Haemost*. 2018; 16 (8): 1487–97. DOI: 10.1111/jth.14157. PMID: 29779246.
66. *Bajaj M. S., Kuppuswamy M. N., Manepalli A. N., Bajaj S. P.* Transcriptional expression of tissue factor pathway inhibitor, thrombomodulin and von Willebrand factor in normal human tissues. *J Thromb Haemost*. 1999; 82 (3): 1047–1052. PMID: 10494762.
67. *Bastarache J. A., Wang L., Wang Z., Albertine K. H., Matthay M. A., Ware L. B.* Intra-alveolar tissue factor pathway inhibitor is not sufficient to block tissue factor procoagulant activity. *Am J Physiol Lung Cell Mol Physiol*. 2008; 294 (5): L874–81. DOI: 10.1152/ajplung.00372.2007. PMID: 18310227.
68. *van den Boogaard F. E., van 'T Veer C., Roelofs J. J. T. H., Meijers J. C. M., Schultz M. J., Broze Jr G., van der Poll T.* Endogenous tissue factor pathway inhibitor has a limited effect on host defense in murine pneumococcal pneumonia. *J Thromb Haemost*. 2015; 114 (07): 115–122. DOI: 10.1160/TH14-12-1053. PMID: 25832548.
69. *Higuchi D. A., Wun T. C., Likert K. M., Broze G. J. Jr.* The effect of leukocyte elastase on tissue factor pathway inhibitor. *Blood*. 1992; 79 (7): 1712–1719. PMID: 1558967.
70. *Yun T. H., Cott J. E., Tapping R. I., Slauch J. M., Morrissey J. H.* Proteolytic inactivation of tissue factor pathway inhibitor by bacterial omptins. *Blood*. 2009; 113 (5): 1139–48. DOI: 10.1182/blood-2008-05-157180. PMID: 18988866.
71. *Massberg S., Grahl L., von Bruehl M.-L., Manukyan D., Pfeiler S., Goosmann C., Brinkmann V., et al.* Reciprocal coupling of coagulation and innate immunity via neutrophil serine proteases. *Nat Med*. 2010; 16 (8): 887–896. DOI: 10.1038/nm.2184. PMID: 20676107.
72. *Maroney S. A., Mast A. E.* Tissue factor pathway inhibitor and bacterial infection. *J Thromb Haemost*. 2011; 9 (1): 119–121. DOI: 10.1111/j.1538-7836.2010.04111.x. PMID: 21210950.
73. *De Moerloose P., De Benedetti E., Nicod L., Vifian C., Reber G.* Procoagulant activity in bronchoalveolar fluids: No relationship with tissue factor pathway inhibitor activity. *Thromb Res*. 1992; 65 (4–5): 507–18. DOI: 10.1016/0049-3848 (92)90202-L. PMID: 1615494.
74. *El Solh A. A., Choi G., Schultz M. J., Pineda L. A., Mankowski C.* Clinical and hemostatic responses to treatment in ventilator-associated pneumonia: role of bacterial pathogens. *Crit Care Med*. 2007; 35 (2): 490–6. DOI: 10.1097/01.CCM.0000253308.93761.09. PMID: 17205031.
75. *Wunderink R. G., Laterre P.-F., Francois B., Perrotin D., Artigas A., Vidal L. O., Lobo S. M., et al.* Recombinant tissue factor pathway inhibitor in severe community-acquired pneumonia: a randomized trial. *Am J Respir Crit Care Med*. 2011; 183 (11): 1561–8. DOI: 10.1164/rccm.201007-1167OC. PMID: 21297074.
76. *Winckers K., Ten Cate H., Hackeng T. M.* The role of tissue factor pathway inhibitor in atherosclerosis and arterial thrombosis. *Blood Rev*. 2013; 27 (3): 119–32. DOI: 10.1016/j.blre.2013.03.001. PMID: 23631910.
77. *Won T., Wood M. K., Hughes D. M., Talor M. V., Ma Z., Schneider J., Skinner J. T., et al.* Endothelial thrombomodulin downregulation caused by hypoxia contributes to severe infiltration and coagulopathy in COVID-19 patient lungs. *EBioMedicine*. 2022; 75: 103812. DOI: 10.1016/j.ebiom.2022.103812. PMID: 35033854.
78. *Griffin J. H., Fernández J. A., Gale A. J., Mosnier L. O.* Activated protein C. *J Thromb Haemost*. 2007; 5 Suppl 1: 73–80. DOI: 10.1111/j.1538-7836.2007.02491.x. PMID: 17635713.
79. *Isshiki T., Sakamoto S., Kinoshita A., Sugino K., Kurosaki A., Homma S.* Recombinant human soluble thrombomodulin treatment for acute exacerbation of idiopathic pulmonary fibrosis: a retrospective study. *Respiration*. 2015; 89 (3): 201–207. DOI: 10.1159/000369828. PMID: 25659984.
80. *Yin Q., Liu B., Chen Y., Zhao Y., Li C.* Soluble thrombomodulin to evaluate the severity and outcome of community-acquired pneumonia. *Inflammation*. 2014; 37 (4): 1271–1279. DOI: 10.1007/s10753-014-9854-9. PMID: 24573987.
81. *Guo S.-C., Xu C.-W., Liu Y.-Q., Wang J.-F., Zheng Z.-W.* Changes in plasma levels of thrombomodulin and D-dimer in children with different types of *Mycoplasma pneumoniae* pneumonia. *Zhongguo Dang Dai Er Ke Za Zhi*. 2013; 15 (8): 619–622. (in Chinese). PMID: 23965872.
82. *Yamazaki A., Nukui Y., Kameda T., Saito R., Koda Y., Ichimura N., Tohda S., et al.* Variation in presepsin and thrombomodulin levels for predicting COVID-19 mortality. *Sci Rep*. 2023; 13 (1): 21493. DOI: 10.1038/s41598-023-48633-0. PMID: 38057335.
83. *Padilla S., Andreo M., Marco P., Marco-Rico A., Ledesma C., Fernández-González M., García-Abellán J., et al.* Enhanced prediction of thrombotic events in hospitalized COVID-19 patients with soluble thrombomodulin. *PLoS ONE*. 2025; 20 (3): e0319666. DOI: 10.1371/journal.pone.0319666. PMID: 40106444.
84. *Rijneveld A. W., Weijer S., Florquin S., Esmon C. T., Meijers J. C.M., Speelman P., Reitsma P. H., et al.* Thrombomodulin mutant mice with a strongly reduced capacity to generate activated protein C have an unaltered pulmonary immune response to respiratory pathogens and lipopolysaccharide. *Blood*. 2004; 103 (5): 1702–9. DOI: 10.1182/blood-2002-05-1380. PMID: 14592828.
85. *Choi G., Schultz M. J., Levi M., van der Poll T., Millo J. L., Garrard C. S.* Protein C in pneumonia. *Thorax*. 2005; 60 (8): 705–706. DOI: 10.1136/thx.2004.037341. PMID: 16061717.
86. *Esmon C.* Inflammation and the activated protein C anticoagulant pathway. *Semin Thromb Hemost*. 2006; 32 (S 1): 049–60. DOI: 10.1055/s-2006-939554. PMID: 16673266.
87. *Eckle I., Seitz R., Egbring R., Kolb G., Havemann K.* Protein C degradation *in vitro* by neutrophil elastase. *Biol Chem Hoppe Seyler*. 1991; 372 (2): 1007–14. DOI: 10.1515/bchm3.1991.372.2.1007. PMID: 1793515.
88. *Yamamoto K., Loskutoff D. J.* Extrahepatic expression and regulation of protein C in the mouse. *Am J Pathol*. 1998; 153 (2): 547–555. DOI: 10.1016/S0002-9440 (10)65597-6. PMID: 9708814.
89. *Warkentin T. E., Pai M.* Shock, acute disseminated intravascular coagulation, and microvascular thrombosis: is ‹shock liver› the unrecognized provocateur of ischemic limb necrosis? *J Thromb Haemost*. 2016; 14 (2): 231–235. DOI: 10.1111/jth.13219. PMID: 26662371.

90. *Ware L. B., Fang X., Matthay M. A.* Protein C and thrombomodulin in human acute lung injury. *Am J Physiol Lung Cell Mol Physiol*. 2003; 285 (3): L514-L521. DOI: 10.1152/ajplung.00442.2002. PMID: 12754194.
91. *Frantzeskaki F., Armaganidis A., Orfanos S. E.* Immunothrombosis in acute respiratory distress syndrome: cross talks between inflammation and coagulation. *Respiration*. 2017; 93 (3): 212–25. DOI: 10.1159/000453002. PMID: 27997925.
92. *Wyjcik K., Bazan-Socha S., Celejewska-Wójcik N., Górka K., Lichołai S., Polok K., Stachura T., et al.* Decreased protein C activity, lower ADAMTS13 antigen and free protein S levels accompanied by unchanged thrombin generation potential in hospitalized COVID-19 patients. *Thromb Res*. 2023; 223: 80–6. DOI: 10.1016/j.thromres.2023.01.016. PMID: 36709678.
93. *De Boer J. D., Kager L. M., Roelofs J. J., Meijers J. C., De Boer O. J., Weiler H., Isermann B., et al.* Overexpression of activated protein C hampers bacterial dissemination during pneumococcal pneumonia. *BMC Infect Dis*. 2014; 14 (1): 559. DOI: 10.1186/s12879-014-0559-3. PMID: 25366058.
94. *Macko R. F., Ameriso S. F., Gruber A., Griffin J. H., Fernandez J. A., Barndt R., Quismorio F. P., et al.* Impairments of the protein C system and fibrinolysis in infection-associated stroke. *Stroke*. 1996; 27 (11): 2005–11. DOI: 10.1161/01.STR.27.11.2005. PMID: 8898806.
95. *Russell J. A.* Genetics of coagulation factors in acute lung injury. *Crit Care Med*. 2003; 31 (Suppl): S243–7. DOI: 10.1097/01.CCM.0000057870.61079.3E. PMID: 12682447.
96. *Ryu K. H., Hindman B. J., Reasoner D. K., Dexter F.* Heparin reduces neurological impairment after cerebral arterial air embolism in the rabbit. *Stroke*. 1996; 27 (2): 303–310. DOI: 10.1161/01.str.27.2.303. PMID: 8571428.
97. *Sims P. J., Wiedmer T.* Induction of cellular procoagulant activity by the membrane attack complex of complement. *Semin Cell Biol*. 1995; 6 (5): 275–282. DOI: 10.1006/scel.1995.0037. PMID: 8562920.
98. *Keragala C. B., Draxler D. F., McQuilten Z.K., Medcalf R. L.* Haemostasis and innate immunity — a complementary relationship: a review of the intricate relationship between coagulation and complement pathways. *Br J Haematol*. 2018; 180 (6): 782–98. DOI: 10.1111/bjh.15062. PMID: 29265338.
99. *Lüscher E. F.* Induction of platelet aggregation by immune complexes. *Ser Haematol*. 1970; 3 (4): 121–129. PMID: 4107202.
100. *Penny R., Castaldi P. A., Whitsed H. M.* Inflammation and haemostasis in paraproteinaemias. *Br J Haematol*. 1971; 20 (1): 35–44. DOI: 10.1111/j.1365-2141.1971.tb00784.x. PMID: 4924493.
101. *Lisiewicz J.* Rola leukocytów w biomorfozie zakrzepów i krzepnieciu krwi [The role of leukocytes in the biomorphosis of thrombosis and blood coagulation]. *Acta Physiol Pol*. 1971; 22 (6): 785–789. (in Polish). PMID: 5292643.
102. *Levine P. H., Weinger R. S., Simon J., Scoon K. L., Krinsky N. I.* Leukocyte-platelet interaction. Release of hydrogen peroxide by granulocytes as a modulator of platelet reactions. *J Clin Invest*. 1976; 57 (4): 955–63. DOI: 10.1172/JCI108372. PMID: 947961.
103. *Vazquez-Garza E., Jerjes-Sanchez C., Navarrete A., Joya-Harrison J., Rodriguez D.* Venous thromboembolism: thrombosis, inflammation, and immunothrombosis for clinicians. *J Thromb Thrombolysis*. 2017; 44 (3): 377–85. DOI: 10.1007/s11239-017-1528-7. PMID: 28730407.
104. *Papayannopoulos V.* Neutrophil extracellular traps in immunity and disease. *Nat Rev Immunol*. 2018; 18 (2): 134–47. DOI: 10.1038/nri.2017.105. PMID: 28990587.
105. *Porembskaya O., Zinserling V., Tomson V., Toropova Y., Starikova E., Maslei V., Bulavinova N., et al.* Neutrophils mediate pulmonary artery thrombosis in situ. *Int J Mol Sci*. 2022; 23 (10): 5829. DOI: 10.3390/ijms23105829. PMID: 35628637.
106. *Brinkmann V., Reichard U., Goosmann C., Fauler B., Uhlemann Y., Weiss D. S., Weinrauch Y., et al.* Neutrophil extracellular traps kill bacteria. *Science*. 2004; 303 (5663): 1532–5. DOI: 10.1126/science.1092385. PMID: 15001782.
107. *Semeraro F., Ammollo C. T., Morrissey J. H., Dale G. L., Friese P., Esmon N. L., Esmon C. T.* Extracellular histones promote thrombin generation through platelet-dependent mechanisms: involvement of platelet TLR2 and TLR4. *Blood*. 2011; 118 (7): 1952–61. DOI: 10.1182/blood-2011-03-343061. PMID: 21673343.
108. *Fuchs T. A., Bhandari A. A., Wagner D. D.* Histones induce rapid and profound thrombocytopenia in mice. *Blood*. 2011; 118 (13): 3708–14. DOI: 10.1182/blood-2011-01-332676. PMID: 21700775.
109. *Luf A., Müller J. P., Brehm M. A.* A biophysical view on von Willebrand factor activation. *J Cell Physiol*. 2018; 233 (2): 799–810. DOI: 10.1002/jcp.25887. PMID: 28256724.
110. *Zhang C., Kelkar A., Neelamegham S.* Von Willebrand factor self-association is regulated by the shear-dependent unfolding of the A2 domain. *Blood Adv*. 2019; 3 (7): 957–68. DOI: 10.1182/bloodadvances.2018030122. PMID: 30936056.
111. *South K., Lane D. A.* ADAMTS-13 and von Willebrand factor: a dynamic duo. *J Thromb Haemost*. 2018; 16 (1): 6–18. DOI: 10.1111/jth.13898. PMID: 29108103.
112. *Grässle S., Huck V., Pappelbaum K. I., Gorzelanny C., Aponte-Santamaría C., Baldauf C., Gräter F., et al.* von Willebrand factor directly interacts with DNA from neutrophil extracellular traps. *Atheroscler Thromb Vasc Biol*. 2014; 34 (7): 1382–9. DOI: 10.1161/ATVBAHA.113.303016. PMID: 24790143.
113. *Yang J., Wu Z., Long Q., Huang J., Hong T., Liu W., Lin J.* Insights into immunothrombosis: the interplay among neutrophil extracellular trap, von Willebrand factor, and ADAMTS13. *Front Immunol*. 2020; 11: 610696. DOI: 10.3389/fimmu.2020.610696. PMID: 33343584.
114. *Fuchs T. A., Brill A., Wagner D. D.* Neutrophil extracellular trap (NET) impact on deep vein thrombosis. *Atheroscler Thromb Vasc Biol*. 2012; 32 (8): 1777–83. DOI: 10.1161/ATVBAHA.111.242859. PMID: 22652600.
115. *Noubouossie D. F., Whelihan M. F., Yu Y.-B., Sparkenbaugh E., Pawlinski R., Monroe D. M., Key N. S. In vitro* activation of coagulation by human neutrophil DNA and histone proteins but not neutrophil extracellular traps. *Blood*. 2017; 129 (8): 1021–9. DOI: 10.1182/blood-2016-06-722298. PMID: 27919911.
116. *Doevelaar A. A.N., Bachmann M., Hölzer B., Seibert F. S., Rohn B. J., Bauer F., Witzke O., et al.* Von Willebrand factor multimer formation contributes to immunothrombosis in coronavirus disease 2019. *Crit Care Med*. 2021; 49 (5): e512-e520. DOI: 10.1097/CCM.0000000000004918. PMID: 33591004.
117. *Pham T. T., Punsawad C., Glaharn S., De Meyer S. F., Viriyavejakul P., van den Steen P. E.* Release of endothelial activation markers in lungs of patients with malaria-associated acute respiratory distress syndrome. *Malar J*. 2019; 18 (1): 395. DOI: 10.1186/s12936-019-3040-3. PMID: 31796023.
118. *Favaloro E. J., Henry B. M., Lippi* G. Increased VWF and decreased ADAMTS-13 in COVID-19: creating a milieu for (micro)thrombosis. *Semin Thromb Hemost*. 2021; 47 (4): 400–418. DOI: 10.1055/s-0041-1727282. PMID: 33893632.
119. *Babkina A. S., Ostrova I. V., Yadgarov M. Y., Kuzovlev A. N., Grechko A. V., Volkov A. V., Golubev A. M.* The role of Von Willebrand factor in the pathogenesis of pulmonary vascular thrombosis in COVID-19. *Viruses*. 2022; 14 (2): 211. DOI: 10.3390/v14020211. PMID: 35215805.
120. *Lüttge M., Fulde M., Talay S. R., Nerlich A., Rohde M., Preissner K. T., Hammerschmidt S., et al. Streptococcus pneumoniae* induces exocytosis of Weibel-Palade bodies in pulmonary endothelial cells. *Cell Microbiol*. 2012; 14 (2): 210–225. DOI: 10.1111/j.1462-5822.2011.01712.x. PMID: 21999205.

121. *Martens C. P., Peetermans M., Vanassche T., Verhamme P., Jacquemin M., Martinod K.* Peptidylarginine deiminase 4 and ADAMTS13 activity in *Staphylococcus aureus* bacteraemia. *Philos Trans R Soc Lond B Biol Sci.* 2023; 378 (1890): 20230042. DOI: 10.1098/rstb.2023.0042. PMID: 37778390.
122. *Голубев А. М., Мороз В. В., Лысенко Д. В., Кузовлев А. Н., Остапченко Д. А.* ИВЛ-индуцированное острое повреждение легких (экспериментальное, морфологическое исследование). *Общая реаниматология.* 2006; 2 (4): 8–12. *Golubev A. M., Moroz V. V., Lysenko D. V., Kuzovlev A. N., Ostapchenko D. A.* Artificial ventilation-induced acute lung lesion: experimental, morphological study. *General Reanimatology = Obshchaya Reanimatologiya.* 2006; 2 (4): 8–12. (In Russ.&Eng.). DOI: 10.15360/1813-9779-2006-4-8-12
123. *Ибадов Р. А., Сабиров Д. М., Эшонходжаев О. Д., Ибрагимов С. Х., Азизова Г. М., Угарова Т. Б.* Факторы риска развития и тяжелого течения вентилятор-ассоциированного трахеобронхита у пациентов на пролонгированной искусственной вентиляции легких. *Общая реаниматология.* 2023; 19 (5): 46–52. *Ibadov R. A., Sabirov D. M., Eshonkhodjaev O. D., Ibragimov S.Kh., Azizova G. M., Ugarova T. B.* Risk factors for the development and severe course of ventilator-associated tracheobronchitis in patients with prolonged mechanical ventilation. *General Reanimatology = Obshchaya Reanimatologiya.* 2023; 19 (5): 46–52. (In Russ.&Eng.). DOI: 10.15360/1813-9779-2023-5-2320.
124. *Yiming M. T., Lederer D. J., Sun L., Huertas A., Issekutz A. C., Bhattacharya S.* Platelets enhance endothelial adhesiveness in high tidal volume ventilation. *Am J Respir Cell Mol Biol.* 2008; 39 (5): 569–575. DOI: 10.1165/rcmb.2007-0332OC. PMID: 18483418.
125. *Klopf J., Brostjan C., Eilenberg W., Neumayer C.* Neutrophil extracellular traps and their implications in cardiovascular and inflammatory disease. *Int J Mol Sci.* 2021; 22 (2): 559. DOI: 10.3390/ijms22020559. PMID: 33429925.
126. *Gao X., Zhao X., Li J., Liu C., Li W., Zhao J., Li Z., et al.* Neutrophil extracellular traps mediated by platelet microvesicles promote thrombosis and brain injury in acute ischemic stroke. *Cell Commun Signal.* 2024; 22 (1): 50. DOI: 10.1186/s12964-023-01379-8. PMID: 38233928.
127. *Laridan E., Denorme F., Desender L., Francois O., Andersson T., Deckmyn H., Vanhoorelbeke K., et al.* Neutrophil extracellular traps in ischemic stroke thrombi. *Ann Neurol.* 2017; 82 (2): 223–232. DOI: 10.1002/ana.24993. PMID: 28696508.
128. *Peca-Martínez C., Durán-Laforet V., García-Culebras A., Ostos F., Hernández-Jiménez M., Bravo-Ferrer I., Pérez-Ruiz A., et al.* Pharmacological modulation of neutrophil extracellular traps reverses thrombotic stroke tPA (tissue-type plasminogen activator) resistance. *Stroke.* 2019; 50 (11): 3228–37. DOI: 10.1161/STROKEAHA.119.026848. PMID: 31526124.
129. *Longstaff C., Varjú I., Sótonyi P., Szabó L., Krumrey M., Hoell A., Bóta A., et al.* Mechanical stability and fibrinolytic resistance of clots containing fibrin, DNA, and histones. *J Biol Chem.* 2013; 288 (10): 6946–56. DOI: 10.1074/jbc.M112.404301. PMID: 23293023.
130. *Patel R. B., Jha A. B., Jain A., Verma A. K., Saini S., Muia J., Gurung P., et al.* Imbalanced VWF-ADAMTS13 axis contributes to the detrimental impact of a preceding respiratory tract infection on stroke. *Blood Adv.* 2025; 9 (6): 1330–41. DOI: 10.1182/bloodadvances.2024014622. PMID: 39787593.
131. *Luka N., South K., Jones R., Unsworth A. J., Coutts G., Mosneag I., Younas M., et al.* The role of the VWF/ADAMTS13 Axis in the thromboinflammatory response in ischemic stroke after SARS-CoV2 infection. *Brain Behav.* 2025; 15 (2): e70348. DOI: 10.1002/brb3.70348. PMID: 39972966.
132. *Li J., Geng Y., Luo Y., Sun X., Guo Y., Dong Z.* Pathological roles of NETs-platelet synergy in thrombotic diseases: from molecular mechanisms to therapeutic targeting. *Int Immunopharmacol.* 2025; 159: 114934. DOI: 10.1016/j.intimp.2025.114934. PMID: 40418882.
133. *Sharma S., Tyagi T., Antoniak S.* Platelet in thrombo-inflammation: unraveling new therapeutic targets. *Front Immunol.* 2022; 13: 1039843. DOI: 10.3389/fimmu.2022.1039843. PMID: 36451834.
134. *Violi F., Cangemi R., Calvieri C.* Pneumonia, thrombosis and vascular disease. *J Thromb Haemost.* 2014; 12 (9): 1391–400. DOI: 10.1111/jth.12646. PMID: 24954194.
135. *Mirsaeidi M., Peyrani P., Aliberti S., Filardo G., Bordon J., Blasi F, Ramirez J. A.* Thrombocytopenia and thrombocytosis at time of hospitalization predict mortality in patients with community-acquired pneumonia. *Chest.* 2010; 137 (2): 416–420. DOI: 10.1378/chest.09-0998. PMID: 19837825.
136. *Kreutz R. P., Bliden K. P., Tantry U. S., Gurbel P. A.* Viral respiratory tract infections increase platelet reactivity and activation: an explanation for the higher rates of myocardial infarction and stroke during viral illness. *J Thromb Haemost.* 2005; 3 (9): 2108–9. DOI: 10.1111/j.1538-7836.2005.01474.x. PMID: 16102122.
137. *Consolo F., Della Valle P., Saracino M., Bonora M., Donadoni G., Ciceri F., Tresoldi M., et al.* Platelet activation state in early stages of COVID-19. *Minerva Anestesiol.* 2022; 88 (6): 472–478. DOI: 10.23736/S0375-9393.22.16054-2. PMID: 35315619.
138. *McMullen P.D., Cho J. H., Miller J. L., Husain A. N., Pytel P., Krausz T.* A descriptive and quantitative immunohistochemical study demonstrating a spectrum of platelet recruitment patterns across pulmonary infections including COVID-19. *Am J Clin Path.* 2021; 155 (3): 354–63. DOI: 10.1093/ajcp/aqaa230. PMID: 33174599.
139. *Leinonen M., Saikku P.* Infections and atherosclerosis. *Scand Cardiovasc J.* 2000; 34 (1): 12–20. DOI: 10.1080/14017430050142341. PMID: 10816055.
140. *Бабкина А. С., Голубев А. М., Острова И. В., Волков А. В., Кузовлев А. Н.* Морфологические изменения головного мозга при COVID-19. *Общая реаниматология.* 2021; 17 (3): 4–15. *Babkina A. S., Golubev A. M., Ostrova I. V., Volkov A. V., Kuzovlev A. N.* Brain morphological changes in COVID-19. *General Reanimatology = Obshchaya Reanimatologiya.* 2021; 17 (3): 4–15. (In Russ.&Eng.). DOI: 10.15360/1813-9779-2021-3-1-0.
141. *Ezzahiri R., Nelissenvrancken H., Kurvers H., Stassen F., Vliegen I., Grauls G., Vanpul M., et al. Chlamydophila pneumoniae* (*Chlamydia pneumoniae*) accelerates the formation of complex atherosclerotic lesions in Apo E3-Leiden mice. *Cardiovasc Res.* 2002; 56 (2): 269–76. DOI: 10.1016/S0008-6363 (02)00544-8. PMID: 12393097.
142. *Vanderwal A. Chlamydia pneumoniae* inside the atherosclerotic plaque — does it affect plaque inflammation and plaque progression? *Cardiovasc Res.* 2002; 56 (2): 178–180. DOI: 10.1016/S0008-6363 (02)00652-1. PMID: 12393086.
143. *Pigarevskii P. V., Mal'tseva S. V., Snegova V. A., Davydova N. G., Guseva V. A. Chlamydia pneumoniae* and immunoinflammatory reactions in an unstable atherosclerotic plaque in humans. *Bull Exp Biol Med.* 2015; 159 (2): 278–81. DOI: 10.1007/s10517-015-2941-6. PMID: 26085364.
144. *Bartlett B., Ludewick H. P., Verma S., Corrales-Medina V. F., Waterer G., Lee S., Dwivedi G.* Cardiovascular changes after pneumonia in a dual disease mouse model. *Sci Rep.* 2022; 12 (1): 11124. DOI: 10.1038/s41598-022-15507-w. PMID: 35778475.
145. *Boumegouas M., Raju M., Gardiner J., Hammer N., Saleh Y., Al-Abcha A., Kalra A., et al.* Interaction between bacteria and cholesterol crystals: implications for endocarditis and atherosclerosis. *PLoS ONE.* 2022; 17 (2): e0263847. DOI: 10.1371/journal.pone.0263847. PMID: 35180238.
146. *Li Y., Zhang M., Li Y., Shen Y., Wang X., Li X., Wang Y., et al.* Flagellar hook protein FlgE promotes macrophage activation and atherosclerosis by targeting ATP5B. *Atherosclerosis.* 2024; 390: 117429. DOI: 10.1016/j.atherosclerosis.2023.117429. PMID: 38278062.

147. *Lanter B. B., Sauer K., Davies D. G.* Bacteria present in carotid arterial plaques are found as biofilm deposits which may contribute to enhanced risk of plaque rupture. *mBio*. 2014; 5 (3): e01206-14.
DOI: 10.1128/mBio.01206-14. PMID: 24917599.
148. *Canducci F., Saita D., Foglieni C., Piscopiello M. R., Chiesa R., Colombo A., Cianflone D., et al.* Cross-reacting antibacterial auto-antibodies are produced within coronary atherosclerotic plaques of acute coronary syndrome patients. *PLoS ONE*. 2012; 7 (8): e42283. DOI: 10.1371/journal.pone.0042283. PMID: 22879930.
149. *Demina E. P., Smutova V., Pan X., Fougerat A., Guo T., Zou C., Chakraberty R., et al.* Neuraminidases 1 and 3 trigger atherosclerosis by desialylating low-density lipoproteins and increasing their uptake by macrophages. *J Am Heart Assoc*. 2021; 10: e018756.
DOI: 10.1161/JAHA.120.018756. PMID: 33554615.
150. *Mezentsev A., Bezsonov E., Kashirskikh D., Baig M. S., Eid A. H., Orekhov A.* Proatherogenic sialidases and desialylated lipoproteins: 35 years of research and current state from bench to bedside. *Biomedicines*. 2021; 9 (6): 600.
DOI: 10.3390/biomedicines9060600. PMID: 34070542.
151. *Jung S.-H., Lee K.-T.* Atherosclerosis by virus infection — a short review. *Biomedicines*. 2022; 10 (10): 2634.
DOI: 10.3390/biomedicines10102634. PMID: 36289895.
152. *Lee H. S., Noh J. Y., Shin O. S., Song J. Y., Cheong H. J., Kim W. J.* Matrix metalloproteinase-13 in atherosclerotic plaque is increased by influenza A virus infection. *J Infect Dis*. 2020; 221 (2): 256–66.
DOI: 10.1093/infdis/jiz580. PMID: 31693113.
153. *Qi X.-Y., Qu S.-L., Xiong W.-H., Rom O., Chang L., Jiang Z.-S.* Perivascular adipose tissue (PVAT) in atherosclerosis: a double-edged sword. *Cardiovasc Diabetol*. 2018; 17 (1): 134.
DOI: 10.1186/s12933-018-0777-x. PMID: 30305178.
154. *Chang L., Milton H., Eitzman D. T., Chen Y. E.* Paradoxical roles of perivascular adipose tissue in atherosclerosis and hypertension. *Circ J*. 2013; 77 (1): 11–8. DOI: 10.1253/circj.CJ-12-1393. PMID: 23207957.
155. *Oseghale O., Liong S., Coward-Smith M., To E. E., Erlich J. R., Luong R., Liong F., et al.* Influenza A virus elicits perivascular adipose tissue inflammation and vascular dysfunction of the aorta in pregnant mice. *PLoS Pathog*. 2022; 18 (8): e1010703.
DOI: 10.1371/journal.ppat.1010703. PMID: 35930608.
156. *Zheng P., Zhang N., Chen Z.* Pulmonary abscess combined with pulmonary vein thrombosis and stroke: a case report. *J Stroke Cerebrovasc Dis*. 2024; 33 (1): 107461.
DOI: 10.1016/j.jstrokecerebrovasdis.2023.107461.
PMID: 38000110.
157. *Albrecht P., Stettner M., Husseini L., Macht S., Jander S., Mackenzie C., Oesterlee U., et al.* An emboligenic pulmonary abscess leading to ischemic stroke and secondary brain abscess. *BMC Neurol*. 2012; 12 (1): 133.
DOI: 10.1186/1471-2377-12-133. PMID: 23121862.
158. *Pasha A. K., Rabinstein A., McBane R. D.* Pulmonary venous thrombosis in a patient with COVID-19 infection. *J Thromb Thrombolysis*. 2021; 51 (4): 985–8.
DOI: 10.1007/s11239-021-02388-5. PMID: 33515360.
159. *Meaney J. F. M., O'Donnell J. S., Bridgewood C., Harbison J., McGonagle D.* Perspective: the case for acute large vessel ischemic stroke in COVID-19 originating within thrombosed pulmonary venules. *Stroke*. 2022; 53 (7): 2411–9.
DOI: 10.1161/STROKEAHA.121.038056. PMID: 35543127.
160. *Ker P. J.* Cryptogenic, embolic stroke — looking backstage. *J Stroke Cerebrovasc Dis*. 2022; 31 (5): 106353.
DOI: 10.1016/j.jstrokecerebrovasdis.2022.106353.
PMID: 35247732.

Received 24.01.2025
Accepted 17.09.2025
Online first 02.10.2025

https://doi.org/10.15360/1813-9779-2025-5-2584

The Intrinsic Network Dynamics Related to Abnormal Delta Rhythm in Consciousness Disorders (Short Review)

Calixto Machado[1]*, Jose J. Sanchez[2], Beata Drobna Saniova[3], Michal Drobný[3], Arthur Schiff[4]

[1] Institute of Neurology and Neurosurgery, Department of Clinical Neurophysiology,
29 y D Vedado, 10400 La Habana, Cuba
[2] Better Call Agency,
1545 NW 15th Street Road, Miami, FL 33125, USA
[3] Clinic of Anaesthesiology and Intensive Medicine, Comenius University in Bratislava,
Jessenius Faculty of Medicine and University Hospital in Martin,
2 Kollarova Str., 03659 Martin, Slovak Republic
[4] Northside Hospital Gwinnett,
500 Medical Center Blvd, Suite 350, Lawrenceville, GA 30046, USA

For citation: *Calixto Machado, Jose J. Sanchez, Beata Drobna Saniova, Michal Drobný, Arthur Schiff.* The Intrinsic Network Dynamics Related to Abnormal Delta Rhythm in Consciousness Disorders (Short Review). *Obshchaya Reanimatologiya = General Reanimatology.* 2025; 21 (5): 73–76. https://doi.org/10.15360/1813-9779-2025-5-2584 [In Engl.]

***Correspondence to:** Calixto Machado, cmachado180652@gmail.com

Summary

Aim: to explore the pathophysiological mechanisms and clinical significance of delta rhythms (⩽4 Hz) in disorders of consciousness (DOC), including coma, unresponsive wakefulness syndrome (UWS), and minimally conscious state (MCS), as biomarkers for diagnosis, prognosis, and therapeutic targeting.

Materials and Methods. A narrative review was conducted, focusing on experimental and clinical findings related to delta rhythm generation and modulation in the disorder of consciousness (DOC). Emphasis was placed on thalamo-cortical interactions, cortical inhibition, neuromodulatory deficits, and the role of glial cells, neuroinflammation, and metabolic disruptions. Quantitative EEG analysis and advanced neuroimaging were highlighted as key tools for assessing delta activity.

Results. Delta rhythms were found to dominate EEGs across DOC states, with high-amplitude global activity in coma and low-amplitude activity in UWS, indicating cortical suppression and thalamocortical disconnection, respectively. In MCS, reduced delta power and improved connectivity correlated with intermittent purposeful behavior. Therapeutic interventions, including TMS, tACS, and pharmacological agents, showed potential for modulating delta rhythms. Additionally, stochastic resonance emerged as a novel mechanism to stabilize neural networks through noise.

Conclusion. Delta rhythms serve as crucial biomarkers in DOC, offering diagnostic, prognostic, and therapeutic value. Multimodal approaches that integrate EEG, neuroimaging, and mechanistic studies are essential for deepening understanding and improving clinical outcomes in DOC management.

Keywords: Delta rhythm; EEG; disorders of consciousness; neural networks; delta-alpha rhythms; neuroimaging

Conflict of interest. The authors declare no conflict of interest.

Introduction

Disorders of consciousness (DOC), including coma, unresponsive wakefulness syndrome (UWS), and minimally conscious state (MCS), represent complex conditions involving disruptions in neural networks. Delta rhythms are prominent in DOC and indicate underlying pathological states. Understanding the mechanisms and implications of delta activity is essential for improving diagnostics, prognostics, and therapeutic approaches. This review synthesizes recent advances in delta rhythm research, emphasizing their mechanistic underpinnings and clinical relevance [1–4].

Mechanisms of Delta Rhythm Generation

Delta rhythms originate from dynamic interactions within the thalamo-cortical circuitry, influenced by [1, 5–8]:

- Thalamic contributions: ıntrinsic oscillatory properties of thalamocortical neurons, mediated by T-type calcium channel dynamics, play a pivotal role in delta generation. Aberrant oscillations within thalamic relay neurons have been linked to hyperpolarized membrane states, resulting in the pathological emergence of delta rhythms.
- Cortical dynamics: cortical neurons contribute to delta activity through synchronized hyperpolarization states, facilitated by GABAergic inhibition. Recent studies have shown that disruptions in interneuron networks can exacerbate the desynchronization seen in DOC.
- Neuromodulatory inputs: cholinergic and dopaminergic systems modulate delta rhythms, with deficits in these pathways observed in DOC patients. Furthermore, noradrenergic and serotonergic systems may indirectly influence delta activity by modulating the arousal network [9–13].

• Role of glial cells: emerging evidence suggests that astrocytes and microglia contribute to rhythm generation by modulating synaptic activity and clearing metabolic byproducts. Neuroinflammation, a common feature in DOC, may alter glial function and impact delta rhythm dynamics [14–16].

Delta Rhythms in Coma

Coma, a profound state of unresponsiveness, is often characterized by pronounced delta activity [17–20] Key features include:

• Global cortical suppression: coma patients typically exhibit high-amplitude, generalized delta rhythms on EEG, reflecting widespread cortical and subcortical dysfunction.

• Thalamic dysfunction: reduced thalamic input in coma is associated with the dominance of slow-wave activity, disrupting normal thalamo-cortical interactions.

• Prognostic insights: while persistent delta activity in coma is indicative of severe brain dysfunction, the gradual re-emergence of faster rhythms may signal recovery potential. Studies have highlighted that early shifts in EEG patterns can predict outcomes in coma patients.

Delta Rhythms in Different DOC States [1, 3, 21]

Distinct delta rhythm profiles differentiate coma, UWS, and MCS:

• *Unresponsive wakefulness syndrome (UWS):* Characterized by widespread, high-amplitude delta activity, reflecting severe cortical disconnection and reduced thalamo-cortical communication.

• *Minimally conscious state (MCS):* Lower delta power and greater functional connectivity compared to UWS, indicating partial preservation of cortical networks. This preservation is often associated with sporadic evidence of purposeful behavior.

• *Emerging patterns in recovery:* Patients transitioning from DOC states often exhibit gradual reductions in delta power, accompanied by increased alpha and beta rhythms, indicative of cortical reorganization.

Diagnostic and Prognostic Value [22–25]

Delta rhythms serve as biomarkers for:

• Diagnosis: Quantitative EEG measures, such as delta power, coherence, and cross-frequency coupling, aid in differentiating DOC states. Combining delta metrics with machine learning approaches has shown promise in improving diagnostic accuracy.

• Prognosis: Changes in delta rhythm characteristics over time correlate with recovery potential, informing clinical decision-making. For instance, a shift from global delta dominance to localized delta activity may indicate partial network restoration.

Therapeutic Implications [1, 20, 26, 27]

1. Neuromodulation: Techniques such as transcranial magnetic stimulation (TMS) and transcranial alternating current stimulation (tACS) target delta activity, showing promise in restoring cortical network function. The use of personalized stimulation protocols, based on individual EEG profiles, may enhance therapeutic outcomes.

2. Pharmacological Approaches: Agents modulating T-type calcium channels or enhancing cholinergic activity offer potential for delta rhythm normalization. Recent trials involving ampakines and GABA-A receptor modulators have demonstrated preliminary efficacy in altering delta dynamics.

3. Noise Modulation: Harnessing the paradoxical stabilizing effects of noise, such as through stochastic resonance, represents an emerging therapeutic avenue. Experimental studies suggest that introducing controlled noise can enhance signal transmission in impaired neural circuits.

Integration with Multimodal Biomarkers [28–32]

Combining delta rhythm analysis with neuroimaging modalities enhances the understanding of DOC pathophysiology. For instance:

• Functional MRI (fMRI): reveals connectivity patterns linked to delta activity, providing insights into network-level disruptions.

• Diffusion Tensor Imaging (DTI): assesses white matter integrity associated with rhythm generation. Studies have shown that reduced fractional anisotropy in thalamic and cortical regions correlates with elevated delta power.

• PET Imaging: investigates metabolic abnormalities that may underlie delta rhythm alterations, such as glucose hypometabolism in key brain regions.

Future Directions

Key areas for further exploration include:

• Mechanistic studies: elucidating the interplay of glial cells, neuroinflammation, and vascular dynamics in delta rhythm generation. Investigating the role of extracellular potassium accumulation in modulating delta activity may also be fruitful.

• Longitudinal studies: examining delta rhythm changes during recovery and their relationship to neural plasticity. Such studies could identify biomarkers predictive of long-term outcomes.

• Clinical trials: evaluating the efficacy of delta-modulating interventions in large patient cohorts. Trials should aim to stratify patients based on baseline EEG features to optimize therapeutic targeting.

• Technological innovations: developing portable, high-density EEG systems to facilitate real-time monitoring of delta activity in clinical settings.

Conclusion

Delta rhythms offer profound insights into the neural disruptions underlying DOC. Advances in understanding their mechanisms and clinical implications hold promise for improving patient outcomes. Future research should focus on bridging experimental findings with translational applications to harness the diagnostic and therapeutic potential of delta rhythms fully. Integrating delta rhythm analysis with multimodal approaches and personalized therapies will likely define the next frontier in DOC management.

References

1. *Wang J., Deng B., Wang J., Yang Y., Liu C.* The abnormal delta rhythm mechanism in disorders of consciousness: intrinsic neuronal properties and network dynamics. *Neurocomputing*. 2025; 620: 129206. DOI: 10.1016/j.neucom.2024.129206.
2. *Casarotto S., Hassan G., Rosanova M., Sarasso S., Derchi C. C., Trimarchi P. D., Vigano A., et al.* Dissociations between spontaneous electroencephalographic features and the perturbational complexity index in the minimally conscious state. *Eur J Neurosci*. 2024; 59: 934–947. DOI: 10.1111/ejn.16299. PMID: 38440949.
3. *Bitar R., Khan U. M., Rosenthale S.* Utility and rationale for continuous EEG monitoring: a primer for the general intensivist. *Crit Care*. 2024; 28 (244): 1–23. DOI: 10.1186/s13054-024-04986-0. PMID: 39014421.
4. *Valomon A., Riedner B. A., Jones S. G., Nakamura K. P., Tononi G., Plante D. T., Benca R. M., et al.* high-density electroencephalography study reveals abnormal sleep homeostasis in patients with rapid eye movement sleep behavior disorder. *Sci Rep*. 2021; 11: 4758. DOI: 10.1038/s41598-021-83980-w. PMID: 33637812.
5. *Naro A., Bramanti A., Leo A., Cacciola A., Manuli A., Bramanti P., Calabro R. S.* Shedding new light on disorders of consciousness diagnosis: The dynamic functional connectivity. *Cortex*. 2018; 103: 316–328. DOI: 10.1016/j.cortex.2018.03.029. PMID: 29684751.
6. *De Stefano P., Carboni M., Pugin D., Seeck M., Vulliemoz S.* Brain networks involved in generalized periodic discharges (GPD) in post-anoxic-ischemic encephalopathy. *Resuscitation*. 2020; 155: 143–151. DOI: 10.1016/j.resuscitation.2020.07.030. PMID: 32795598.
7. *Llinás R. R.* Thalamo-cortical dysrhythmia syndrome: neuropsychiatric features. *An R Acad Nac Med (Madr.)*. 2003; 120 (2): 267–290. PMID: 14619543.
8. *Jones B. E.* Arousal systems. *Front Biosci*. 2003; 8: s438–451. DOI: 10.2741/1074. PMID: 12700104.
9. *Brudzynski S. M., Burgdorf J. S., Moskal J. R.* From emotional arousal to executive action. Role of the prefrontal cortex. *Brain Struct Funct*. 2024; 229: 2327–2338. DOI: 10.1007/s00429-024-02837-w. PMID: 39096390.
10. *Babiloni C., Del Percio C., Pascarelli M. T., Lizio R.,. Noce G., Lopez S., Rizzo M., et al.* Abnormalities of functional cortical source connectivity of resting-state electroencephalographic alpha rhythms are similar in patients with mild cognitive impairment due to Alzheimer's and Lewy body diseases. *Neurobiol Aging*. 2019; 77: 112–127. DOI: 10.1016/j.neurobiolaging.2019.01.013. PMID: 30797169.
11. *Carracedo L. M., Kjeldsen H., Cunnington L., Jenkins A., Schofield I., Cunningham M. O., Davies C. H., et al.* A neocortical delta rhythm facilitates reciprocal interlaminar interactions via nested theta rhythms. *J Neurosci*. 2013; 33 (26): 10750–10761. DOI: 10.1523/JNEUROSCI.0735-13.2013. PMID: 23804097.
12. *Dimpfel W.* Pharmacological modulation of cholinergic brain activity and its reflection in special EEG frequency ranges from various brain areas in the freely moving rat (Tele-Stereo-EEG). *Eur Neuropsychopharmacol*. 2005; 15 (6): 673–682. DOI: 10.1016/j.euroneuro.2005.03.006. PMID: 16009538.
13. *Philippu A., Prast H.* Importance of histamine in modulatory processes, locomotion and memory. *Behav Brain Res*. 2001; 124 (2): 151–159. DOI: 10.1016/s0166-4328(01)00226-1. PMID: 11640968.
14. *Hao W., Liu S., Liu H., Mu X., Chen K., Xin Q., Zhang X.-D. In vivo* neuroelectrophysiological monitoring of atomically precise Au (25) clusters at an ultrahigh injected dose. *ACS Omega*. 2020; 5 (38): 24537–24545. DOI: 10.1021/acsomega.0c03005. PMID: 33015471.
15. *Grigorovsky V., Bardakjian B. L.* Low-to-high cross-frequency coupling in the electrical rhythms as biomarker for hyperexcitable neuroglial networks of the brain, IEEE. *Trans Biomed Eng*. 2018; 65 (7): 1504–1515. DOI: 10.1109/TBME.2017.2757878. PMID: 28961101.
16. *Gavilanes A. W., Gantert M., Strackx E., Zimmermann L. J., Seeldrayers S., Vles J. S., Kramer B. W.* Increased EEG delta frequency corresponds to chorioamnionitis-related brain injury. *Front Biosci (Schol Ed)*. 2010; 2 (2): 432–438. DOI: 10.2741/s76. PMID: 20036959.
17. *Kumar G. P., Panda R., Sharma K., Adarsh A., Annen J., Martial C., Faymonville M. E., et al.* Changes in high-order interaction measures of synergy and redundancy during non-ordinary states of consciousness induced by meditation, hypnosis, and auto-induced cognitive trance. *Neuroimage*. 2024; 293: 120623, 1–10. DOI: 10.1016/j.neuroimage.2024.120623. PMID: 38670442.
18. *Rayi A., Asuncion R. M. D., Mandalaneni K.* Encephalopathic EEG patterns. In: StatPearls [Internet]. Treasure Island (FL): *StatPearls Publishing*; 2025. 2024 Aug 11. PMID: 33232041. Bookshelf ID: NBK564371.
19. *Huang Y., Xia X., Meng X., Bai Y., Feng Z.* Single session of intermittent theta burst stimulation alters brain activity of patients in vegetative state. *Aging*. 2024; 16 (8): 7119–7130. DOI: 10.18632/aging.205746. PMID: 38643463.
20. *Li M., Tang Z., Yu L., Li Y., Ma W., Li J., Li G., Xiong L., et al.* The arousal effect of An-Gong-Niu-Huang-Wan on alcoholic-induced coma rats: a research based on EEG. *J Ethnopharmacol*. 2024; 328: 117974. DOI: 10.1016/j.jep.2024.117974. PMID: 38467317.

21. *Espinosa E. P., Zang D., Buccellato A., Qi Z., Wu X., Abbasi S., Catal Y., et al.* Spectral peak analysis and intrinsic neural timescales as markers for the state of consciousness. *Neuroimage Clin.* 2024; 44: 103698. DOI: 10.1016/j.nicl.2024.103698. PMID: 39509990.
22. *Li C., Wang Y., Li W., Yang Y., Xia X.* Measure functional network and cortical excitability in post-anoxic patients with unresponsive wakefulness syndrome diagnosed by behavioral scales. *Front Neurosci.* 2022; 16: 1071594. DOI: 10.3389/fnins.2022.1071594. PMID: 36711155.
23. *Bai Y., Xia X., Wang Y., He J., X. Li X.* Electroencephalography quadratic phase self-coupling correlates with consciousness states and restoration in patients with disorders of consciousness. *Clin Neurophysiol.* 2019; 130: 1235–1242. DOI: 10.1016/j.clinph.2019.04.710. PMID: 31163368.
24. *Stefan S., B. Schorr B., Lopez-Rolon A., Kolassa I. T., Shock J. P., Rosenfelder M., Heck S., et al.* Consciousness indexing and outcome prediction with resting-state EEG in severe disorders of consciousness. *Brain Topogr.* 2018; 31 (5): 848–862. DOI: 10.1007/s10548-018-0643-x. PMID: 29666960.
25. *Bagnato S., Boccagni C., Prestandrea C., Fingelkurts A. A., Fingelkurts A. A., Galardi G.* Changes in standard electroencephalograms parallel consciousness improvements in patients with unresponsive wakefulness syndrome. *Arch Phys Med Rehabil.* 2017; 98 (4): 665–672. DOI: 10.1016/j.apmr.2016.09.132. PMID: 27794486.
26. *Anzolin A., Das P., Garcia R. G., Chen A., Grahl A., Ellis S., Purdon P., et al.* Delta power during sleep is modulated by EEG-gated auricular vagal afferent nerve stimulation (EAVANS). *Annu Int Conf IEEE Eng Med Biol Soc.* 2023: 1–4. DOI: 10.1109/EMBC40787.2023.10340971. PMID: 38082663.
27. *Landau J., Baulac M., Durand G., A. de Billy A., Philippon J.* Impairment of consciousness induced by valproate treatment following neurosurgical operation. *Acta Neurochir (Wien).* 1993; 125 (1–4): 92–96. DOI: 10.1007/BF01401834. PMID: 7993403.
28. *Bonfiglio L., Olcese U., Rossi B., Frisoli A., Arrighi P., Greco G., Carozzo S., et al.* Cortical source of blink-related delta oscillations and their correlation with levels of consciousness. *Hum Brain Mapp.* 2013; 34 (9): 2178–2189. DOI: 10.1002/hbm.22056. PMID: 22431380.
29. *Duda A. T., Clarke A. R., Barry R. J., De Blasio F. M.* Mindfulness meditation is associated with global EEG spectral changes in theta, alpha, and beta amplitudes. *Int J Psychophysiol.* 2024; 206: 112465. DOI: 10.1016/j.ijpsycho.2024.112465. PMID: 39557128.
30. *Babiloni C., Lopez S., Noce G., Ferri R., Panerai S., Catania V., Soricelli A., et al.* Relationship between default mode network and resting-state electroencephalographic alpha rhythms in cognitively unimpaired seniors and patients with dementia due to Alzheimer's disease. *Cereb Cortex.* 2023; 33 (20): 10514–10527. DOI: 10.1093/cercor/bhad300. PMID: 37615301.
31. *Belov D., Fesenko Z., Efimov A., Lakstygal A., Efimova E.* Different sensitivity to anesthesia according to ECoG data in dopamine transporter knockout and heterozygous rats. *Neurosci Lett.* 2022; 788: 136839. DOI: 10.1016/j.neulet.2022.136839. PMID: 35964824.
32. *Jombik P., Drobny M., Saniova B., Fischer M., Kaderjakova P., Lajciakova M., Bakosova E., et al.* Some quantitative EEG features in default mode resting state network under general anaesthesia. *Neuro Endocrinol Lett.*2017; 38 (4): 261–268. PMID: 28871712.

Received 24.01.2025
Accepted 17.09.2025
Online first 02.10.2025

ФОРУМЫ АНЕСТЕЗИОЛОГОВ И РЕАНИМАТОЛОГОВ РОССИИ
2023, 2024 и 2025 года

	2023	2024	2025
количество очных участников	3725	4015	4267
количество онлайн подключений	15323	13281	14298
количество компаний на выставке	58	63	62

2023	2024	2025
395 докладчиков и модераторов	394 докладчиков и модераторов	493 докладчиков и модераторов
35 секционных заседаний	37 секционных заседаний	42 секционных заседаний
151 лекция	132 лекции	132 лекции
11 сателлитных симпозиумов и мастер классов	6 сателлитных симпозиумов и мастер классов	9 сателлитных симпозиумов и мастер классов
11 постерных секций	12 постерных секций	12 постерных секций
Всероссийский конкурс ординаторов по специальности анестезиология и реаниматология «Профессионалы 2023»	II Всероссийский конкурс ординаторов по специальности анестезиология и реаниматология «Профессионалы 2024»	III Всероссийский конкурс ординаторов по специальности анестезиология и реаниматология «Профессионалы 2025»
	Конкурс научно-исследовательских работ молодых ученых	Конкурс научно-исследовательских работ молодых ученых
		Выездная секция «Открытая территория: знание, лечение, диалог» в ММКЦ «Коммунарка»
		14-ая международная конференция «Актуальные аспекты экстракорпорального очищения крови в интенсивной терапии»

23 страны
412 городов

25 стран
340 городов

26 стран
341 город

ФОРУМ АНЕСТЕЗИОЛОГОВ И РЕАНИМАТОЛОГОВ РОССИИ ФАРР-2025
СЪЕЗД ФЕДЕРАЦИИ АНЕСТЕЗИОЛОГОВ И РЕАНИМАТОЛОГОВ

более 18 500
очных и заочных участников

Доклады	327
Лекции	132
Секционные заседания	42
Симпозиумы	7
Мастер-классы	2
Коммерческих докладов	12

26 стран

Абхазия
Австралия
Азербайджан
Армения
Беларусь
Бразилия
Венгрия
Вьетнам
Германия
Израиль
Ирак
Казахстан
Киргизия
Китай
Латвия
Молдова
Россия
Саудовская Аравия
Словакия
США
Туркмения
Турция
Узбекистан
Украина
Эквадор
Эстония

341 город РОССИИ

В РАМКАХ ФОРУМА ПРОШЕЛ
III Всероссийский конкурс ординаторов по специальности анестезиология и реаниматология
«Профессионалы 2025»

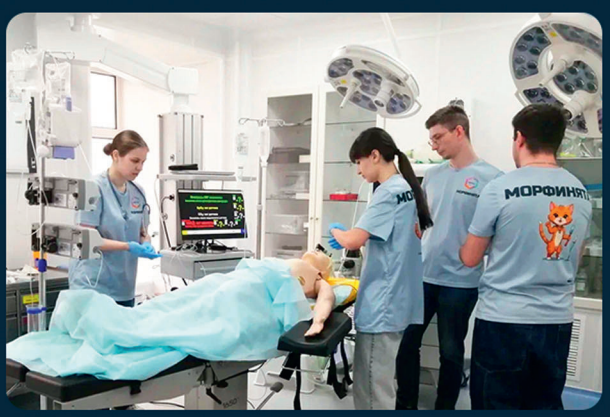

41 команда участие в отборе

16 команд очный раунд

ФЕДЕРАЛЬНОЕ ГОСУДАРСТВЕННОЕ БЮДЖЕТНОЕ НАУЧНОЕ УЧРЕЖДЕНИЕ
"Федеральный научно-клинический центр реаниматологии и реабилитологии"
ФНКЦ РР

Федеральное государственное бюджетное научное учреждение **«Федеральный научно-клинический центр реаниматологии и реабилитологии» (ФНКЦ РР)**

Симуляционный центр ФНКЦ РР

Лаборатория перспективных симуляционных технологий

СИМУЛЯЦИОННЫЕ ОБРАЗОВАТЕЛЬНЫЕ ПРОГРАММЫ:

/ Первая помощь
/ Подготовка инструкторов первой помощи
/ Базовая сердечно-легочная реанимация
/ Расширенная сердечно-легочная реанимация
/ Ультразвуковой мониторинг и навигация в анестезиологии-реаниматологии
/ Трудный дыхательный путь
/ Респираторная поддержка
/ Критические состояния в анестезиологии-реаниматологии
/ Подготовка к первичной специализированной аккредитации
/ Обучение преподавателей симуляционных центров

Все образовательные программы обеспечены баллами НМО
Возможно формирование образовательных циклов по требованию

Тел.: 8(495)650-96-77
www.fnkcrr.ru/edu
edu@fnkcrr.ru